Silviculture for Forest Diversity: Mixed Species Management to Meet Multiple Objectives

Stacey Elaine Dixon

A dissertation

submitted in partial fulfillment of the

requirements for the degree of

Doctor of Philosophy

University of Washington

2026

Reading Committee:

Gregory J. Ettl, Chair

Bernard T. Bormann

Robert J. McGaughey

Maureen C. Kennedy

Program Authorized to Offer Degree:

Environmental and Forest Sciences

University of Washington

Abstract

Silviculture for Forest Diversity:

Mixed Species Management to Meet Multiple Objectives

Stacey Elaine Dixon

Chair of the Supervisory Committee:
Gregory J. Ettl
School of Environmental and Forest Sciences

Mixed species forest management is valued for the potential to increase productivity while generating other important co-benefits that may reduce risks associated with monocultures, such as varied species responses to drought, improved insect and disease resistance, enhanced wildlife habitat, and additional insurance against uncertain ecological change. However, diverse forest systems add a layer of complexity to management, including challenges with seedling regeneration and predicting varied forest development. This dissertation addresses three components of diverse forest management and research: (1) comparison of growth of five Pacific Northwest tree species in monoculture and mixed species forests, (2) browse deterrent strategies for regeneration of high-value timber species such as western redcedar (*Thuja plicata* Donn ex D. Don) and Douglas-fir (*Pseudotsuga menziesii* (Mirb.) Franco), and (3) quantifying understory biomass response to forest management prescriptions using remote sensing methods. This work takes advantage of two long-

term permanent plot datasets (20-year and 50-year) to explore mixed species and monoculture competition, six field trials to compare browse deterrent methods, and two remote sensing datasets to assess predictive model performance of understory biomass. Generalized linear mixed effect models were used to evaluate growth performance for species in mixtures versus monocultures and to investigate browse deterrent strategies alongside χ^2 Tests of Independence; five different machine learning models allowed for comparison of remote sensing methods.

Intraspecific competition is stronger than interspecific competition in mixed, mesic forested stands in the Pacific Northwest. The following pairings showed positive, small growth effects for both species under certain species basal area proportions: (1) Douglas-fir and bigleaf maple (*Acer macrophyllum* Pursh); (2) Douglas-fir and western redcedar; and (3) red alder (*Alnus rubra* Bong.) and western hemlock (*Tsuga heterophylla* (Raf.) Sarg.). Douglas-fir and western hemlock growth responses were also positive under some conditions but inconsistent across two datasets. Interspecific interactions were largely explained by competition or complementarity for limiting resources; positive growth pairings include shade-intolerant species paired with more shade-tolerant species.

Browse deterrence for western redcedar showed effectiveness, ranked in terms of impacts on growth and tree form, from highest to lowest as fenced exclosures, Vexar® tubing, co-planting, Plantskydd and flexible fencing. For Douglas-fir, co-planting with Sitka spruce was more effective than Vexar tubing; fenced exclosures produced varying results, with the presence of invasive species and robust shrub cover associated with reduced Douglas-fir growth. Plantskydd® showed early promising results for western redcedar browse prevention, but challenges with application timing and need for consistent, sustained reapplication reduce utility. Reported costs for deterrent methods indicate large fenced exclosures are the most expensive method to implement, followed

by chemical repellent, Vexar tubing, and Sitka spruce co-planting in that order.

Lastly, low understory biomass values in an open forest system can be predicted using a stochastic gradient boosting model built with unmanned aerial vehicle (UAV) acquired LiDAR and multispectral data. Data acquisition and post-processing were more important than model selection in optimizing model performance and predictions. This study provides a framework for evaluating understory biomass efficiently in open canopy conditions, using limited ground measurements via calibrated photos and UAV remotely sensed data.

Together, these results allow for streamlined decision-making for forest managers and researchers to identify complementary species pairings, increase regeneration success of high-value timber species, and produce wall-to-wall remotely sensed metrics for novel forest prescriptions with limited in-field data. In an era of ecological and societal change, alternative management options mitigate these risks, and this work equips managers with additional tools when monoculture forestry no longer meets objectives.

TABLE OF CONTENTS

LIST OF FIGURES

LIST OF TABLES

ACKNOWLEDGEMENTS

At times, this degree felt like a herculean effort. I am indebted to those who reenergized me through thoughtful guidance, technical input, caring conversation, exceptional childcare and delicious food. I will look back on these years and wonder how I got to the finish line, and then I'll remember your support.

First, I'd like to thank my advisor Gregory Ettl, who was willing to mentor me when I was an overly eager master's student, and has stayed patient, encouraging and reliable for all the years. One of the best parts about working with Dr. Ettl is his ability to focus: his full and individual attention was provided at every meeting and his engagement with the work was steadfast. I will forever be grateful for your mentorship as it has now shaped my early career.

To my committee members, Robert McGaughey, Maureen Kennedy, and Bernard Bormann, your willingness to meet and coach me through this process was essential. Bob, I would never have been able to complete a remote sensing chapter without your help, and I learned so much from you along the way. Thank you for making that possible. Maureen, thank you for the countless statistics coaching sessions—I will refer to them for years to come. Bernard, your enthusiasm for this field is inspiring, and from you, I've learned that no worthy project is too large to take on, and that one should do so with gusto.

I'm grateful for my numerous collaborators that played essential roles in the completion of these chapters. David Diaz, your mentorship and guidance was critical, and I aspire to cultivate such a whip-smart scientific approach. Others who were essential to the process and the completion of this work include: Ariana Mendible, Patrick Tobin, Courtney Bobsin, Ally Kruper, Violet Harris, Chase Beyer, Chris Erickson, Miles Micheletti, the Townsend Family and Port Blakely.

Dano Holt, any student would be so lucky to have you as an advisor, and I've benefitted tenfold from your apt input and persistent encouragement. Thank you to David Peterson who provided extremely valuable edits and feedback in the final weeks. I owe much to the data collectors: decades of Pack Forest interns who helped collect CFI data, ONRC summer crews who helped with biomass data collection, and the students who helped measure seedlings for browse data. Thank you for your tireless work.

To those at the Snohomish Conservation District, my days in the field with you were what reminded me that what I was studying had meaning. Thank you to Paisley Blume, Nolan Kitts, Sara Rocero and Thomas Bulthuis for supporting me with this endeavor, keeping the program and projects running while I was gone for long stretches, and being great friends along the way. To Linda Lyshall, thank you for prioritizing and encouraging growth and education at the district. To Kristin Marshall, my fantastic supervisor, your dedication to my success and flexibility with this degree was unmatched—I could not have done this without you.

To my family, I'm fortunate to always have someone to call when I need to be uplifted—what an incredible gift. To the Hunt family, thank you for welcoming me in and encouraging me always. Thank you to Dennis Dixon, Jackie Dixon, Iain Thatcher, Eric Dixon, Lauren Murphy, Brian Dixon, Melissa Dixon, Gary Dixon, and Jacky Lee—what an absolutely fantastic group of individuals. Thank you for being a source of inspiration, laughter and comfort. To my mother, Sandra Cosca, who provided months of childcare that was essential for the completion of this degree. Thank you for being my loudest cheerleader and a superb example of a mother. Having you in my corner is what gave me the confidence to start this project.

To my friends, hard work is only worth it when you can relax with excellent people, and I have so many in my life. Ben Strom and Isabel Scherl, Lopez trips revived me more than once;

thank you for providing a home away from home and the highest quality of friendship. Brittany and Conor, thank you for caring for Aidan and me through humor and bird walks. Courtney Bobsin, my friend and colleague, you helped me launch this PhD with your wise advice, and you got me to the end with your effective feedback and caring check-ins. Menaka, thank you for the phone calls filled with wisdom—you helped me keep my feet moving forward. To my fellow Mom, PhD student and forest dweller, Meredith Jacobson, it has been an honor to go through this process alongside you. With a final defense at the same hour of the same day, I loved that our stars were so perfectly aligned, giving me a profound sense of being seen. Hannah Tennent, your reliable and warm friendship got me through many challenging weeks and long workdays; you make life more fun. To Curty Rusch, Sarah Edwards, Trevor Harrison and Ariana Mendible, our regular family dinners brought laughter and music to our home. The volleyball games were essential for the home stretch. Thank you for raising Maya with us and making these years so bright.

To my husband, Aidan Hunt, you have supported me not only as an incredibly generous and loving husband but also as a rigorous scientist with astutely helpful comments and technical support. Having a baby and finishing a PhD are not always compatible, but you made that possible through weekly fresh-made bread, long dog walks, weekend childcare after an already hard work week, divinely prepared meals and more. Thank you for all that you sacrificed to get us here—it is an honor and privilege to be your partner and we live an enviable life together.

To Maya, you're curious and unafraid, and I'm so lucky to be your mom. Thank you for your patience as I completed this degree—I'll make it count.

DEDICATION

To Maya, may you also find joy in hard work and trees.

CHAPTER 1. INTRASPECIFIC COMPETITION CONSISTENTLY OUTWEIGHS INTERSPECIFIC COMPETITION IN MIXED-SPECIES FORESTRY

1.0 ABSTRACT

Mixed-species forest management has the potential to increase productivity, reduce risks associated with a changing climate, and provide a wide range of other benefits relative to monoculture. We used two long-term (20-year and 50-year) permanent plot datasets and linear mixed-effects models to explore growth of sympatric species pairings of five common species in the Pacific Northwest USA: Douglas-fir (*Pseudotsuga menziesii* (Mirb.) Franco), western hemlock (*Tsuga heterophylla* (Raf.) Sarg.), western redcedar (*Thuja plicata* Donn ex D. Don), red alder (*Alnus rubra* Bong.) and bigleaf maple (*Acer macrophyllum* Pursh). All species showed significant signs of negative intraspecific (competition within monoculture) effects on growth compared to varying interspecific (mixed species) effects. Of the significant interspecific relationships, 80% resulted in positive growth responses, indicating a pattern of weak interspecific competition. The following pairings showed significant positive and bilateral growth effects under certain species proportions: (1) Douglas-fir and bigleaf maple; (2) Douglas-fir and western redcedar; and (3) red alder and western hemlock. Responses for Douglas-fir and western hemlock showed promise for complementarity but were inconsistent across datasets. Interspecific interactions were largely explained by competition or complementarity for limiting resources; positive-growth pairings include shade-intolerant species paired with more shade-tolerant species. In most cases, intraspecific competition is stronger than interspecific competition in mixed, mesic forested stands

in the Pacific Northwest, and individual tree growth maximization may occur under mixed-species conditions.

1.1 Introduction

Mixed-species forest plantations offer an opportunity to achieve a diversity of ecosystem functions beyond what is provided in monoculture plantations (Liu et al., 2018). Co-benefits of mixed-species forest management may be increasingly useful under high-emission climate change scenarios for their potential to produce varied species responses to drought (Pardos et al., 2021), increase insect and disease resistance, enhance wildlife habitat (Felton et al., 2010), and provide insurance against uncertain ecological change (Jactel et al., 2017; Jansen et al., 2021; Puettmann, 2011). Among these co-benefits, a growing body of literature asserts higher productivity with mixed-species forests compared to monocultures for many species pairings, termed overyielding (Feng et al., 2022; Pretzsch and Schütze, 2021; Zhang et al., 2012). Despite these potential high-value outcomes, comprehensive information for mixed-species forest management in the Pacific Northwest—one of the leading timber producing regions globally—is lacking (but see Himes and Puettmann, 2020). This paper aims to increase knowledge of competition dynamics of common tree species in monoculture vs. mixed-species stands in western Washington State, USA.

In monoculture plantings, intraspecific competition—competition among individuals of the same species—is well understood as an interaction between the number and size of individuals per unit area (Postma et al., 2021). In forestry there are multiple metrics describing this phenomenon for stands of trees. For example, stand density index (SDI), integrates both stocking level and tree size to drive models of crown closure and self-thinning (Reineke, 1933). Intraspecific competition is greater at higher stocking as individual trees compete for limited resources, leading to stagnation

of growth (Oliver and Larson, 1996) or eventual density-related mortality (Yoda et al., 1963). Stand density metrics guide timing and intensity of thinning and final harvest for monoculture stands (Curtis, 1982; Tappeiner, 2015). Timely management interventions are particularly critical for fast-growing timber species where intraspecific pressure may be especially pronounced (Puettmann et al., 1993; Radosevich et al., 2006). Many of the strongest competitors are the most valuable timber species as competition can improve growth form through straighter stems (Höwler et al., 2019), and rapid growth allows for shorter rotations, enabling managers to use intraspecific pressures to increase timber quality and yield (Kelty, 1992; Tappeiner, 2015).

The role of interspecific competition—competition between individuals of differing species—in stand management is less clear (Chen et al., 2003; Tappeiner, 2015), and improved understanding is critical for incorporating mixed species into silvicultural prescriptions. Regardless of shade tolerance, certain species can be strong competitors both aboveground and belowground, leading to superior growth in the forest and an environment of competitive exclusion (Rewald and Leuschner, 2009). Or, beneficial species pairings can arise through complementarity, such as resource partitioning and/or facilitation. Beneficial aboveground resource partitioning may occur when mixed-species stands have higher absorbed photosynthetically active radiation (APAR) or light use efficiency (LUE) compared to monoculture stands. This can be a product of a variety of processes that interact with different tree species, including canopy stratification, crown shapes, crown architecture, crown plasticity and more (Forrester et al., 2025).

In part, physiological traits, such as shade tolerance and shade intolerance, can help explain growth benefits for some mixed-species pairings, in alignment with the niche complementarity hypothesis (H. Lu et al., 2016; Tilman et al., 2001). For example, although shade-intolerant species dominate the upper canopy, shade-tolerant species can persist in the understory for long periods

of time, creating higher density plantations compared to monocultures (Kobe and Coates, 1997; Pretzsch, 2014). Different functional strategies in relation to light allow species to vary their use and response to canopy openings and maximize layering in vertical canopy space (Stan and Daniels, 2014; Urgenson et al., 2013). Stand architecture, as an interaction of assembling species of different growth forms (Van de Peer et al., 2017), and crown features that integrate past growth dynamics and shading effects, such as crown size and shape (Bravo et al., 2001), can further create spatial partitioning of the canopy and enhance productivity (Williams et al., 2017). Under certain contexts, mixtures of shade-intolerant and shade-tolerant species allow for increased yield (Chen et al., 2003) and higher maximum stand densities compared to pure stands (Heiderman and Kimsey, 2023), indicating a more efficient use of the resources controlling growth.

Predicting competition and complementarity in mixed-species forests is complex. Empirical evidence suggests that interspecific competition is often much weaker (20-25%) than intraspecific competition in many plant communities (Adler et al., 2018), yet these effects are mediated by stand characteristics like density and spacing (Amoroso and Turnblom, 2006; Fang et al., 2019). In some forest types, asymmetric competition may exist, with one species dominating the growth of another, depending on vertical placement, above or below another species in the canopy (Nishimura et al., 2003). Variation in the establishment of mixed-species stands also adds complexity to the relationship: planting one species before the other can influence the strength of interspecific competition and resulting mortality. For example, delayed red alder (*Alnus rubra* Bong.) planting into a Douglas-fir (*Pseudotsuga menziesii* (Mirb.) Franco) plantation can help reduce red alder shading of Douglas-fir seedlings (Shainsky and Radosevich, 1992). Site conditions and growing conditions can tip the balance of this relationship, with interspecific

competition decreasing under stressful climatic conditions, yet this response can be species specific and related to life-history strategies (Käber et al., 2023).

Increased tree biomass production compared to monoculture stands may depend on a small range of initial density and percentages of mixture values, with values outside of that range resulting in net decreases in growth (Amoroso and Turnblom, 2006). Regional variation exists: the diversity and productivity relationship are negatively related in portions of the Pacific Northwest but are positively related in other areas of the United States, where productivity is higher when diversity is higher (Watson et al., 2015). Mixed-species relationships are context dependent, with outcomes changing depending on site productivity, species traits and shifts in resource use over time, making generality challenging yet critical for positioning future research (Cole and Newton, 2023; Pardos et al., 2021).

Higher species richness increases not only the complexity of individual tree interactions and stand management but also the ability to develop models which account for these interactions (Coll et al., 2018). Knowledge of beneficial species pairings is largely a result of field mixed-species experimental trials with long time lags for findings or assessment of naturally regenerated stands (Bravo et al., 2001). Mixed-species plantations are rare and usually do not span the full complement of species ratios; often limited to 50:50 or 75:25 reciprocal comparisons to monocultures of each species in the pair. Studies that explore these topics are difficult to install, track, and review at meaningful time intervals, adding difficulty to comparing experimental studies and reaching broad conclusions (De Montigny, 2007; Erickson et al., 2009). Reliance on field trials skews understanding to young stands, where interplay between intra- versus interspecific competition may not yet be fully developed (Pretzsch and Schütze, 2021). As time goes on,

repeated measurements of field trials can result in shifting conclusions that make definitive interpretation challenging (Courtin and Harper, 2018; Harper et al., 2023).

Long-term observational datasets offer an opportunity to compare stand conditions over decades to better refine understanding of beneficial species pairings. This study leverages permanent plot networks with repeated measurements to identify significant detectable effects of species pairings on growth across many forest stand types, guide future experimentation and management, and compare scientific findings. A variety of stand ages, densities and species proportions allow for the creation of baseline averages that can then be used to benchmark past and future experimental outcomes. Two long-term (20-year and 50-year) permanent plot datasets, were used to explore optimal species pairings for five common species of western Washington—Douglas-fir, western hemlock (*Tsuga heterophylla* (Raf.) Sarg.), western redcedar (*Thuja plicata* Donn ex D. Don), red alder and bigleaf maple (*Acer macrophyllum* Pursh)—and address the following questions:

1. What is the relative influence of intraspecific competition versus interspecific competition on tree growth across species pairings and stand densities?
2. Where interspecific interactions with growth are observed, are they positive or negative, and do they show potential for complementarity or competitive exclusion between species?

These questions are addressed by evaluating growth responses of the five species in turn, with each species treated as the focal species when it serves as the response variable in statistical models.

1.2 Materials and Methods

Permanent Plot Data

We used data from two sources to complete this study (Table 1.1.). The first is a continuous forest inventory (CFI) permanent plot dataset collected at the University of Washington Center for Sustainable Forestry at Pack Forest (Pack Forest) (46.8432N, 122.3176W), a research and demonstration forest located in the Cascade Range foothills near Mount Rainier in Washington, USA (Figure 1.1). The second is the US Forest Service (USFS) Forest Inventory and Analysis (FIA) dataset for the western half of Washington State, USA (Gray et al., 2012) (Figure 1.2). The regional climate for the area is Mediterranean, characterized by cold, moist winters and dry summers, with periods of drought. For Pack Forest, mean annual temperature in this region is 10.4°C (16°C from May-September) and annual precipitation is 961.04 mm (40.64 mm from May-September) (PRISM Climate Group, Oregon State University, 2026).

Pack Forest Continuous Forest Inventory

The Pack Forest CFI dataset provides a useful contribution to this study because it contains multiple repeat measurements of trees, tracking growth for up to five decades, and most of the plots in this dataset have only the five study species. Additionally, management history of this forest is extremely well documented, and sites can be revisited to further explore species pairings. Pack Forest is a working forest, managed for both timber production and research objectives. Plots lie within a diverse array of forest types including Douglas-fir dominated plantations, mixed-species plantations, mixed-species conifer-hardwood old-growth forests and hardwood-dominated habitat reserves.

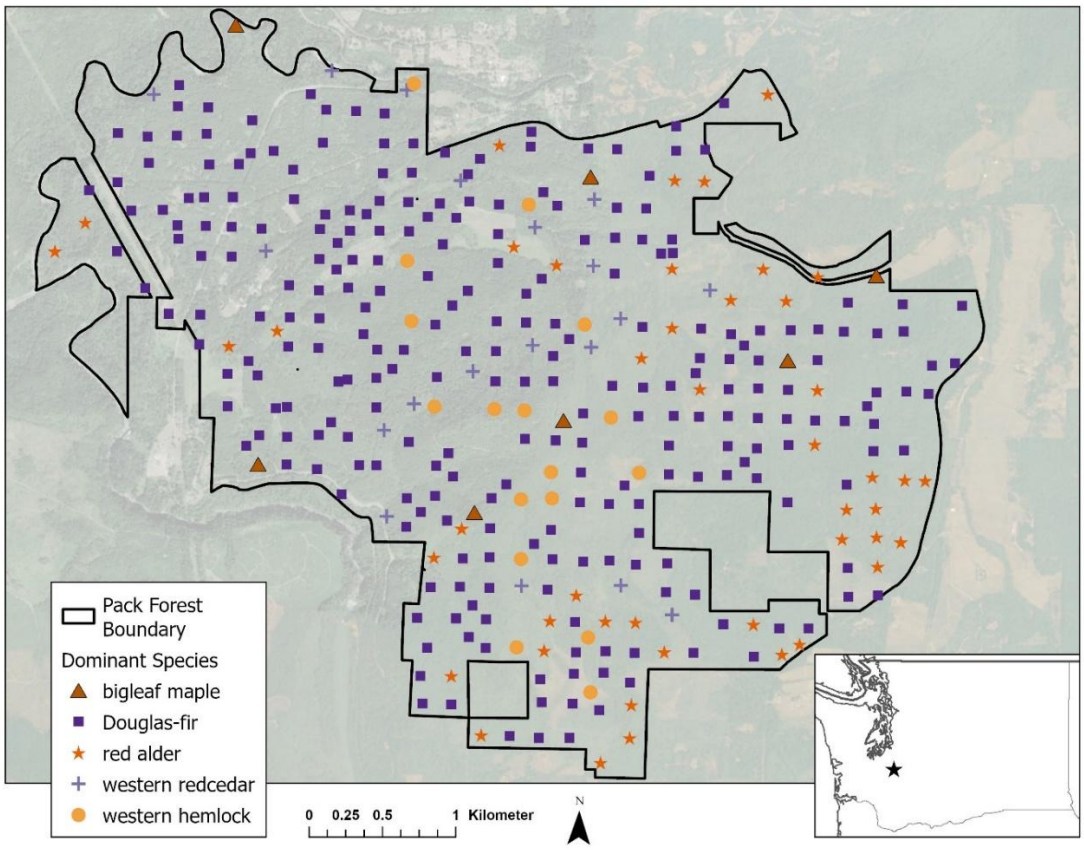

Figure 1.1. Continuous Forest Inventory Plots at the University of Washington research forest, Pack Forest, near Mount Rainier in Washington, USA.

The Pack Forest CFI program was established in 1975 as a network of 440 permanent plots located throughout the research forest to track forest conditions and changes over time (Figure 1.1.). We used measurements from 1975–2023 for this study. The CFI plots follow a grid sampling design and are measured on a rolling basis at a five-year measurement interval. CFI plots are fixed-area 0.04 hectare (1/10th acre) circular plots. For each plot, all trees are tagged with metal tree tags, creating a unique plot and tree number combination that is tracked over time.

Data collection cadence and staffing for the CFI network have varied since establishment with changes in personnel and programmatic support. Inventory data are maintained in database files maintained for discrete (typically five-year) periods. Data were combined from these distinct

databases and records for individual trees were included for analysis in this study based on ability to track a tree over time. Trees that were measured only once across the 50 years were removed from the dataset as plot boundary errors. Plots with less than 95% consistency in tree tag numbers from the previous measurement to the next were excluded from analyses (362 plots were retained out of 440).

United States Forest Service Forest Inventory and Analysis

To allow a broader and more robust regional scope of inference, we incorporated field observations from the USFS FIA, which was purpose-built to enable timely and accurate findings covering a wide range of forest attributes across the United States. Data from Washington were filtered to include only plots with one "condition" observed across the four subplots and limited to the following forest types: Douglas-fir, western redcedar, bigleaf maple, red alder and western hemlock (Figure 1.2.). This resulted in plots limited to the western half of the state, with inventory years ranging from 2002 to 2020, and with all plots remeasured on a 10-year interval.

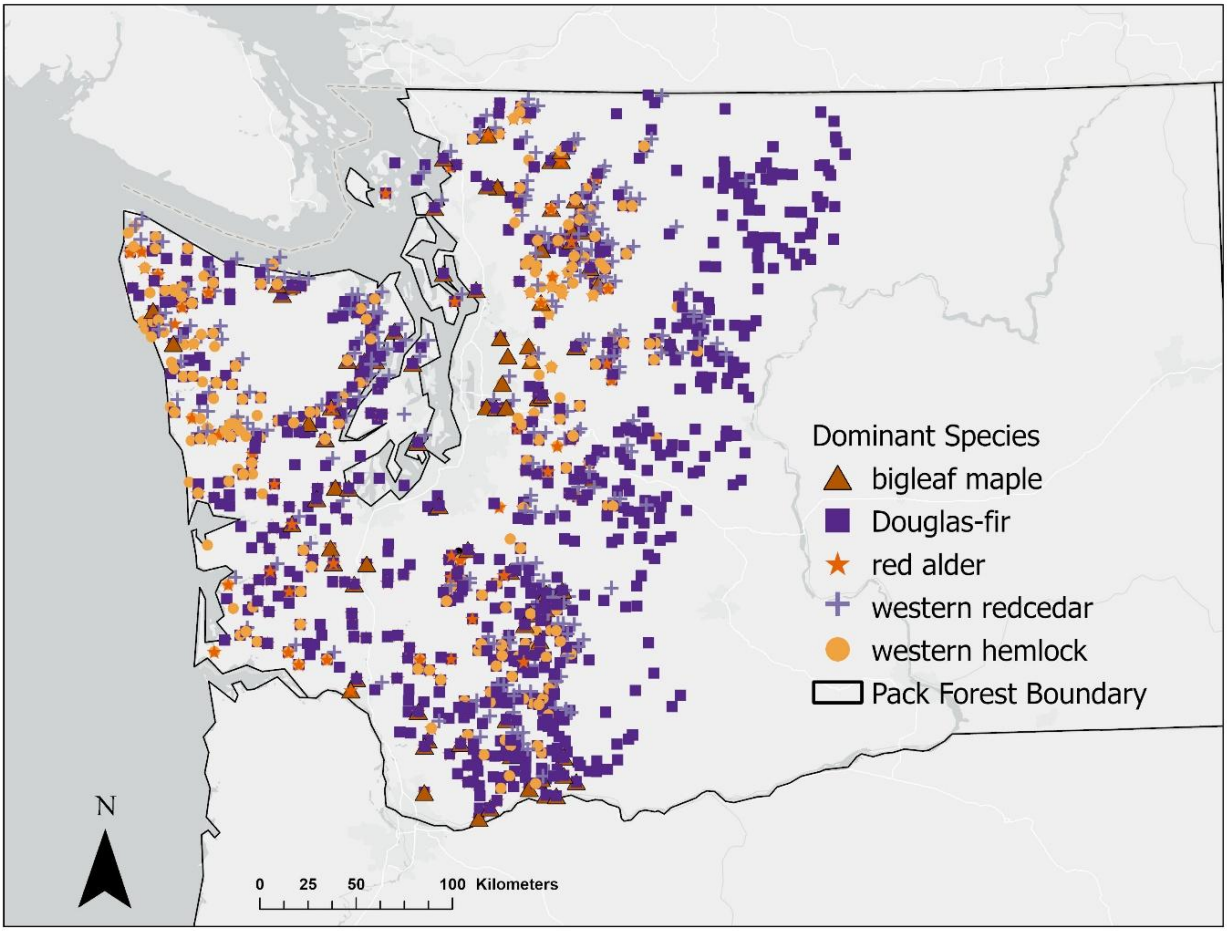

Figure 1.2. USFS Forest Inventory and Analysis plots used in this study and filtered to contain plots in Washington with forest types of either bigleaf maple, Douglas-fir, red alder, western redcedar or western hemlock.

Table 1.1. General characteristics of the two datasets used in this study: Pack Forest Continuous Forest Inventory (CFI) and USFS Forest Inventory and Analysis (FIA). The dataset contains plots with other species than the five study species for this paper, and the percentage of the plots with other species is shown in the rightmost column.

Dataset	Tree Age Range	Elevation Range	Tree Diameter Range	% of dataset comprised of five focal species	% of plots with other species than the five focal species
CFI	0-221	150–610 m	2.5–165 cm	96%	21%
FIA	0-200	30–1800 m	2.5–227 cm	86%	61%

Dataset Processing

We followed the same data processing and analysis steps for both the CFI and FIA datasets. All measurements were processed and analyzed using packages in both the Python (version 3.11.5) and R languages (version 4.3.2) (Python Software Foundation, 2016; R Core Team, 2022). Generative artificial intelligence (ChaptGPT-4o. and ChatGPT-5.2) (OpenAI, 2025) was used to aid in R coding, including exploring functions, refining code, editing code to generate figures and debugging code. The authors reviewed and edited the content of all outputs and take full responsibility for the content of the published article. No portion of the manuscript was written with AI. All data were acquired and processed in Imperial units and converted to SI units at the end of the analysis for presentation only.

Basal Area Increment

We calculated basal area from diameter in Imperial units at standard height (DSH–1.38m above ground) for each individual tree in the plot according to:

$$Basal\ Area = (DSH^2 \times 0.005454) \times Tree\ Expansion\ Factor, \quad \text{(Eq. 1.1.)}$$

where the tree expansion factor is the number of trees per acre represented by each plot tree, which is distinct for the different plot sizes within FIA and CFI.

From these values, we calculated annualized basal area increment (BAI) for each individual tree, using the following formula:

$$Annualized\ Basal\ Area\ Increment\ (BAI) = \frac{\Delta\ Basal\ Area}{\Delta\ Time}, \quad \text{(Eq. 1.2.)}$$

where time is the time interval between two consecutive measurements in years. Each individual tree record was processed separately to account for any variation in measurement intervals or plot size, creating annualized values for each tree. BAI values were used as the principal response variable in our analysis.

Species Proportions

We focused our analysis on five common western Washington species, which comprise most species in the two datasets (Table 1.1.): bigleaf maple, Douglas-fir, red alder, western hemlock, and western redcedar. To assess the impact of species presence and density in the stand on growth, we calculated the proportion of basal area for each species as a fraction of the total plot basal area at each measurement period. Plots were not removed from the dataset if they had species other than the five analyzed species, meaning "other" species were included in the total basal area value. We used the plot-level species proportions for the five tested species as a predictor variable in modeling BAI growth for each tracked tree.

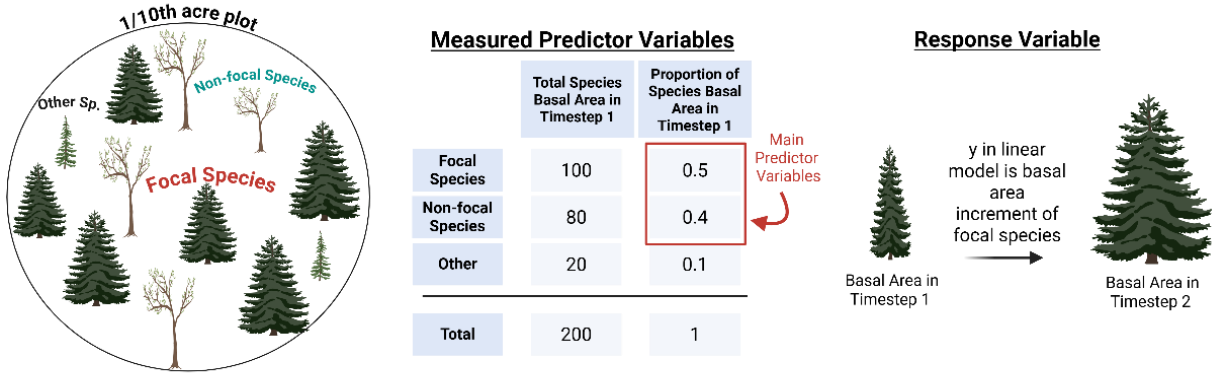

Figure 1.3. Example plot from the CFI dataset showing how predictor and response variables were generated. The proportion of species basal area in any given plot was used to understand the marginal effects of species on individual tree growth, as measured in basal area increment. For each of the five species, we rotated through which species we considered the focal species and which species we considered the non-focal species to make all possible combinations of interspecific models, as well as a focal species only model (intraspecific).

Prior to statistical analysis and after plot-level calculations of total basal area and species proportion, we filtered both the CFI and FIA individual tree records to include only trees with positive BAI growth values, with the thought that negative values were due to inconsistent or

irregular measurements. We used the FIA dataset to benchmark reasonable growth values for the CFI dataset, which resulted in BAI values between 0 and 0.23 m^2y^{-1} (final FIA n=35,491; final CFI n = 18,032). When one of the five species BAI was the response variable for the statistical analysis, that species was termed the focal species, and the other four species were considered non-focal species, irrespective of the basal area proportions in the plot (Figure 1.3.). Prior to fitting a model for each focal species, we filtered the dataset to only include plots where that species was present.

Species-Informed Linear Growth Models

To identify the role of species basal area proportion on growth of the five species, we used an adapted and simplified non-recursive version of the Wykoff diameter growth model, used as the conceptual foundation for the USFS Forest Vegetation Simulator (FVS), based on Diaz (2023). The Wykoff model uses three main components to model tree diameter growth: static site conditions, the size of the subject tree, and competition. We further simplified the Wykoff model to estimate the natural log of BAI instead of the change of squared inside-bark diameter. We added species effect as a fourth component to this model, expressed through the species basal area proportion in the plot. Species effect was the main term of interest when evaluating model performance and species interactions. We added random effects to the model to account for repeat measurements and variation in growth across measurement years as a result of climatic, weather-related or other causes. We used the following linear equation:

$$ln\,(BAI\ of\ focal\ species)\ = Size_t + Site + Comp_t + Species + Random\ Effects$$

Where:

$$Size_t = ln(DSH) + (DSH^2);$$

$$Site = \ ln(site\ index)\ + slope + elevation;$$

$$Comp_t = \frac{BA\ of\ the\ larger\ trees}{ln(DBH + 1)}\ +\ Total\ BA;$$

$$Species = proportion\ basal\ area\ of\ non\ focal\ species;$$

$$Random\ Effects = \ (1|year)\ +\ (1|plot{:}\,tree), \qquad \text{(Eq. 1.3.)}$$

For each of the five species tested, we ran a separate statistical analysis. This model was further evaluated using a variance inflation factor (VIF), which is a measure of the amount of multicollinearity in the model. Terms with a VIF greater than 10 were removed from species-specific analyses. This resulted in most models generated with the CFI dataset having a simplified competition term of total BA only (see supplemental material for exact equations of all models generated). For the FIA dataset, plots selected had no more than two measurements throughout the dataset history, resulting in only one growth increment value for each tree in each plot, so random effects for the FIA analysis were adjusted from what is shown above to (1|year:plot) in R to account for lack of repeat tree growth increment measurements.

Focal species growth in terms of BAI was assessed by estimating four different models, each with a different species basal area proportion term representing the four non-focal species. Interaction effects for all focal and non-focal species pairs were also tested separately. If a significant interaction existed between focal and non-focal species basal area proportions, that model was prioritized over one without an interaction term because growth response could not be explained by a single species' basal area proportion alone; both proportions were required to

interpret the response. In addition, we tested the role of intraspecific growth by building a model with a basal area proportion term for the focal species itself. This process was repeated five times for each species, so that each species had five final models for comparison: four models with four different non-focal species effects and an intraspecific model with a focal species (same species) effect.

Predictions for beneficial proportions

For species pairings that lacked significant interactions between focal and non-focal species basal area proportions, we used the devtools package in R to predict overall species effects on growth, holding all other variables in the model constant (Wickham et al., 2026). For models with significant interaction effects between basal area proportions of focal and non-focal species, we used the effects package in R, to create predictions for growth across a range of values, holding all other model parameters constant (Fox, 2003; Fox and Weisberg, 2019). Using the linear model equations and model coefficients, threshold values were identified for when species proportions benefit or reduce focal species growth in interactive relationships. For species pairs that demonstrated a positive bilateral growth response within the FIA dataset, implications for total yield at the plot level were calculated by comparing (1) predicted basal area increment from a model without the species effect term to (2) the predicted basal area increment from a model with a species effect term. Predictions were summed for each individual focal species tree in the plot to estimate total plot yield for the focal species and the relative importance of the species effect term on total plot yield.

1.3 RESULTS

Species Growth Effects

All focal species showed a significant decrease in individual tree basal area growth with an increase in proportion of the focal species itself, indicating high intraspecific competition across all five species (Figure 1.4.). Model results for the species term for all pairings are presented in Table 1.2., with all coefficients and fits reported in the supplementary materials (Table S1.5 and S1.6). For the 10 tested intraspecific (same species) models across the two datasets, 80% produced a significant species effect, all of which were negative in terms of focal species growth, and results were dispersed across the five species. Five of these significant effects resulted in p values that were less than 0.001.

Table 1.2. Model results for the species effect terms for all species pairs. Full model results are available in the supplementary materials. For models with significant interactions, the direction of the effect is reported conditionally rather than as a single coefficient. Breakdown of repeated measurements are shown in the right most columns, with "total *n*", signifying the number of individual tree measurements. Abbreviations: bigleaf maple (BM), Douglas-fir (DF), red alder (RA), western hemlock (WH), and western redcedar (WRC).

Dataset	Focal Species	Non-focal Species	Species Effect Coefficient	*p*-value	R^2	# Unique Trees	# Unique Plots	Total *n*
CFI	BM	BM	-0.66	0.05	0.85	340	92	523
FIA	BM	BM	-0.22	0.65	0.50	509	86	513
CFI	BM	DF	Positive DF effect if BM proportion < 0.1*	<0.01	0.83	319	85	478
FIA	BM	DF	-0.16	0.72	0.48	462	81	466
CFI	BM	RA	0.13	0.65	0.89	219	56	335
FIA	BM	RA	0.22	0.75	0.44	393	54	397
CFI	BM	WH	0.39	0.42	0.84	156	50	273
FIA	BM	WH	-0.76	0.42	0.54	234	53	238
CFI	BM	WRC	-0.08	0.91	0.88	77	27	120
FIA	BM	WRC	1.86	0.30	0.65	152	35	153
CFI	DF	BM	0.19	0.43	0.90	1251	101	1861
FIA	DF	BM	0.63	0.04	0.55	1478	86	1558
CFI	DF	DF	-0.38	<0.01	0.85	6013	345	11486
FIA	DF	DF	-0.3	<0.01	0.56	16755	1016	17916
CFI	DF	RA	Negative RA effect*	0.03	0.90	2833	192	4905
FIA	DF	RA	0.13	0.56	0.53	3107	200	3348
CFI	DF	WH	Positive WH effect if DF proportion < 0.5*	<0.01	0.87	2936	185	5397
FIA	DF	WH	0.4	<0.01	0.60	8378	495	8946

CFI	DF	WRC	Positive WRC effect if DF proportion > 0.3*	0.01	0.88	1254	88	2562
FIA	DF	WRC	-0.22	0.28	0.60	4634	315	4870
FIA	RA	BM	0.64	0.15	0.54	251	49	262
CFI	RA	BM	Positive BM effect if RA proportion < 0.5*	<0.01	0.77	354	58	496
FIA	RA	DF	0.06	0.75	0.56	1064	178	1113
CFI	RA	DF	0.13	0.08	0.66	1366	173	2228
FIA	RA	RA	-0.53	0.02	0.55	1306	205	1355
CFI	RA	RA	-0.3	<0.01	0.65	1642	186	2669
FIA	RA	WH	0.48	0.03	0.53	1037	154	1084
CFI	RA	WH	0.12	0.61	0.70	751	106	1164
FIA	RA	WRC	0.46	0.58	0.53	445	76	478
CFI	RA	WRC	0.59	0.07	0.74	288	57	424
FIA	WH	BM	0.54	0.30	0.42	291	56	295
CFI	WH	BM	-0.51	0.29	0.93	325	57	564
FIA	WH	DF	Positive DF effect if WH proportion < 0.4*	0.02	0.48	5894	487	6113
CFI	WH	DF	Negative DF effect*	0.01	0.89	788	167	1564
FIA	WH	RA	0.11	0.58	0.47	2163	173	2365
CFI	WH	RA	Positive RA effect if WH proportion < 0.1*	0.04	0.94	504	108	834
FIA	WH	WH	-0.13	0.14	0.45	7463	566	7937
CFI	WH	WH	-0.6	<0.001	0.89	800	173	1594
FIA	WH	WRC	0	0.99	0.43	4385	283	4574
CFI	WH	WRC	Positive WRC effect if WH proportion > 0.2*	0.04	0.92	418	67	852
FIA	WRC	BM	1.3	0.03	0.49	212	39	222
CFI	WRC	BM	Positive BM effect if WRC proportion < 0.09*	<0.001	0.83	172	30	322
FIA	WRC	DF	0.6	<0.001	0.53	2384	307	2439
CFI	WRC	DF	0.35	<0.001	0.88	443	82	939
FIA	WRC	RA	-0.56	0.24	0.53	420	86	434
CFI	WRC	RA	-0.02	0.96	0.85	342	57	566
FIA	WRC	WH	-0.4	0.02	0.49	2066	276	2103
CFI	WRC	WH	-0.21	0.49	0.87	360	64	778
FIA	WRC	WRC	-0.65	<0.001	0.50	2730	349	2796
CFI	WRC	WRC	-0.5	<0.001	0.87	478	87	1001

*These models had a significant interaction between the focal species basal area proportion and the non-focal species basal area proportion, so growth impact depends on the ratios of the two species in the plot.

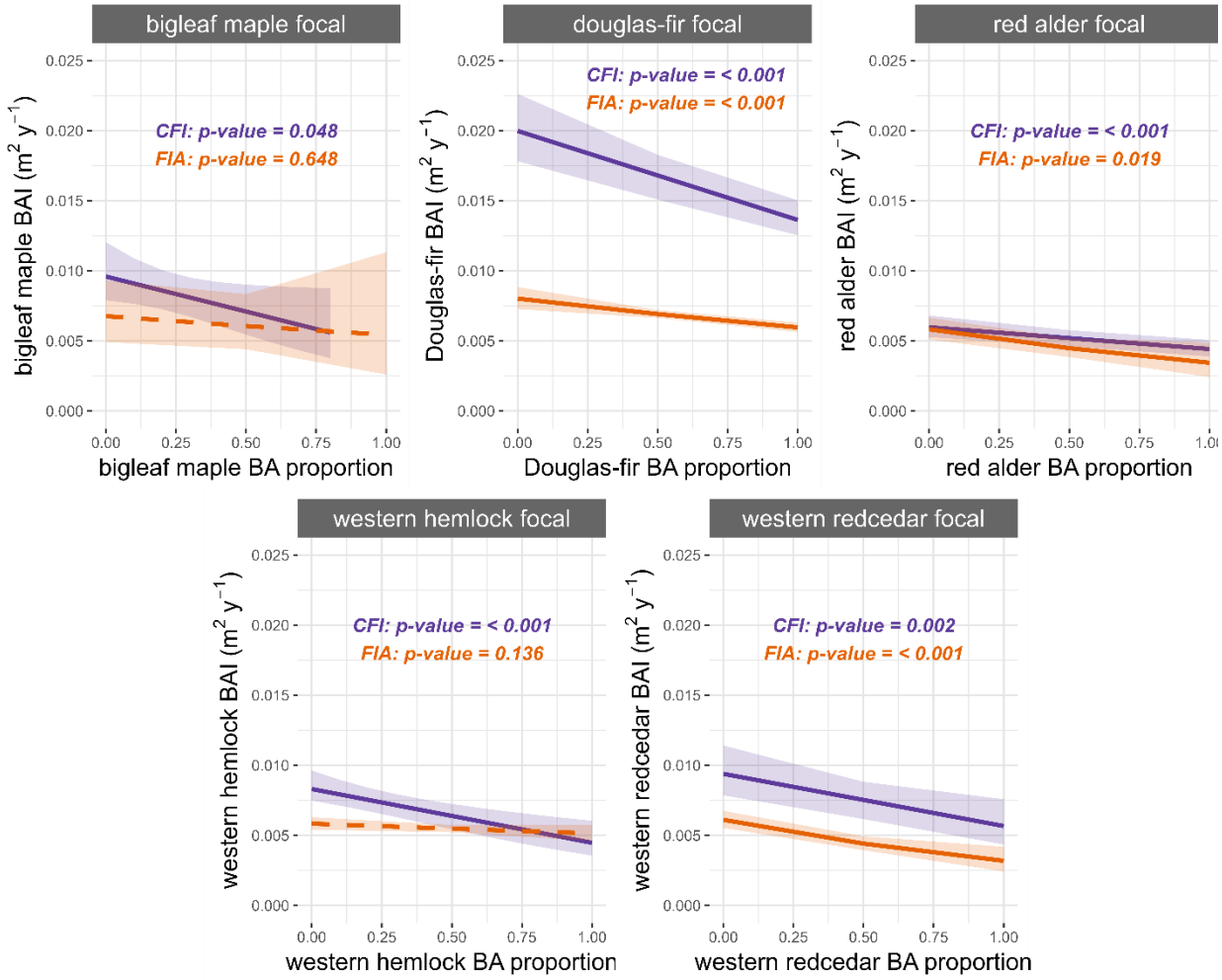

Figure 1.4. Intraspecific growth response for each of the five tested species and when all other model parameters are held constant. In each species, the negative slopes indicate the presence of intraspecific competition. Solid lines represent a significant effect ($p < 0.05$), dashed lines represent a non-significant effect.

Of the 40 tested interspecific relationships, 17 species effects were significant. Three of the significant relationships had a negative growth effect: (1) Douglas-fir focal and red alder non-focal, (2) western hemlock focal and Douglas-fir non-focal, and (3) western redcedar focal and western hemlock non-focal. However, western hemlock focal and Douglas-fir non-focal pairing was a significant positive relationship in the FIA dataset, reducing the strength of this result. All other significant relationships between two different species resulted in positive effects on growth rates, indicating a pattern of interspecific facilitation. The following pairings showed

evidence for significantly positive and bilateral growth effects (positive slopes) for both species in the pair under specific species proportions: (1) Douglas-fir and bigleaf maple; (2) Douglas-fir and western redcedar; and (3) red alder and western hemlock (Figure 1.5.). Other relationships may be complementary but lacked significance for both species. For example, both datasets provided evidence that bigleaf maple may benefit western redcedar growth, but results were inconclusive for the effect of western redcedar growth on bigleaf maple.

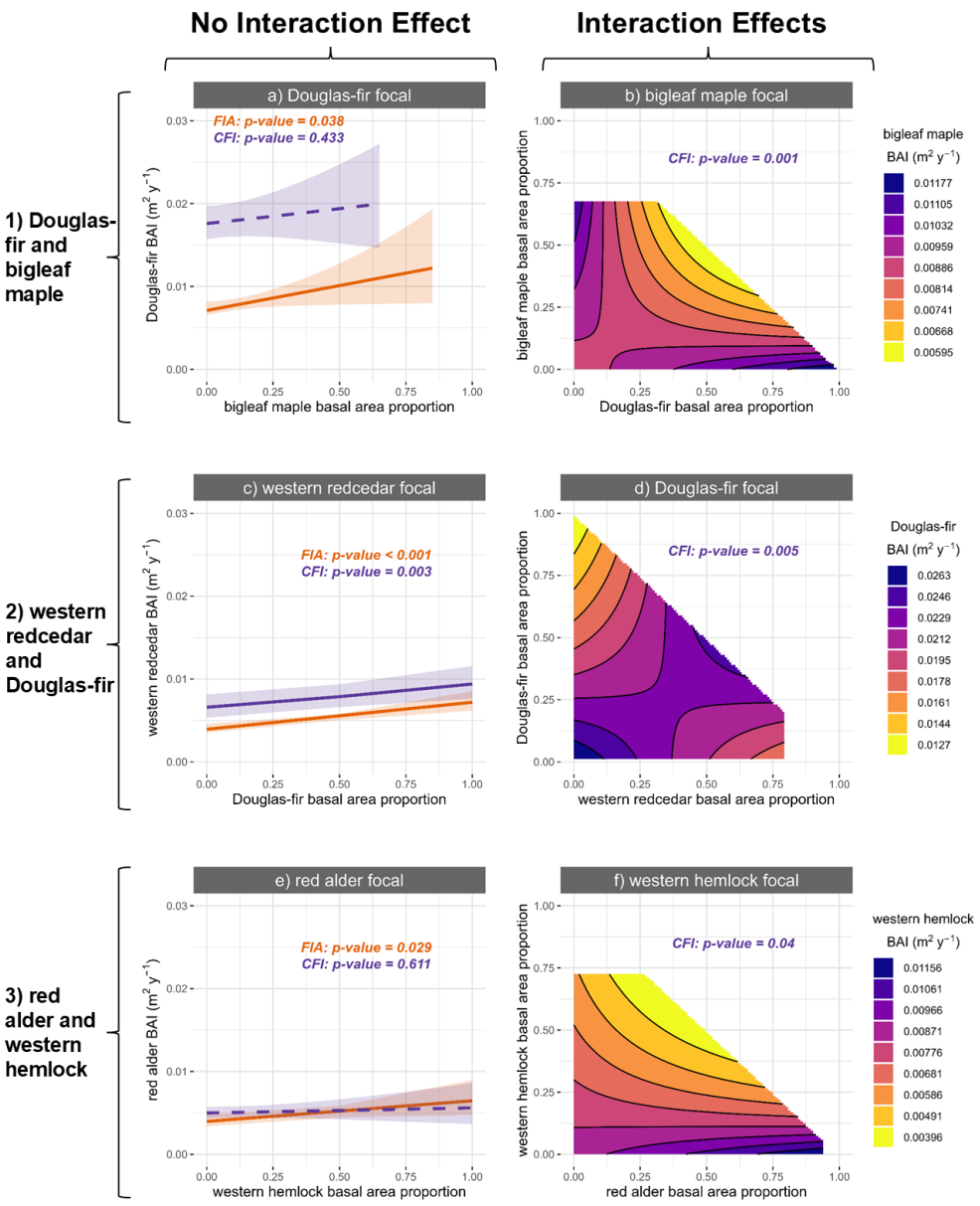

Figure 1.5. Basal area increment model relationships for the three species pairs with significantly positive bilateral growth responses depending on species proportions: (1) Douglas-fir and bigleaf maple; (2) Douglas-fir and western redcedar; (3) red alder and western hemlock. Interaction plots (1b, 2d, 3f) are shown when the interaction between the focal species basal area proportion and the non-focal species basal area proportion was significant in the linear model, indicating that just one species proportion effect on growth would create an incomplete prediction. Contour lines denote changes in growth response to different species proportions in m^2y^{-1}. All predictions are produced by holding all other model variables constant and predicting for only the available basal area plot proportions in the datasets. Solid lines represent a significant effect ($p < 0.05$), dashed lines represent a non-significant effect.

For mutually beneficial species pairs in the FIA dataset, we quantified the relative impact of species effect on total yield by finding the difference in predicted focal species BAI for an entire plot using a model with and without the species effect term. For all pairs, the addition of the species effect term resulted in very minor improvements in BAI, if at all: under 0.34% of average total focal species BAI growth for all tested models. This result indicates that although positively associated species pairs for maximizing individual tree growth exist, total plot yield is still largely driven by the cumulative effects of other growth determinants in the model formation, such as site conditions, tree size, and plot density.

Interaction Models

For certain models, the focal species growth depended on both the focal species and non-focal species proportion as identified through a significant interaction between the basal area proportion of each in the linear model. Many of these interactions contained a threshold at which certain basal area ratios would tip the balance of the relationship from negative to positive. Threshold values were highly variable indicating inconsistent interspecific effects across the species (Table 1.2.).

In some cases, a threshold value was detected between two species in one dataset but not the other. For example, the CFI western hemlock focal species and Douglas-fir non-focal species model indicated that for all ratios of the two species, there is a negative effect on western hemlock growth. In contrast, the FIA dataset suggests Douglas-fir positively influences western hemlock growth if western hemlock basal area is below 40%. When considering Douglas-fir as the focal species, a similar threshold exists in the CFI dataset (when <50% BA of the plot is Douglas-fir, then the effect of western hemlock on Douglas-fir is positive) but not in the FIA dataset (when at all ratios the effect of western hemlock on Douglas-fir is positive). Holistically,

these results may indicate the mixing benefit for Douglas-fir and western hemlock can be lost if the plot is too dominated by either species, though conflicting results on species response between the two datasets reduce the strength of the findings.

Wykoff model performance for CFI and FIA

Model performance for the modified Wykoff model fit CFI data better (training R^2 values = 0.65–0.94) than FIA data (training R^2 values = 0.42–0.70) (reported in Table S1.5 and S1.6). When focusing on the effects of the species proportion term, CFI and FIA showed good agreement in directionality of species effects on growth except for conflicting results for western hemlock focal species and Douglas-fir non-focal. Threshold values in the significant interactions complicate definitive conclusions across the two datasets because the relationship is no longer a binary positive or negative, and overall, indicate highly variable interspecific interactions and consistently negative intraspecific interactions.

1.4 Discussion

What is the role of intraspecific competition versus interspecific competition on tree growth across species pairings and stand densities?

Intraspecific competition was negative and observed as statistically significant more often than interspecific competition, matching previously identified trends in terrestrial plant communities (Adler et al., 2018; Pretzsch, 2022; Reineke, 1933). These intraspecific patterns were also consistent with prior research on Pacific Northwest tree species, which has reported stronger intraspecific competition in some species, especially Douglas-fir (Table 1.3.) (Amoroso and Turnblom, 2006; Slesak et al., 2025; Wierman and Oliver, 1979), the primary timber species in the Pacific Northwest. Fang et al. (2019) reported that competitive effects of red alder were lower than the effects of a mix of Douglas-fir and western redcedar competition on Douglas-fir

growth. Amoroso and Turnblom (2006) observed interspecific release (improved growth) in Douglas-fir and western hemlock mixtures compared to monocultures. As noted in Slesak et al. (2025), these results were not surprising, as robust competitive ability gives Douglas-fir an advantage, making it a clear choice for production systems. Similarly, past studies have found red alder intraspecific pressure to be higher than interspecific competition between red alder and western redcedar, or between red alder and Douglas-fir (HSC, 2017; Radosevich et al., 2006; Shainsky and Radosevich, 1992). There is also evidence of intraspecific competition for limited resources in western redcedar-dominated stands; this competition can be reduced through fertilizer applications and thinning (Devine and Harrington, 2009). This study and others suggest that reducing intraspecific pressure through species mixing may help maximize individual tree growth, though this should not be equated to overall increases in stand yield, because monocultures of primary timber species still often outperform mixtures in volume production (Slesak et al., 2025).

In contrast to the consistent negative intraspecific effects, interspecific relationships were variable in the growth effects for focal species. Several positive interspecific relationships were observed, but threshold values in the interaction space point to specific—and sometimes very small—windows for complementarity. When interspecific relationships were positive for each species in a pair, the addition of the species-effect term resulted in marginal if any improvement in overall plot yield. Although we observed statistically significant species effects, these effects do not result in meaningful changes to plot-level growth; other model effects (site, size, competition) cumulatively determine most stand level growth outcomes. Because our model structure measures individual tree responses, we cannot infer whether or not these results indicate overyielding. Mixed-species forests can in some cases increase the carrying capacity of

a site (Heiderman and Kimsey, 2023). Therefore, future work should adjust model formation from the individual-tree level to the plot level to further explore overyielding possibilities with positively associated species pairs.

Where interspecific interactions with growth are observed, are they positive or negative, and do they show potential for complementarity or competitive exclusion?

Three species pairings showed evidence for complementarity with positive growth for both species in the pair. All three of the pairs (1. Douglas-fir and bigleaf maple; 2. Douglas-fir and western redcedar; 3. red alder and western hemlock) align along functional-trait space, balancing a shade-intolerant species (Douglas-fir or red alder) with a more shade-tolerant species (western hemlock, western redcedar, and bigleaf maple). The opportunity for species layering, with a shade-intolerant species in the upper canopy and the shade tolerant species capturing diffuse light conditions below, may explain why these pairings are successful (Kelty, 1992). Differing crown architecture of these species may further allow for resource sharing and growth optimization. For example, for the combination of Douglas-fir and western redcedar, rapid Douglas-fir growth promotes occupation of the upper canopy, while western redcedar shade tolerance allows for longevity of lower branches in low light conditions in the lower canopy—albeit at the expense of western redcedar timber quality (Devine and Harrington, 2009). Additionally, Douglas-fir lower branches may be naturally pruned by the presence of the shade-tolerant western redcedar (Tappeiner, 2015; Wierman and Oliver, 1979).

Conversely, in terms of crown architecture, Douglas-fir and bigleaf maple are a surprising complementary pair in that forest managers often seek to remove bigleaf maple from production stands because broad canopies of individual bigleaf maple can occupy a disproportionately larger growing space (Knowe et al., 1995), contributing to a blanket preference for monoculture and

competition control. This pairing may better be explained by differing leaf phenology, which may allow for temporally staggered resource use throughout the year, and increased nutrient availability through leaf drop (Krishna and Chandra Garkoti, 2022; Richards et al., 2010). Deciduous tree leaf drop can return almost double the amount of nutrients to the soil as evergreen forests (Bigger, 1988), creating a larger pool of nutrients for evergreen species plus an absence from light competition in the deciduous leafless period (Kelty, 1992). Bigleaf maple may cause an increase in soil fertility through higher cation exchange capacity, higher nitrogen concentrations, and higher exchangeable potassium, calcium and magnesium (Turk et al., 2008) as well as faster turnover rates for forest floor biomass (Fried et al., 1990). Bigleaf maple may moderately improve water availability via throughfall and stemflow, which may increase with high precipitation (Hamdan and Margaret Schmidt, 2012). Improved soil fertility may also help explain the observed benefit of bigleaf maple on the growth of western redcedar in our results.

Belowground stratification of resources allows for another possible explanation for the positively associated pair of Douglas-fir and western redcedar, aligning with the complementarity hypothesis. The evergreen pair have differing belowground root environments with Douglas-fir having a larger root spread, larger diameter roots, and smaller root taper than western redcedar (Eis, 1974). Douglas-fir can also develop a deep-reaching taproot, which decreases vulnerability to drought (Leuschner and Meinzer, 2024) and may help vertical diversification of soil space. Hydraulic redistribution of water from deeper soil layers (Brooks et al., 2002) may be one of many mechanisms for higher drought tolerance in mixed-species forests, yet drought stress reduction is variable across mixtures (Forrester et al., 2016).

However, the laborious nature of studying the belowground environment limits our ability to clarify belowground interactions and their connections with aboveground mixed-species

dynamics. For example, intermingling root systems may also provide benefits through signaling (Wang et al., 2021) that aids with plant defenses (Erb et al., 2009). Fine root productivity can be higher in mixed stands, yet this need not be connected to aboveground yield (Brassard et al., 2011). Increased root length density in nutrient-rich soil layers in mixed-species stands suggest higher resource-use efficiency, but mixtures supported on average less fine-root biomass (Wambsganss et al., 2021). Facilitation, the improvement of a species growth or survival by its neighboring species, can occur through the presence of N_2-fixing trees that increase pools of soil nitrogen and organic matter, leading to higher water and nutrient holding capacity, although the benefits of N_2-fixation on overall yield depend on site quality (Binkley, 2003; Courbaud et al., 2015). Notably, soil space use can be asymmetric with aboveground biomass, in which certain species are underrepresented in the belowground space yet dominate aboveground light use (Rewald and Leuschner, 2009). Additional investigation of the belowground environment to achieve better understanding of species-specific partitioning of resources is needed.

The negative interspecific interactions we identified may partly be explained by similar light resource requirements, resulting in a lack of aboveground resource partitioning (Collet et al., 2014). Chen et al. (2003) reported that western hemlock and western redcedar mixtures lacked stratification in the vertical canopy space, which led to comparable volume output to monocultures. In their study, western hemlock grew faster than western redcedar, leading to overall less volume in the mixture than the western hemlock monoculture (Chen et al., 2003). This aligns with the directionality of the relationship in our study, with western hemlock as the dominant species of the two: western hemlock had a negative effect on western redcedar but not necessarily the other way around (Table 1.2.). Belowground, these two species have overlapping and intermingling root systems leading to intense competition for available soil resources (Wang

et al., 2002). Overlapping functional ecology (canopy architecture and root systems) may be creating niche similarity in this pairing that prevents coexistence (Blackstone et al., 2025).

The remaining significant interspecific relationships (Douglas-fir and western hemlock; Douglas-fir and red alder; red alder and bigleaf maple) lack clear complementarity or competitive exclusion explanations. This finding is consistent with experimental trials designed to systematically test mixed-species relationships showing inconsistent patterns, with slim margins for overyielding (Kelty, 1992). Our results for western hemlock growth when paired with Douglas-fir differed between the FIA and CFI datasets, although this accurately reflects the experimental literature (Table 1.3.) in which this pair varies for western hemlock and is consistently positive for Douglas-fir (Wierman and Oliver, 1979). Amoroso and Turnblom (2006) documented a decline in western hemlock growth in a mixture with Douglas-fir, yet the reduction in intraspecific competition for Douglas-fir, with the added volume of western hemlock, led to overyielding under high stocking conditions.

Another variable pair was identified with the CFI dataset: increasing red alder basal area proportion was significantly associated with reduced Douglas-fir growth, while there were no significant responses for red alder in the pair for either dataset. Many previous studies have found this pairing to be potentially beneficial to both species and particularly to Douglas-fir, although results are inconsistent (Binkley, 2003; Cortini and Comeau, 2008; Eskelson and Huberman, 2023; Fang et al., 2019; Radosevich et al., 2006; Shainsky and Radosevich, 1992; Table 1.3.). The benefit of red alder to Douglas-fir depends on timing of establishment as rapid juvenile growth of red alder will overtop Douglas-fir and reduce Douglas-fir growth on many sites (Kelty, 1992). Benefits of red alder growth are more often found on low-productivity sites (especially with a history of intense wildfire), where nitrogen fixation can increase available

resources (Binkley, 2003). Our results from the CFI dataset may also be influenced by the fact that these data are collected in a working forest where Douglas-fir is the primary production species. In stands where red alder is dominant, Douglas-fir has not been prioritized for production for a variety of reasons, such as if soils are seasonally hydric, and confounding factors may be contributing to the lower growth of Douglas-fir. Red alder may also be present in low numbers in highly productive Douglas-fir stands that were thinned to extend rotations, occupying growing space between older thinned trees, which would contribute to low red alder numbers being associated with higher Douglas-fir growth. Considering these nuances, negative interspecific relationships are unsurprising for our study results, regardless of the observed complementarity of the pair in the literature (Binkley, 2003; Miller and Murray, 1978).

Table 1.3. Literature review of previous studies of the five focal species as mixtures compared to this study. Experimental outcomes of other studies were assessed as to whether the pairing benefitted the growth each species. ✓ = growth benefit observed in this study; ✗ = no growth benefit observed in this study; ? = inconclusive; * = benefit depends on basal area proportions.

Species Pair	Growth Benefit in This Study	Findings from the Literature
Douglas-fir - - - - - western hemlock	✓	**Yes:** higher densities resulted in stratification of resources (Amoroso & Turnblom, 2006) **Yes:** mixed-species stands can replicate thinning treatments due to resource efficiency (Carsky, 2019) **Yes:** mixtures had greater yield (Erickson et al., 2009; Slesak et al., 2025) (same study site) **Yes:** mixtures had greater yield (Wierman and Oliver, 1979)
	?	**No:** lower overall yield but better diameter growth in mixtures (Amoroso & Turnblom, 2006) **Yes:** improved basal area growth (Carsky, 2019) Neutral compared to monocultures (Erickson et al., 2009; Slesak et al., 2025) (same study site) **No:** Douglas-fir suppressed hemlock growth (Wierman and Oliver, 1979)
Douglas-fir - - - - - red alder	✗	**Yes:** red alder improved growth on poor site after 72 years (Binkley, 2003; Miller and Murray, 1978) (same study site) **Yes**: red alder improved growth of Douglas-fir even decades after red alder died out (Bormann et al., 2023)

Species Pair	Growth Benefit in This Study	Findings from the Literature
		Yes: low alder densities (200–300 alders/ha) benefitted Douglas-fir (Cortini and Comeau, 2008; Eskelson and Huberman, 2023) (same study site) **Yes:** best yield with 100 to 200 alder trees/ha (Fang et al., 2019) **Yes:** improved relative land output when red alder was planted five years after Douglas-fir (Radosevich et al., 2006) **Yes:** can help increase relative growth rates at high densities of red alder and Douglas-fir (Shainsky and Radosevich, 1992)
	?	**Yes:** improved relative land output when red alder and Douglas-fir are planted simultaneously (Radosevich et al., 2006) **No:** increasing Douglas-fir had little effect on alder relative growth rate (Shainsky and Radosevich, 1992)
Douglas-fir - - - - - western redcedar	✓*	**No:** at age 14, authors suggest stand was too young to properly explore mixing effects; at age 22 stand volume declined with increasing western redcedar (De Montigny, 2007; Omari et al., 2021) (same study site)
	✓	**No:** authors suggest stand was too young at age 14 and 22 to properly explore mixing effects (De Montigny, 2007; Omari et al., 2021) (same study site)
Douglas-fir - - - - - bigleaf maple	✓	**Yes and No:** higher BAI for Douglas-fir in plots with bigleaf maple compared to plots with Douglas-fir yet negative model coefficients for bigleaf maple presence (Jamrozik, 2016) **No:** proximity to bigleaf maple decreased diameter and height (Knowe et al., 1995)
	✓*	NA
western hemlock - - - - - bigleaf maple	?	**Yes:** higher BAI for western hemlock in plots with bigleaf maple compared to plots with Douglas-fir (Jamrozik, 2016)
	?	NA
western hemlock - - - - - red alder	✓*	**No:** red alder reduced height and diameter compared to monoculture due to overtopping alder (Cole and Newton, 2023) **Yes:** low alder densities (200–300 alders/ha) benefitted western hemlock (Cortini and Comeau, 2008; Eskelson and Huberman, 2023) (same study site)
	✓	**No:** early gains suggested potential overyielding but 14-year measurement suggests better yields with pure alder (Cole and Newton, 2023)
western hemlock - - - - - western redcedar	✓*	**No:** no mixed-species effect was detected (Chen et al., 2003; Collins, 2001) (same study site)
	✗	**No:** no mixed-species effect was detected (Chen et al., 2003; Collins, 2001) (same study site)

Species Pair	Growth Benefit in This Study	Findings from the Literature
western redcedar - - - - - red alder	?	**Yes:** 13 year measurements saw cedar volumes increase with increasing alder proportion; 20 year measurements saw no significant difference in stand volumes but higher values in mixture (Courtin and Harper, 2018; Harper et al., 2023) (same study site) **No:** increasing broadleaf density inhibited growth(Cortini and Comeau, 2008; Eskelson and Huberman, 2023) (same study site) **Yes:** best yield at 100 alder trees/hectare (Fang et al., 2019) **No:** lower DSH and height in mixtures (HSC, 2017)
	?	**Yes and No**: at 13 years relative yield was less in mixtures than monoculture; at 20 years no significant difference in volume, but better growth in mixtures (Courtin and Harper, 2018; Harper et al., 2023) (same study site) **Yes:** relative yield higher for alder in mixtures due to less intraspecific competition (HSC, 2017)

Differences between our results and previously published work from experimental trials may be associated with temporal differences. Experimental trials explore species pairings early in their development, such as stand ages 10–25, and authors may note fluctuations in these relationships over the study period (Cole and Newton, 2023; De Montigny, 2007; Omari et al., 2021). Early inhibition of growth from one species to another, such as bigleaf maple shading early development of Douglas-fir, may contribute to negative growth effects in the short term between conifer and hardwood pairings (Jamrozik, 2016). However, long-term gains in conifer dominance to surpass hardwoods, like red alder or bigleaf maple, can result in higher yields over the long-term once hardwood mortality increases (Binkley, 2003). Benefits of red alder on Douglas-fir growth, attributed to increased mineral soil organic matter and soil nitrogen, can extend well beyond the death of red alder in the stand (Bormann et al., 2023). In some instances, our study may be identifying long-term signals rather than short-term interactions.

Our study can help inform future research on understudied mixed-species pairs. We found positive growth outcomes for both Douglas-fir and western redcedar in that pairing, yet

the literature lacked evidence for this, with one experimental trial established in Vancouver, British Columbia (Canada), needing more growth time to fully explore species mixing (De Montigny, 2007; Omari et al., 2021). In addition, Douglas-fir and bigleaf maple are a potentially positive pairing, but few publications or experimental trials on this pairing exist. Our study found better growth of red alder with high proportions of bigleaf maple ($p < 0.001$), as well as better growth of western redcedar when grown amid a dominant maple stand ($p = 0.03$). Less commonly grown species combinations in production systems may increasingly become important under a high-emission climate change scenario if keeping more diverse forest stands leads to meaningful risk reduction through increased adaptability (Puettmann, 2011). Additive and/or replacement trials with novel species pairs would provide greater insight into their potential and inform management options.

Management implications and opportunities for future research

This study discovered varying basal area proportions of species pairs with positive growth responses, which can inform management decisions for landowners interested in mixed-forest stands. Landowner objectives determine suitability for mixed-species pairings, with stand-level production volume still likely higher for monoculture Douglas-fir forests than mixed-species forests (Slesak et al., 2025). However, our results highlight avenues for improved individual tree growth in mixtures. For Douglas-fir and western redcedar, our results indicate that at least 30% basal area in Douglas-fir is needed for this pairing to maximize individual tree growth responses. For Douglas-fir and western hemlock, despite our conflicting results between our two datasets regarding western hemlock growth, this pair benefitted Douglas-fir growth, consistent with the literature (Amoroso and Turnblom, 2006; Wierman and Oliver, 1979). If managers are most interested in Douglas-fir growth and willing to accept poorer western hemlock production, a 50:50

BA mixture may optimize Douglas-fir growth and minimize reductions in western hemlock growth. The other positively associated species combinations (Douglas-fir and bigleaf maple; red alder and western hemlock) have small windows for complementarity and can be facilitated through minor changes in management. Managers should consider leaving low numbers of bigleaf maple in Douglas-fir stands, rather than systematically removing it in the thinning stage, though this practice may be best suited for landowners not primarily motivated by commercial timber utilization or financial returns from timber harvesting. Managers can increase bigleaf maple proportions in areas with laminated root rot (*Coniferiporia sulphurascens*), as bigleaf maple is resistant and may provide a barrier for root-to-root transmission, thereby potentially reducing Douglas-fir mortality. Western hemlock can be added opportunistically in the understory of red alder to improve use of vertical growing space.

Table 1.4. Basal area proportions for species pairs that warrant further investigation, where pairings and proportions could lead to improved individual tree growth. Note: Douglas-fir and western hemlock pairing produced conflicting results in this study for western hemlock response but consistent positive effects for Douglas-fir growth.

Pairings with Significant and Positive Growth Responses	Growth Maximizing Proportions
Douglas-fir and bigleaf maple	90% BA in DF, 10% or less BA in BM
Douglas-fir and western redcedar	At least 30% BA in DF
Douglas-fir and western hemlock	50% or less BA in DF; 40% or less in WH
red alder and western hemlock	90% BA in red alder, 10% or less in WH

1.5 Conclusion

More consistent intraspecific competition was observed than interspecific competition for all species investigated. Variable interspecific relationships provide evidence that individual tree

growth maximization may occur under mixed-species stand conditions, but this effect may be marginal if overall plot-level yield is influenced more by cumulative factors, such as site conditions, tree size, and competition. For species pairs with mutually positive responses, complementarity can be explained by stratification of resource use and depends on basal area proportions within a stand. We identified understudied pairings that can be explored by future research that includes experimental trials. The European triplets network—sets of three plots (two monospecific and one mixed-species stand with both species) located along a productivity gradient across Europe—could be expanded to the Pacific Northwest to help fill research gaps on pairings and create broader conclusions for species pairings (Pretzsch et al., 2019). Researchers should work with forest managers to create guidelines for mixed-species forests that achieve both production goals and co-benefits.

1.6. SUPPLEMENTARY MATERIAL

Table S1.5. Coefficient estimates (p-value) from linear mixed-effects models for the CFI dataset. BM = bigleaf maple; DF = Douglas-fir; RA = red alder; WH = western hemlock; WRC = western redcedar. — indicates term not included in that model.

Focal Sp.	Non-focal Sp.	Intercept	ln(DSH)	DSH²	Total BA	Plot:Tree	Growth Year	Residual	BAL/ln(DSH+1)	Focal Species Coefficient	Non-focal Species Coefficient	Interaction Term (Focal × Non-focal)
BM	BM	-2.254 (0)	0.924 (0)	0.037 (0.524)	-0.221 (0)	0.65 (NA)	0.264 (NA)	0.645 (NA)	—	-0.661 (0.048)	—	—
BM	Base Model	-2.388 (0)	0.871 (0)	0.025 (0.66)	-0.186 (0)	0.656 (NA)	0.273 (NA)	0.644 (NA)	—	—	—	—
BM	DF	-2.339 (0)	0.921 (0)	0.094 (0.393)	-0.238 (0)	0.579 (NA)	0.294 (NA)	0.658 (NA)	—	0.387 (0.425)	0.329 (0.194)	-3.377 (0.001)
BM	RA	-2.256 (0)	0.866 (0)	0.031 (0.607)	-0.324 (0)	0.688 (NA)	0.389 (NA)	0.597 (NA)	—	—	0.13 (0.651)	—
BM	WH	-2.502 (0)	0.797 (0)	0.063 (0.323)	-0.137 (0.039)	0.566 (NA)	0.45 (NA)	0.623 (NA)	—	—	0.39 (0.422)	—
BM	WRC	-2.612 (0)	0.634 (0.001)	0.147 (0.409)	-0.109 (0.302)	0.682 (NA)	0.596 (NA)	0.658 (NA)	—	—	-0.084 (0.915)	—
DF	BM	-1.835 (0)	0.883 (0)	-0.148 (0)	-0.053 (0.262)	0.511 (NA)	0.212 (NA)	0.501 (NA)	-0.422 (0)	—	0.194 (0.433)	—
DF	Base Model	-1.865 (0)	0.82 (0)	-0.171 (0)	-0.155 (0)	0.472 (NA)	0.204 (NA)	0.581 (NA)	-0.466 (0)	—	—	—
DF	DF	-1.532 (0)	0.832 (0)	-0.18 (0)	-0.157 (0)	0.468 (NA)	0.207 (NA)	0.581 (NA)	-0.463 (0)	-0.38 (0)	—	—
DF	RA	-1.436 (0)	0.851 (0)	-0.179 (0)	-0.092 (0.001)	0.51 (NA)	0.158 (NA)	0.515 (NA)	-0.493 (0)	-0.46 (0)	-0.006 (0.968)	-0.646 (0.028)
DF	WH	-1.504 (0)	0.919 (0)	-0.17 (0)	-0.196 (0)	0.53 (NA)	0.441 (NA)	0.584 (NA)	-0.412 (0)	-0.345 (0)	0.847 (0.002)	-1.769 (0)
DF	WRC	-1.189 (0)	0.841 (0)	-0.141 (0)	-0.2 (0)	0.558 (NA)	0.546 (NA)	0.562 (NA)	-0.444 (0)	-0.879 (0)	-0.611 (0.18)	2.479 (0.005)
RA	BM	-2.931 (0)	0.63 (0)	0.092 (0.054)	-0.429 (0)	0.374 (NA)	0.598 (NA)	0.588 (NA)	—	0.15 (0.406)	3.216 (0)	-6.013 (0)
RA	Base Model	-2.883 (0)	0.535 (0)	-0.031 (0.327)	-0.112 (0.02)	0.41 (NA)	0.222 (NA)	0.681 (NA)	-0.193 (0)	—	—	—

Focal Sp.	Non-focal Sp.	Intercept	ln(DSH)	DSH²	Total BA	Plot:Tree	Growth Year	Residual	BAL/ln(DSH+1)	Focal Species Coefficient	Non-focal Species Coefficient	Interaction Term (Focal × Non-focal)
RA	DF	-2.948 (0)	0.586 (0)	-0.126 (0.002)	-0.14 (0.014)	0.401 (NA)	0.186 (NA)	0.678 (NA)	-0.223 (0)	—	0.133 (0.083)	—
RA	RA	-2.74 (0)	0.536 (0)	-0.039 (0.215)	-0.114 (0.017)	0.396 (NA)	0.231 (NA)	0.684 (NA)	-0.236 (0)	-0.3 (0)	—	—
RA	WH	-2.863 (0)	0.642 (0)	-0.011 (0.783)	-0.242 (0.002)	0.41 (NA)	0.247 (NA)	0.667 (NA)	-0.011 (0.879)	—	0.117 (0.611)	—
RA	WRC	-3.001 (0)	0.55 (0)	0.014 (0.805)	-0.219 (0)	0.41 (NA)	0.232 (NA)	0.645 (NA)	—	—	0.594 (0.068)	—
WH	BM	-2.597 (0)	0.933 (0)	0.075 (0.17)	-0.386 (0)	0.645 (NA)	0.199 (NA)	0.473 (NA)	—	—	-0.507 (0.287)	—
WH	Base Model	-2.511 (0)	0.943 (0)	0.044 (0.273)	-0.488 (0)	0.615 (NA)	0.207 (NA)	0.565 (NA)	—	—	—	—
WH	DF	-2.256 (0)	0.974 (0)	0.056 (0.162)	-0.544 (0)	0.604 (NA)	0.232 (NA)	0.563 (NA)	—	-0.314 (0.292)	-0.012 (0.94)	-1.816 (0.008)
WH	RA	-2.319 (0)	1.128 (0)	-0.006 (0.916)	-0.529 (0)	0.647 (NA)	0.19 (NA)	0.451 (NA)	—	-0.68 (0.003)	0.35 (0.19)	-3.087 (0.04)
WH	WH	-2.393 (0)	0.968 (0)	0.062 (0.124)	-0.53 (0)	0.61 (NA)	0.203 (NA)	0.564 (NA)	—	-0.605 (0)	—	—
WH	WRC	-2.522 (0)	1.085 (0)	0.011 (0.824)	-0.483 (0)	0.67 (NA)	0.652 (NA)	0.511 (NA)	—	-0.429 (0.096)	-0.567 (0.137)	3.156 (0.038)
WRC	BM	-2.248 (0)	1.339 (0)	-0.061 (0.283)	-0.558 (0)	0.244 (NA)	0.422 (NA)	0.712 (NA)	—	-0.57 (0.089)	0.989 (0.348)	-10.45 (0.004)
WRC	Base Model	-2.423 (0)	1.168 (0)	-0.028 (0.563)	-0.602 (0)	0.484 (NA)	0.324 (NA)	0.645 (NA)	—	—	—	—
WRC	DF	-2.564 (0)	1.188 (0)	-0.019 (0.697)	-0.589 (0)	0.486 (NA)	0.338 (NA)	0.625 (NA)	—	—	0.354 (0.003)	—
WRC	RA	-2.344 (0)	1.181 (0)	-0.013 (0.807)	-0.594 (0)	0.429 (NA)	0.35 (NA)	0.679 (NA)	—	—	-0.015 (0.963)	—
WRC	WH	-2.437 (0)	1.164 (0)	0.007 (0.885)	-0.597 (0)	0.473 (NA)	0.396 (NA)	0.639 (NA)	—	—	-0.206 (0.487)	—

Focal Sp.	Non-focal Sp.	Intercept	ln(DSH)	DSH²	Total BA	Plot:Tree	Growth Year	Residual	BAL/ln(DSH+1)	Focal Species Coefficient	Non-focal Species Coefficient	Interaction Term (Focal × Non-focal)
WRC	WRC	-2.283 (0)	1.186 (0)	-0.013 (0.791)	-0.567 (0)	0.477 (NA)	0.325 (NA)	0.644 (NA)	—	-0.499 (0.002)	—	—

Table S1.6. Coefficient estimates (p-value) from linear mixed-effects models for the FIA dataset. BM = bigleaf maple; DF = Douglas-fir; RA = red alder; WH = western hemlock; WRC = western redcedar. — indicates term not included in that model.

Focal Sp.	Non-focal Sp.	Intercept	SD (Intercept)	SD (Obs.)	ln(DSH)	DSH²	Total BA	BAL/ln(DSH+1)	Focal Species Coefficient	Non-focal Species Coefficient	Interaction Term (Focal × Non-focal)
BM	BM	-2.619 (0)	0.781 (NA)	0.904 (NA)	0.196 (0.113)	-0.154 (0.07)	0.308 (0.033)	-0.748 (0)	-0.22 (0.648)	—	—
BM	Base Model	-2.675 (0)	0.766 (NA)	0.905 (NA)	0.188 (0.127)	-0.152 (0.073)	0.321 (0.023)	-0.748 (0)	—	—	—
BM	DF	-2.574 (0)	0.752 (NA)	0.924 (NA)	0.145 (0.283)	-0.002 (0.992)	0.316 (0.049)	-0.705 (0)	—	-0.155 (0.72)	—
BM	RA	-2.688 (0)	0.54 (NA)	0.914 (NA)	-0.009 (0.945)	-0.121 (0.188)	0.374 (0.023)	-1.01 (0)	—	0.221 (0.752)	—
BM	WH	-2.635 (0)	0.847 (NA)	0.889 (NA)	0.146 (0.554)	-0.209 (0.107)	0.377 (0.116)	-0.862 (0)	—	-0.759 (0.416)	—
BM	WRC	-2.891 (0)	1.108 (NA)	0.833 (NA)	-0.259 (0.405)	-0.122 (0.535)	0.631 (0.048)	-1.002 (0)	—	1.861 (0.296)	—
DF	BM	-2.574 (0)	0.346 (NA)	0.735 (NA)	0.342 (0)	-0.279 (0)	0.176 (0.007)	-0.699 (0)	—	0.625 (0.038)	—
DF	Base Model	-2.648 (0)	0.492 (NA)	0.749 (NA)	-0.03 (0.034)	-0.218 (0)	0.364 (0)	-0.743 (0)	—	—	—
DF	DF	-2.449 (0)	0.49 (NA)	0.748 (NA)	-0.027 (0.056)	-0.219 (0)	0.347 (0)	-0.741 (0)	-0.297 (0)	—	—
DF	RA	-2.281 (0)	0.458 (NA)	0.745 (NA)	0.504 (0)	-0.303 (0)	-0.001 (0.978)	-0.661 (0)	—	0.131 (0.558)	—
DF	WH	-2.579 (0)	0.475 (NA)	0.728 (NA)	0.252 (0)	-0.272 (0)	0.086 (0.003)	-0.621 (0)	—	0.397 (0.001)	—

Focal Sp.	Non-focal Sp.	Intercept	SD (Intercept)	SD (Obs.)	ln(DSH)	DSH²	Total BA	BAL/ln(DSH+1)	Focal Species Coefficient	Non-focal Species Coefficient	Interaction Term (Focal × Non-focal)
DF	WRC	-2.575 (0)	0.447 (NA)	0.711 (NA)	0.128 (0)	-0.24 (0)	0.209 (0)	-0.67 (0)	—	-0.217 (0.283)	—
RA	BM	-3.076 (0)	0.435 (NA)	0.675 (NA)	-0.117 (0.405)	0.125 (0.145)	-0.064 (0.703)	-0.661 (0)	—	0.642 (0.149)	—
RA	Base Model	-2.885 (0)	0.542 (NA)	0.718 (NA)	-0.03 (0.616)	-0.054 (0.195)	0.047 (0.492)	-0.68 (0)	—	—	—
RA	DF	-2.888 (0)	0.556 (NA)	0.717 (NA)	-0.067 (0.294)	-0.035 (0.428)	0.053 (0.478)	-0.676 (0)	—	0.063 (0.745)	—
RA	RA	-2.768 (0)	0.528 (NA)	0.719 (NA)	-0.026 (0.664)	-0.045 (0.287)	0.037 (0.589)	-0.679 (0)	-0.526 (0.019)	—	—
RA	WH	-3.118 (0)	0.555 (NA)	0.728 (NA)	0.092 (0.235)	-0.091 (0.05)	-0.028 (0.73)	-0.622 (0)	—	0.483 (0.029)	—
RA	WRC	-3.203 (0)	0.656 (NA)	0.738 (NA)	0.18 (0.158)	-0.086 (0.226)	-0.12 (0.369)	-0.534 (0)	—	0.461 (0.576)	—
WH	BM	-2.749 (0)	0.29 (NA)	0.876 (NA)	0.085 (0.485)	-0.135 (0.066)	0.041 (0.731)	-0.692 (0)	—	0.538 (0.304)	—
WH	Base Model	-2.815 (0)	0.399 (NA)	0.848 (NA)	0.04 (0.103)	-0.124 (0)	0.039 (0.138)	-0.635 (0)	—	—	—
WH	DF	-2.95 (0)	0.396 (NA)	0.833 (NA)	0.094 (0.001)	0.07 (0.005)	-0.064 (0.032)	-0.538 (0)	0.162 (0.37)	0.388 (0.008)	-0.998 (0.02)
WH	RA	-2.872 (0)	0.332 (NA)	0.842 (NA)	-0.066 (0.149)	-0.073 (0.017)	0.222 (0)	-0.997 (0)	—	0.111 (0.583)	—
WH	WH	-2.767 (0)	0.399 (NA)	0.848 (NA)	0.04 (0.105)	-0.123 (0)	0.043 (0.104)	-0.637 (0)	-0.126 (0.136)	—	—
WH	WRC	-2.909 (0)	0.358 (NA)	0.855 (NA)	0.07 (0.036)	-0.093 (0)	0.019 (0.572)	-0.55 (0)	—	-0.003 (0.987)	—
WRC	BM	-3.126 (0)	0.336 (NA)	0.841 (NA)	0.145 (0.251)	-0.132 (0.035)	0.062 (0.628)	-0.637 (0)	—	1.298 (0.027)	—
WRC	Base Model	-2.866 (0)	0.464 (NA)	0.804 (NA)	-0.018 (0.632)	-0.062 (0.01)	0.09 (0.02)	-0.662 (0)	—	—	—
WRC	DF	-3.109 (0)	0.445 (NA)	0.774 (NA)	0.037 (0.363)	-0.098 (0.001)	0.014 (0.736)	-0.667 (0)	—	0.595 (0)	—

Focal Sp.	Non-focal Sp.	Intercept	SD (Intercept)	SD (Obs.)	ln(DSH)	DSH²	Total BA	BAL/ln(DSH+1)	Focal Species Coefficient	Non-focal Species Coefficient	Interaction Term (Focal × Non-focal)
WRC	RA	-2.704 (0)	0.545 (NA)	0.867 (NA)	0.234 (0.017)	-0.097 (0.097)	-0.036 (0.754)	-0.649 (0)	—	-0.556 (0.237)	—
WRC	WH	-2.791 (0)	0.453 (NA)	0.833 (NA)	-0.06 (0.199)	-0.039 (0.143)	0.133 (0.003)	-0.671 (0)	—	-0.403 (0.019)	—
WRC	WRC	-2.721 (0)	0.45 (NA)	0.804 (NA)	-0.017 (0.652)	-0.056 (0.019)	0.068 (0.079)	-0.663 (0)	-0.65 (0)	—	—

CHAPTER 2. BROWSE DETERRENTS FOR FOREST REGENERATION IN WESTERN WASHINGTON, USA: A COMPARATIVE STUDY

2.0 ABSTRACT

Tree seedling herbivory by ungulates, such as Columbian black-tailed deer (*Odocoileus hemionus columbianus*) and Roosevelt elk (*Cervus elaphus roosevelti*), creates challenges for forest regeneration, especially when planting high value forage tree species like western redcedar (*Thuja plicata* Donn ex D. Don). Six independent experimental trials exploring browse deterrent techniques in the Pacific Northwest USA reveal relative effectiveness in promoting the growth and survival of two high-value timber species, western redcedar and Douglas-fir (*Pseudotsuga menziesii* (Mirb.) Franco). Trials explore the following treatments: large multi-hectare fenced exclosures, small 0.03- and 0.04-hectare fenced exclosures, co-planting seedlings with Sitka spruce (*Picea sitchensis* (Bong.) Carrière) to act as a physical deterrent, Vexar® tubing, flexible fencing, and the application of the chemical repellent Plantskydd®. Browse deterrents were species specific. For western redcedar, fenced exclosures were most effective at reducing browse, followed by Vexar tubing, co-planting with Sitka spruce, Plantskydd and flexible fencing, in order of effectiveness and impact on timber quality. For Douglas-fir, co-planting with Sitka spruce was more effective than Vexar tubing, and fenced exclosures produced varying results, with the presence of invasive species and robust shrub cover associated with reduced Douglas-fir growth within some fenced exclosures. Plantskydd showed early promising results for western redcedar browse prevention, but challenges with application timing and need for consistent, sustained reapplication reduce utility. Reported costs for deterrent methods indicate large fenced exclosures are the most expensive method to implement, followed by chemical

repellent, Vexar tubing and Sitka spruce co-planting in that order. Managers should consider species, maintenance demands and ability for follow-through when selecting a browse prevention option, noting differences in cost and impact on timber production.

2.1 Introduction

Mammalian herbivores are active components of ecological systems (Woodward et al., 1994). Forest management can both aggravate herbivory forage deficits, through prolonged closed canopy conditions that reduce palatable plants, and ameliorate wildlife forage by creating post-harvest open conditions with many edible options (Leopold et al., 1947). Ungulates affect ecosystem processes (Endress et al., 2016; Woodward et al., 2021), and their presence can have ramifications for long-term forest trajectories through reduced plant community diversity, reduced shrub density (Woodward et al., 1994), and repeat tree recruitment failure (Ramirez et al., 2019; Rooney, 2001). Vegetation responses to ungulate browse can persist for decades (Woodward et al., 1994).

Herbivory, which causes deformity and/or mortality in forest plantations, is a challenge for forest managers (Beguin et al., 2016). In areas where deer and elk lack significant predation and hunting pressure, excessive grazing of certain forage species can cause a fundamental change in the forested systems which deer and elk inhabit, creating a conflict between regeneration objectives and ungulate browse preference (Kay, 2001). Herbivory can cause indirect effects in ecosystems, such as plant compositional changes that alter vertebrate species densities, effects that can be more pronounced on low productivity sites (Larson and Paine, 2007). Managing herbivory to ensure desired tree species composition is critical, especially in mixed-species forest management (Löf et al., 2023) and for forest restoration efforts (Hart et al., 2020).

Complete regeneration failure of western redcedar (*Thuja plicata* Donn ex D. Don) in the Pacific coastal and western Cascade forests is common due to severe and repeated ungulate browse (Stroh et al., 2008). Western redcedar is a preferred food source for the Columbian black-tailed deer (*Odocoileus hemionus columbianus*) and Roosevelt elk (*Cervus elaphus roosevelti*), the most common deer and elk species west of the Cascade Range crest in Washington (Coates et al., 1985; Puettmann et al., 2024). Despite the high timber market value of western redcedar (Antos et al., 2016), planting of this species in post-harvest stands is limited in part due to extreme challenges with browse (LePage and Banner, 2014). A loss of western redcedar has been tied to a lack of natural regeneration, providing a limitation to multi-cohort stand development (Keeton and Franklin, 2005). Western redcedar is especially underrepresented in young forests in the Pacific Northwest, where it is often completely absent (LePage and Banner, 2014), though this depends on land-use history and ownership. Herbivory of western redcedar can reduce radial growth; severe and repetitive defoliation can reduce the ability of trees to produce defense chemicals, thereby increasing palatability of browsed trees and creating a cycle of repeated browse (Vourc'h et al., 2002).

Western redcedar holds value beyond timber production goals. It remains a culturally important species for Pacific Northwest tribal nations (Gunther, 1973) and is a critical component of Pacific Northwest habitat and forest function (Antos et al., 2016). Western redcedar can offer an important species alternative for forest landowners who are managing laminated root rot (*Coniferiporia sulphurascens*) on site since it is more resistant than other species (Goheen and Willhite, 2021). Meanwhile, changing climate regimes may cause accelerated large tree mortality in the western United States (McNellis et al., 2021), putting added pressure on forest regeneration and health. Western redcedar is experiencing anomalously

high mortality and crown dieback in some locations due to increasingly severe summer drought conditions (Andrus et al., 2024). Successful regeneration of this species through proactive planting and protection from browse is essential for maintaining its representation on the landscape and its economic, cultural, and ecological role (LePage and Banner, 2014).

Deer and elk similarly impact Douglas-fir (*Pseudotsuga menziesii* (Mirb.) Franco), the primary timber species in the Pacific Northwest, with animal damage—primarily in the form of browsing—affecting an average of 30 percent of all Douglas-fir trees in Oregon and Washington that lack browse protection (Black et al., 1979), though this estimate needs to be updated. Past work suggests that the cumulative effects of animal damage cost the timber industry hundreds of millions of dollars each year (Brodie, 1979). Early herbivory of Douglas-fir, often in the form of nipping at terminal buds (Crouch, 1968), can lead to multiple leaders or other manifestations of poor growth form, reducing growth (Mitchell, 1964) and timber value (Brodie, 1979). Simulated herbivory through mechanical clipping of Douglas-fir and western redcedar buds leads to reduced diameter growth and less overall volume (Cockle and Ettl, 2010). Although Douglas-fir is not as severely browsed as western redcedar (Nolte, 1998), its premier role in timber production increases the importance of browse reduction.

Multiple browse prevention methods have been implemented—with varying success—to reduce the impact of deer and elk browsing (Campbell and Evans, 1988; Gourley et al., 1990; Kimball et al., 2008). Survival of high-value species in areas with abundant deer and elk often depends on silvicultural interventions such as physical barriers (fencing and tubing) (Vercauteren et al., 2006), larger nursery stock (Puettmann et al., 2024; Takanobu Yagi, 2022), or chemical repellents (Nolte, 1998). Some land managers have used co-planting of tree seedlings with Sitka spruce (*Picea sitchensis* (Bong.) Carrière), where the sharp needles of Sitka spruce are a physical

deterrent for deer and elk (Murray, 2021). This technique involves planting one Sitka spruce with one focal species seedling (often Douglas-fir or western redcedar) in the same hole, using the same stock type for each species (Murray, 2021). Once the focal species has surpassed browse height, usually within 7 to 10 years, the Sitka spruce can be cut out, high enough that the focal species is not at risk of damage from a chainsaw, reducing the competitive effects of the Sitka spruce and increasing resource availability for the focal species (Murray, 2021).

All browse prevention methods have tradeoffs in effectiveness, impact on seedling growth, installation time, cost, and management interventions required (Iijima and Oka, 2023; Puettmann et al., 2024). These tradeoffs vary across the landscape where ungulate migration, ungulate density, and site quality affect herbivory outcomes (Thyroff et al., 2022; Villemaire-Côté et al., 2017). Responses can also be species specific, which complicates outcomes (Endress et al., 2016). Identifying when one technique is better suited than another is challenging but critical for land management decisions.

This study analyzes and synthesizes six independent trials in the Pacific Northwest, Washington, USA that are investigating browse prevention techniques for the high-value timber species Douglas-fir and western redcedar. Trials test the following treatments to determine their effects on seedling browsing, mortality, and long-term timber development: (1) large multi-hectare fenced exclosures, (2) small 0.03-0.04 hectare fenced exclosures, (3) co-planting seedlings with Sitka spruce, (4) Vexar® tubing, (5) flexible fencing, and (6) the application of the chemical repellent Plantskydd®. To our knowledge, this is the first peer-reviewed study to assess the relative success of co-planting seedlings with Sitka spruce (but see Clifton and Smith, 2018), despite its popularity with practitioners in the Pacific Northwest (Murray, 2021; Townsend,

2019). This work aims to answer the following questions to provide forest managers with more tools to combat herbivory pressure:

1. How do browse prevention techniques (fencing, chemical repellent, tubing, co-planting with Sitka spruce) affect the survival and growth of Douglas-fir and western redcedar regeneration?
2. What are the tradeoffs of browse prevention tools when considering ease of installation, maintenance, and cost?
3. Using the results of this study, what impact does browse have on the regeneration and development of diverse forests in the Pacific Northwest?

2.2 Materials and Methods

Study Design

This work examines the effects of browse protection on seedling establishment from six experimental trials based in western Washington (Table 2.1.). Three trials are located within the University of Washington Center for Sustainable Forestry at Pack Forest (Pack Forest) (46.8432N, 122.3176W), a research and demonstration forest located in the western Cascade Range foothills in Pierce County, Washington, USA. Two trials were located at nearby Tree Farms: Port Blakely Tree Farm in Lewis County and Coburg Tree Farm in Pierce County. Lastly, one trial is located near Forks, WA in Clallam County on the Olympic Peninsula on Washington Department of Natural Resources (DNR) land (Figure 2.1.). These six trials were initiated independently, starting in 2011 onward, with varying data collection efforts throughout their duration. Therefore, data available for each trial is distinct and retroactively compiled to create this synthesis.

The regional climate for the area is Mediterranean, characterized by cold, moist winters and dry summers, with periods of drought. Near Pack Forest and the nearby Tree Farms, mean annual temperature is 10.4 C (16 C for May–September), and average annual precipitation is 961 mm (average of 41 mm for May–September) (PRISM Climate Group, Oregon State University, 2026). On the Olympic Peninsula, mean annual temperature is 10.4 C (14.9 C for May–September), and average annual precipitation is 2959 mm (average of 90 mm for May–September) (PRISM Climate Group, Oregon State University, 2026).

Table 2.1. Stand information, management history and data collection information for the six trials included in this study. All trials were conducted independently and compiled for this study. Site class is a measure of how productive a site is for growing trees and is based on the height of dominant and codominant trees at the age of 50, with a lower site class indicating better growing conditions.

	Co-Planting and Tubing Trial in Eatonville	Fencing and Plantskydd Trial on the Olympic Peninsula	Large Fence Trial at Pack Forest	Large Fence and Co-Planting Trial near Riffle Lake	Small Fence and Weeding Trial at Pack Forest	Treatment Strips at Pack Forest
Elevation	472 m	157 m	482 m	450 m	495 m	267 m–519 m
Soil Series	Cinebar (silt loam)	Ilwaco (silt loam)	Scamman (fine, mixed)	Cinebar (silt loam)	Wilkeson (fine-loamy)	Wilkeson (fine-loamy), Scamman (fine, mixed), Barneston (sandy-skeletal)
Site Class	2	3	2–3	2	2	2–3.5
Year Planted	2019	2021	2016	2011	2016	2015
Initial Planting Density	741 TPH	890 TPH	988 TPH	1680 TPH	1,235 TPH	20 trees in each treatment strip; three replicates
Measured Species	Douglas-fir	Douglas-fir	Douglas-fir and western redcedar	western redcedar	Douglas-fir and western redcedar	western redcedar, Sitka spruce
Data Collection Years	2024	2025	2016, 2018, 2024	2011	2019, 2024	2015, 2024
Response Variables in Models	deformity, number of leaders, height, diameter	browse presence, mortality, height, diameter	browse presence, deformity, number of leaders, rotation risk, height, diameter	seedling survival	browse presence, deformity, rotation risk, mortality, height, diameter	browse presence, deformity, rotation risk, mortality, height, diameter

Figure 2.1. Trial site locations in western Washington, USA for all six trials. The following trials were located within the University of Washington Pack Forest: Large Fence Trial, Small Fence and Weeding Trial, and Treatment Strips. Fencing and Plantskydd Trial on the Olympic Peninsula is located on WA Department of Natural Resources (DNR) land. Co-Planting and Tubing Trial is at the Coburg Tree Farm near Eatonville. The Large Fence and Co-Planting Trial is on Port Blakely land near Riffle Lake.

Co-Planting and Tubing Trial in Eatonville

A trial was established to compare effectiveness of mesh tubing and Sitka spruce co-planting protection on Douglas-fir growth at the Coburg Tree Farm, near Eatonville, WA. Douglas-fir seedlings were planted in 2019 at a density of 741 trees per hectare (TPH) (300 trees per acre (TPA)). For one half the unit, Douglas-fir was protected with Vexar tubing, a flexible plastic mesh tubing 10.2 cm wide and 91.5 cm tall, which was secured over the seedling with bamboo stakes, woven into the mesh, ensuring a connection with the ground. For the other half of the trial, Douglas-fir was co-planted with Sitka spruce in the same hole and allowed to grow side-by-side until the Douglas-fir was tall enough to not be browsed, at which point the Sitka spruce was removed, just prior to data collection in 2024 (Figure 2.2.). Co-planted trees were tied together with survey ribbon to ensure proximity of the Sitka spruce to the Douglas-fir. Trials were separated by a forest road.

Figure 2.2. Douglas-fir co-planted with Sitka spruce into the same hole, so Sitka spruce sharp needles act as a physical deterrent to browse.

Data were collected once during the summer of 2024. Circular plots of 0.05 hectare in size were established randomly in both Vexar tubing and co-planting zones. Measurements included presence or absence of stem deformity, number of leaders, risk of tree not reaching timber rotation age (rotation risk), height, and diameter at 1 m. Deformity was measured through the presence or absence of the following characteristics: spike knot, multiple leaders, sweep, lean, or bole damage. To assess severity of deformity, crews assessed the risk that one or more

deformities was severe enough that the tree would die before it reaches commercial timber age, or the age of rotation into a new tree cohort. Referred to as rotation risk, this was measured as a binary yes or no and was subjective based on the data collector's assessment of the severity of the deformities present. Analysis for this trial was performed for Douglas-fir growth only.

Fencing and Plantskydd Trial on Olympic Peninsula

Fencing and Plantskydd Trial is part of an existing randomized-block experiment on the Olympic Peninsula outside of Forks, WA in Clallam County (see Bobsin, 2023), a portion of which was analyzed for this study. The unit received a variable retention harvest in 2018, leaving an average of 20 trees per hectare, and an herbicide application in August 2020, followed by planting from January to April 2021. This trial explored three separate treatments: (1) installation of 2.4 m (8 ft) tall fencing made with galvanized metal attached to fence posts (Figure 2.3.), (2) application of Plantskydd 4 times per year for the first 2 years, and (3) no treatment, open to browse; control. Each treatment area was 20 x 20 m (0.04 hectare). The portion of the trial used in this study was planted with Douglas-fir plugs at 890 TPH (360 TPA). Data were collected on browsing presence (binary yes/no), seedling height, and root collar diameter. Understory naturally regenerated at this site over time with a

Figure 2.3. Fencing installed as part of the Fencing and Plantskydd Trial on the Olympic Peninsula. Fencing was 2.4 m tall and made with galvanized metal.

mixture of graminoids, forbs, shrubs, and ferns. Statistical analysis evaluated Douglas-fir performance for the three treatments.

Large Fence Trial at Pack Forest

The Large Fence Trial at Pack Forest is a 7.8-hectare (19.3-acre) fully fenced stand designed to study how large exclosures impact western redcedar and Douglas-fir growth. The unit was harvested in 2015 with a variable retention harvest, after which a 2.4 m (8 ft) tall fence with a perimeter of ~1135 m, was constructed around most of the unit. Fencing was built with square welded wire mesh and secured with wooden posts. The western and eastern edges of the unit were left unfenced so seedling growth could be compared inside and outside the fence. The unit was planted in 2016 at 988 TPH (400 TPA) with a ratio of 3:1 western redcedar to a mix of Douglas-fir, western white pine and Sitka spruce (data was only collected on western redcedar and Douglas-fir). Seedlings were planted as plug +1 nursery stock. Pre-commercial thinning and mechanical vegetation control of non-commercial species was performed as needed within the fenced unit, determined by whether vegetation overtopped seedlings.

Data were collected across four zones (two inside and two outside the fence) separated by roughly 100 m. Presence of browse damage, height, and diameter at root collar were collected for Douglas-fir and western redcedar in spring of 2016 and summer of 2018. A third round of measurements was collected during the summer of 2024, eight years after planting. This third round of measurements included data on deformity, risk of tree not reaching rotation age (rotation risk), height, and diameter at 1 m. Deformity presence and rotation risk were evaluated in the same way as the Co-Planting and Tubing Trial in Eatonville, see above. Statistical analysis evaluated both Douglas-fir and western redcedar performance.

Large Fence and Co-Planting Trial near Riffle Lake

The Large Fence and Co-Planting Trial was located just south of Riffle Lake in Lewis County, WA, managed by Port Blakely, a private timber company. This trial includes two experiments side-by-side. First, a 10.5-hectare (26-acre) stand planted entirely with western redcedar was fully fenced with an 2.4 m (8 foot) tall fence, built with welded wire mesh and wooden posts. Second, adjacent to this unit, a western redcedar-Sitka spruce co-planting trial across 3.4 hectare (8.5 acres) was installed, where western redcedar and Sitka spruce were planted in the same hole at the same time. Similar to the Co-Planting and Tubing Trial near Eatonville, the intention was that Sitka spruce would act as a physical deterrent to prevent western redcedar browse. For both experiments, seedlings were 1 year old when planted. For the large-fence study, seedling stock type was Styro-15, which were seedlings grown in a Styroblock container with a cavity size of 15 cubic inches. For the co-planting trial, the stock type planted was Styro-6, which has a cavity size of 6 cubic inches. The entire trial had a target planting density of 1,680 TPH (680 TPA). Pre-commercial thinning and vegetation control on non-commercial species was performed as needed within the fenced unit, determined by vegetation overtopping seedlings. Data collected on this experiment were limited, but seedlings were measured for regeneration success just short of a year after planting. Analysis focused on western redcedar survival.

Small Fence and Weeding Trial at Pack Forest

The combination of fencing and weeding was explored through a randomized block design at Pack Forest (Figure 2.4.). This trial was installed in a unit that was harvested in 2016 within four randomly placed clear-cut patches. Each block consisted of four randomly selected treatments: fencing, weeding, weeding and fencing, and no-action control. Weeding was

performed with brush cutters and completed on an as needed basis, determined by whether vegetation overtopped seedlings, in the spring and summer of 2017, 2018, 2019, and 2021. Fencing was 2.4 m (8 ft) tall, built with welded wire mesh and wooden posts. Fencing was secured to the ground or buried to preclude animal entry. Each treatment block was 0.12 hectares with 0.03 hectares per treatments, and to avoid edge effects, treatment units are separated by roughly 3 m within each block.

Even-age patches were planted in 2017 with a mix of western redcedar and Douglas-fir at a density of 1235 TPH (500 TPA) (~37 trees within each treatment unit). Mortality after the first growing season prompted infill planting of western redcedar the following year (2018); Douglas-fir seeded into the study units naturally, making final TPH counts variable across the blocks.

Seedlings were measured in 2019 for species, height, diameter at root collar, and browse presence. Data were collected in the summer of 2024 for three of the replicated blocks (Blocks B, C, and D). Block A was not measured due to a compromised fence and the presence of an active bear den. Measurements in 2024 included deformity presence, number of leaders, risk of tree not reaching rotation age (rotation risk), height, and diameter at 1 m. Deformity and rotation risk were measured consistent with the Co-Planting and Tubing Trial near Eatonville (see above). Measurements and statistical analysis in 2024 included all western redcedar and only Douglas-fir that were clearly planted and not naturally regenerated, identified by larger heights and diameters indicative of a different age cohort.

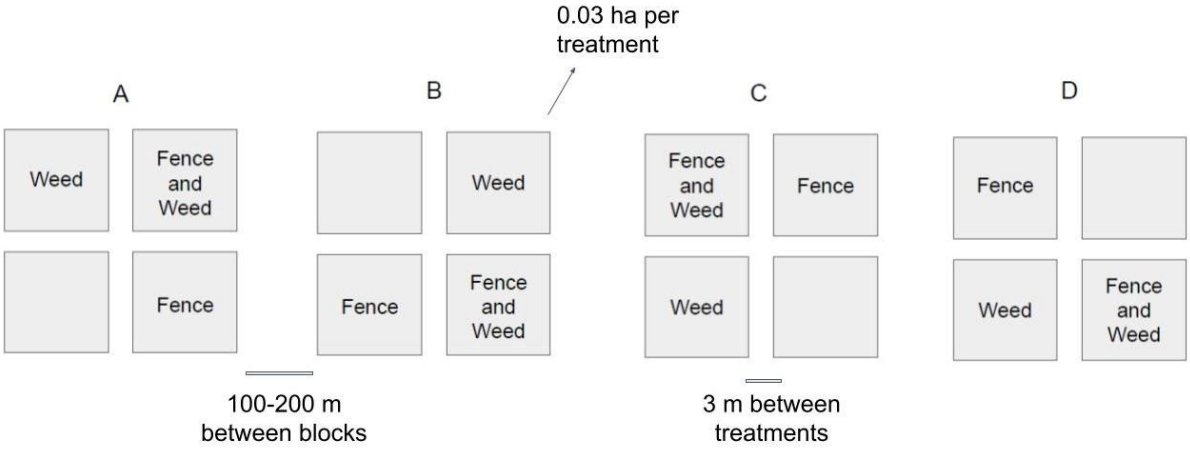

Figure 2.4. Experimental layout of Small Fence and Weeding Trial located at Pack Forest. The trial consisted of four blocks, each with four treatments: (1) no fence, no weeding, (2) fence, no weeding, (3) fence and weeding, (4) no fence and weeding.

Treatment Strips at Pack Forest

Multiple browse deterrent methods were explored using row planting across three replicated blocks at Pack Forest. Replicates were installed in spring of 2015 in units that were harvested between 2013 and 2015. Browse deterrents were tested in rows using the following treatments: (1) no action western redcedar control, (2) Sitka spruce co-planting (both western redcedar and Sitka spruce were measured), (3) flexible plastic 2.4-m tall deer fencing, (4) Plantskydd application, (5) Vexar tubing, and (6) Sitka spruce without western redcedar as a control. The flexible fencing treatment for this experiment was created using metal posts and vertically installed plastic fencing, which gradually formed a tent over the entire line of seedlings as fencing was weighed down by competing vegetation and/or snow during storm events. Vexar tubing and Sitka spruce co-planting installation followed the same protocol as those described in the trials above. The 20 trees in each treatment were planted 0.6 m apart in a straight line, perpendicular to the nearest road and 3 to 6 m from the road edge (Figure 2.5.). The six lines of

treatments within each experimental block were spaced 3 m apart. The order of the six treatments was randomized for each replicate. One year-old western redcedar plugs and Sitka spruce plugs were used for this study.

Initial measurements were collected in the summer of 2015, four months after planting, and measured browse presence or absence, mortality, height, and diameter at root collar. A final round of measurements was collected in the summer of 2024, nine years after installation. Final measurements included deformity presence, risk of tree not reaching rotation age (rotation risk), height, and diameter at 1 m. Spruce were removed from co-planting in the summer 2024 at the time of final measurement. Statistical analysis focused on western redcedar response; Sitka spruce growth was also included in statistical analyses to assess degree of Sitka spruce competition on western redcedar growth outcomes.

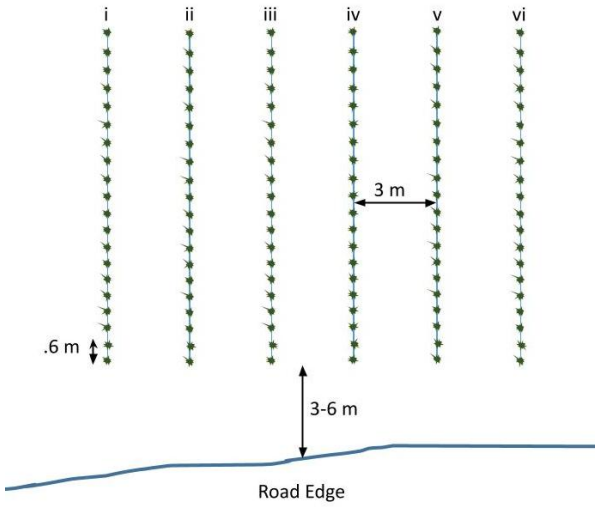

Figure 2.5. Experimental layout of treatment strips at Pack Forest. The trial consisted of three blocks, each with six treatments: (1) no action western redcedar control, (2) Sitka spruce co-planting (both western redcedar and Sitka spruce were measured), (3) flexible fencing, (4) Plantskydd application, (5) Vexar tubing, and (6) Sitka spruce control. Treatment order was randomized for each block. Treatments were replicated across three blocks.

Statistical analysis

Statistical analyses were conducted in R version 4.3.2 (R Core Team, 2022). Each trial was analyzed independently using generalized linear models, generalized linear mixed effects models and χ^2 Test of Independence. In the case of multiple plots within a trial, we assessed whether random effects accounting for within-plot variability improved model performance as measured by the Akaike Information Criterion. If yes, we included a random effect of plot in all models built for that trial to ensure that effect was captured. To assess treatment effects on the continuous response variables (height and diameter), we fit linear fixed-effect and linear mixed-effect models with a Gaussian distribution. To assess binary response variables (presence or absence of browse, rotation risk, and survival), we fit generalized linear and generalized linear mixed models with a binomial distribution. For browse, rotation risk, and survival, if there were only two treatments in a trial and no random effects—creating a 2 x 2 matrix structure—we used a χ^2 Test of Independence to evaluate statistical independence between treatments. Models for count data (the number of leaders on seedlings for each treatment) were estimated with a Poisson distribution with a log link. For models without interaction terms, the *emmeans* package in R was used to create pairwise comparisons between treatments (Lenth and Piaskowski, 2026). For models with interaction terms, no post hoc tests were performed, because the large number of contrasts that it would create would reduce interpretability.

Prior to interpretation, all models were evaluated for outliers and uniform residuals with the R package DHARMa (Hartig, 2022). We used an alpha level of 0.05 to indicate significant treatment effects. Generative artificial intelligence (Sonnet 4.6) (Anthropic, 2025) was used to write and debug code. All code was reviewed and edited, and we take full responsibility for the

content of the published article. Results were visualized with R packages *ggplot2* (Wickham, 2016) and *patchwork* (Pedersen, 2024).

Economic Data

Forest Managers from Pack Forest, Port Blakely, University of Washington Olympic Natural Resource Center, and Pilchuck Tree Farm (a privately owned timber producing forest in western Washington) reported costs for the following browse deterrent methods: chemical repellent, large fenced exclosure, Sitka spruce co-planting, and Vexar tubing (Table S2.10). These costs were compiled and converted to January 2026 dollars using the U.S. Bureau of Labor Statistics Consumer Price Index Inflation Calculator ("CPI Inflation Calculator," 2026). When two costs for the same deterrent method were reported, 2026 prices were averaged. Compiled costs do not include typical forest management activities (e.g., the cost of herbicide applications) and were limited to the additional expenses related to specific browse deterrent methods.

2.3 Results

Table 2.2 summarizes significant results from all trials; model outcomes for all trials can be found in Table S2.4–Table S2.9 in the supplementary materials.

Table 2.2. Summary of statistically significant treatment effects and whether they (1) reduced browse, deformity, and rotation risk, and (2) increased survival, height, and diameter for western redcedar (WRC) and Douglas-fir (DF). For some trials, treatments were compared to each other, without a control, which is noted in the footnotes. Age of trial at time of observed significant effect is denoted in parenthesis. Y = yes; N = no; yr = year; mo = month.

	Browse Reduction?		Deformity Reduction?		Rotation Risk Reduction?		Increased Survival?		Increased Height?		Increased Diameter?	
Treatments	**WRC**	**DF**	**WRC**	**DF**	**WRC**	**DF**	**WRC**	**DF**	**WRC**	**DF**	**WRC**	**DF**
Large multi-hectare fenced exclosures	Y (yr 1, yr 3)	Y (yr 1, yr 3)	Y (yr 8)		Y (yr 8)		Y (yr 1)[1]		Y (yr 3, yr 8)	Y (yr 3, yr 8)	Y (yr 3)	
Small 0.03 and 0.04 hectare fenced exclosures		Y (yr 4)				Y (yr 7)[2]		Y (yr 4)	Y (yr 2, yr 7)	N (yr 2)[3]; Y (yr 4)[4]	Y (yr 2, yr 7)	N (yr 2, yr 7)[3]; Y (yr 4)[4]
Co-planting seedlings with Sitka spruce	Y (mo 4)			Y (yr 5)[5]			N (yr 1)[6]		Y (mo 4)	Y (yr 5)[5]		Y (yr 5)[5]
Vexar tubing	Y (mo 4)			N (yr 5)[1]			N (mo 4)		Y (mo 4, yr 10)	N (yr 5)[1]	Y (yr 10)	N (yr 5)[1]
Chemical repellent Plantskydd	Y (mo 4)								Y (mo 4)		Y (mo 4)	
Flexible fencing[7]	Y (mo 4)		N (yr 10)						Y (mo 4)		Y (mo 4, yr 10)	

[1]In comparison to co-planting

[2]In conjunction with weeding

[3]Results from Treatment Strips at Pack Forest

[4]Results from Fencing and Plantskydd Trial on the Olympic Peninsula

[5]In comparison to Vexar tubing

[6]In comparison to large fenced exclosure

[7]Flexible fencing lost rigidity over time and formed a tent over seedlings

Co-Planting and Tubing Trial in Eatonville

This trial compared Douglas-fir growth in response to Sitka spruce co-planting and Vexar tubing (Figure 2.6.). Vexar tubing resulted in significantly higher Douglas-fir deformity than Sitka spruce co-planting. This deformity did not produce a significant risk of trees not reaching rotation age. Co-planting Douglas-fir with Sitka spruce significantly increased the height of Douglas-fir seedlings compared to Douglas-fir in Vexar tubes. The same was true for diameter: Douglas-fir co-planted with Sitka spruce had significantly larger diameters than Douglas-fir protected by Vexar tubing. There were no significant treatment effects on number of leaders.

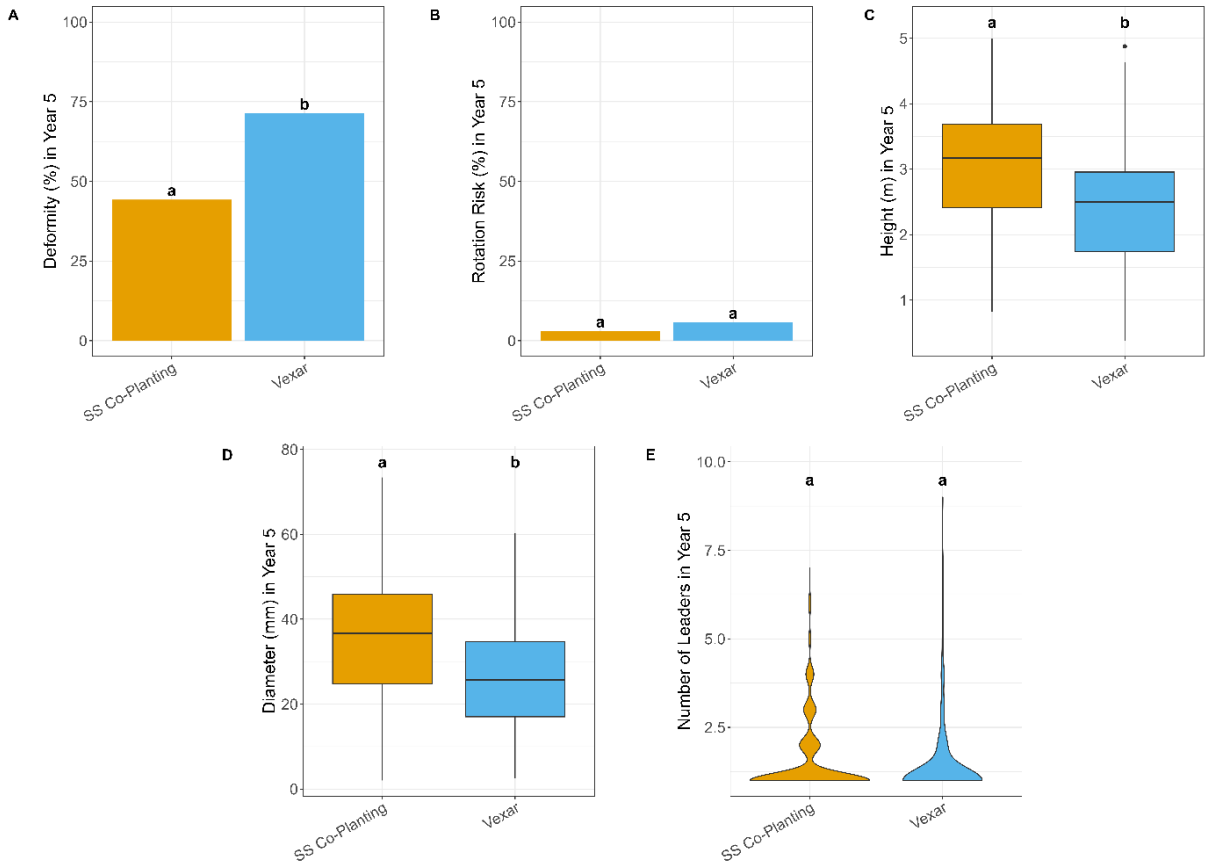

Figure 2.6. Douglas-fir growth responses to Sitka spruce co-planting versus Vexar tubing at the Co-Planting and Tubing Trial at Coburg Tree Farm in Eatonville. Deformity measurements (A) were a binary yes or no with presence of any of the following indicating deformity: spike knot (irregularity in wood caused by embedded tree branches), crook (abrupt bend in tree), sweep (gradual bend), pistol butt (distinct bend at base), lean or trunk damage. Rotation risk (B) was an in-field determination as to whether the individual tree would likely make it to timber harvest age based on degree of deformities. Height (C) in meters and diameter (D) at 1 m were measured in year 5. Number of leaders (E) is a count of the number of vertical shoots at the top of each seedling for each treatment. Post hoc pairwise tests were used to identify significant differences ($p < 0.05$) between treatments, documented with lowercase letters.

Fencing and Plantskydd Trial on Olympic Peninsula

This trial tested the effects of 0.04-hectare fenced exclosures and the application of Plantskydd on Douglas-fir growth (Figure 2.7.). The fencing treatment eliminated browse in year 4 for Douglas-fir, whereas browse for the Plantskydd treatment was not significantly different than the control ($p = 0.49$). Survival was significantly higher in the fencing treatment than in the control, as were height and diameter in year 4. The Plantskydd treatment did not significantly affect survival, height, or diameter in year 4.

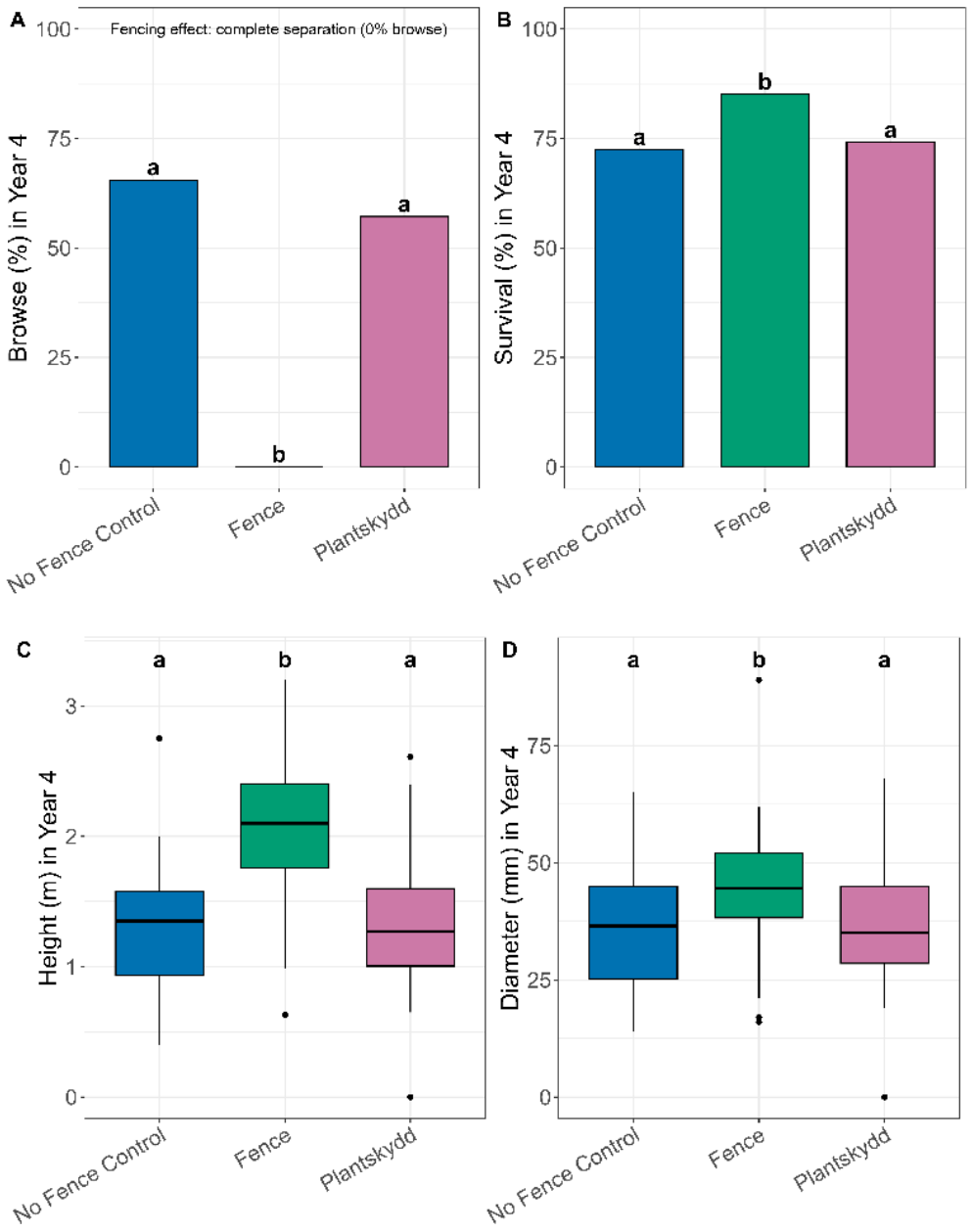

Figure 2.7. Douglas-fir growth responses at year 4 to a 20 x 20 m (0.04 hectare) exclosure and the application of the chemical repellent Plantskydd (4 times per year for the first 2 years) for the Fencing and Plantskydd Trial on the Olympic Peninsula. Browse (A) was measured as the presence or absence of signs of herbivory. Survival (B), height (C), and diameter (D) at root collar were measured four years after planting. Treatments were compared to no fence control using generalized linear mixed effects models. Post hoc pairwise tests were used to identify significant differences ($p < 0.05$) between treatments, documented with lowercase letters.

Large Fence Trial at Pack Forest

The Large Fence Trial tested treatment effects from a 7.8-hectare fenced exclosure for Douglas-fir and western redcedar (Figure 2.8.). In year 1 and 3 of the trial, a χ^2 Test of Independence indicated that treatment significantly affected browse outcomes, with less browse inside the fence. In year 1, western redcedar diameter outside the fence was significantly smaller than Douglas-fir; no other treatment effects were significant. In year 3, western redcedar diameter outside the fence was still significantly smaller than Douglas-fir outside the fence, and western redcedar had a much greater positive response to fencing than Douglas-fir, with diameter values between the two species being similar inside the fence. In year 1 and 3, species, treatment, and interaction of species and treatment were significant for height. Western redcedar height outside the fence was significantly shorter than Douglas-fir outside the fence. Both Douglas-fir and western redcedar heights were significantly higher inside the fence; the effect was stronger for western redcedar, which was taller than Douglas-fir inside the fence at year 3.

In year 8 of the study, western redcedar outside the fence had significantly more deformity than Douglas-fir outside the fence, and there was an interaction between the fencing treatment and western redcedar deformity. Fencing caused a much greater reduction in deformity for western redcedar than Douglas-fir. Rotation risk followed the same pattern: outside the fence, western redcedar was significantly more at risk than Douglas-fir for long-term form issues that would cause mortality before rotation age, and the fencing treatment resulted in greater reduction in that risk for western redcedar than Douglas-fir. Diameter was significantly smaller for western redcedar than Douglas-fir outside the fence, but there were no significant treatment effects on diameter. Height was significantly smaller for western redcedar than Douglas-fir outside the fence, and both Douglas-fir and western redcedar heights were significantly taller inside the

fence, with the effect being stronger for western redcedar. Fencing significantly reduced the number of leaders for western redcedar inside the fence ($p < 0.001$), going from an average of two leaders to one leader; western redcedar had significantly more terminal leaders than Douglas-fir outside the fence ($p < 0.001$).

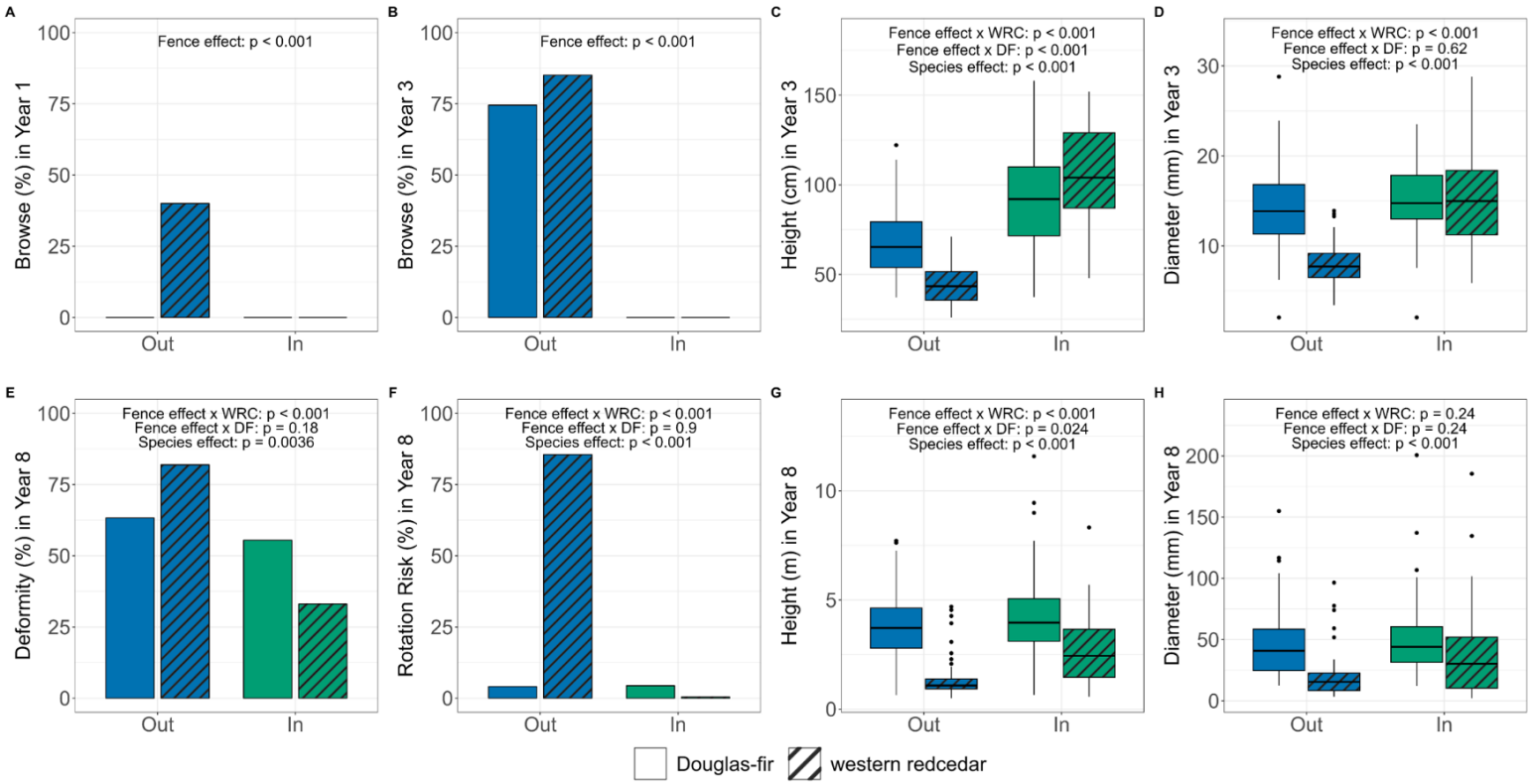

Figure 2.8. Douglas-fir (solid bars) and western redcedar (hatched bars) growth responses to a large fenced exclosure surrounding 7.8 hectares. Results are separated by inside and outside the fence. Repeat measurements allow for tracking the experiment over time. The presence or absence of browse was measured in year 1 (A) and year 3 (B). Height (C) and diameter (D) at root collar were measured in year 3. In year 8, deformity measurements (E) were a binary yes or no with presence of any of the following indicating deformity: spike knot, crook, sweep, pistol butt, lean or bole damage (refer to definitions in Figure 2.6.). Rotation risk (F) was a field-based determination as to whether the individual tree would likely make it to timber harvest age based on degree of deformities. In year 8, height (G) and diameter (H) at 1 m were measured. Effects were tested against the Douglas-fir growth outside the fence (control), and significant differences ($p < 0.05$) are described at the top of each graph and available in supplementary material. No post hoc pairwise tests were performed for this trial as interaction effects increase the number of contrasts and limit interpretability.

Large Fence and Co-Planting Trial near Riffle Lake

This trial evaluated western redcedar survival in two treatments: a 10.5-hectare (26-acre) exclosure and 3.4 hectares (8.5 acres) of western redcedar co-planting with Sitka spruce (Figure 2.9.). The χ^2 Test of Independence indicated that treatment significantly affected survival outcomes for western redcedar; the large fence exclosure resulted in higher survival for western redcedar than Sitka spruce co-planting.

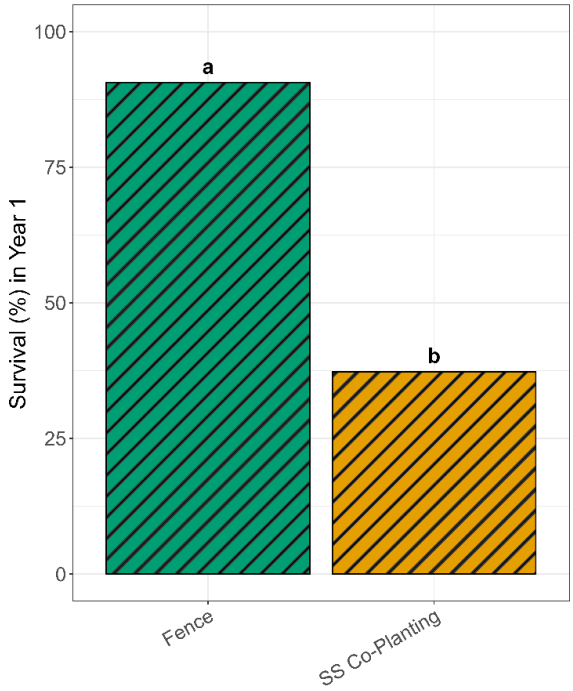

Figure 2.9. Western redcedar growth responses to a large fenced exclosure surrounding 10.5 hectares (26 acres), and a separate trial on 3.4 hectares (8.5 acres) of Sitka spruce co-planting. Survival data were collected as part of a regular survey one year after planting. Letters a and b indicate a significant difference ($p < 0.05$) in survival between treatments.

Small Fence and Weeding Trial at Pack Forest

This randomized block trial tested treatment effects of small 0.03-hectare fences and weeding on western redcedar and Douglas-fir growth (Figure 2.10.). In year 2 of the study, there were no significant treatment or species effects on browse. For height in year 2, fencing significantly reduced Douglas-fir height and significantly increased western redcedar height.

Western redcedar height outside the fence was significantly lower than Douglas-fir outside the fence, and treatments allowed western redcedar to recover height differences: fencing and weeding treatments significantly decreased height for Douglas-fir but increased height for western redcedar. Similarly, for diameter at year 2, Douglas-fir diameter outside the fence was significantly greater than western redcedar diameter outside the fence, and both fencing treatments (F/NW and F/W) significantly reduced Douglas-fir diameter compared to no fence or weed control, and increased western redcedar diameter. The weeding treatment did not significantly impact western redcedar diameter.

In year 7 of the study, there were no significant treatment effects of species on deformity. The fencing and weeding treatment significantly reduced Douglas-fir rotation risk. For height and diameter, patterns from year 2 continued. In terms of height, western redcedar was significantly shorter outside the fence than Douglas-fir and the fencing treatment significantly increased western redcedar height. The same was true for diameter: western redcedar had a significantly smaller diameter than Douglas-fir outside the fence and both fencing treatments (F/NW and F/W) increased western redcedar diameter. Distinctly, the F/NW treatment significantly reduced Douglas-fir diameter for year 7. For all year 7 models, weeding alone did not result in significant differences

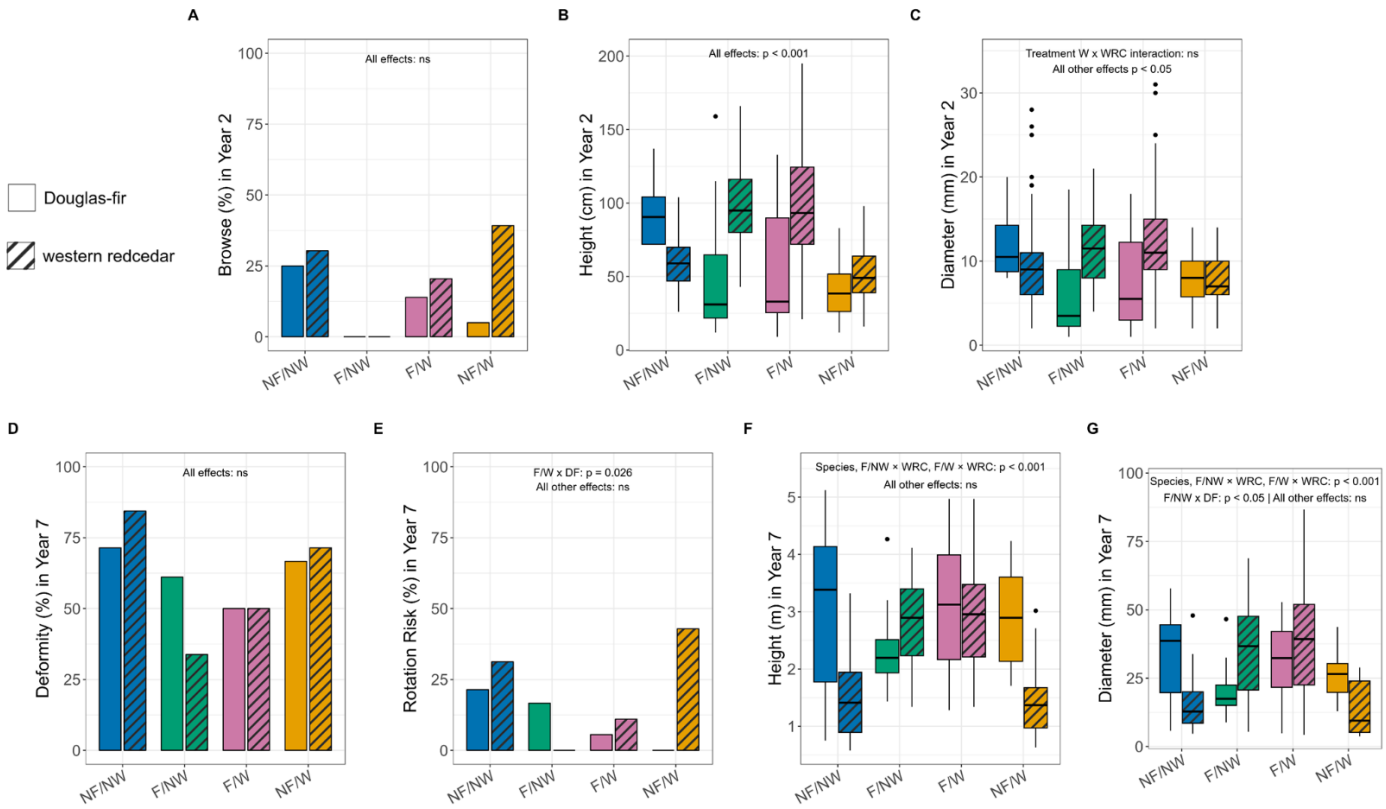

Figure 2.10. Douglas-fir (solid bars) and western redcedar (hatched bars) growth responses to a randomized block trial of 0.03 hectare exclosures and weeding as part of the Small Fence and Weeding Trial at Pack Forest. Results are separated by the four treatments: (1) no fence, no weeding (NF/NW), (2) fence, no weeding (F/NW), (3) fence and weeding (F/W), (4) no fence and weeding (NF/W). Repeat measurements allow for tracking the experiment over time. The presence or absence of browse (A), height (B) and diameter (C) at root collar were measured in year 2. In year 7, deformity measurements (D) were a binary yes or no with presence of any of the following indicating deformity: spike knot, crook, sweep, pistol butt, lean or bole damage (refer to definitions in Figure 2.6.). Rotation risk (E) was a field-based determination as to whether the individual tree would likely make it to timber harvest age based on degree of deformities. In year 7, height (F) and diameter (G) at 1 m were measured. Effects were tested against the no-fence and no-weed control, and significant differences ($p < 0.05$) are described at the top of each graph and available in supplementary material. No post hoc pairwise tests were performed for this trial as interaction effects increase the number of contrasts and limit interpretability.

Treatment Strips at Pack Forest

This trial focused on western redcedar response to the following treatments: (1) no action western redcedar control, (2) Sitka spruce co-planting (both western redcedar and Sitka spruce were measured), (3) flexible fencing, (4) Plantskydd application, (5) Vexar tubing, and (6) Sitka spruce control (Figure 2.11.). At four months, all treatments significantly reduced browse compared to the control. Mortality at four months was significantly higher for the Vexar tubing treatment and lower for the Sitka spruce compared to the western redcedar control. For height at four months, all treatments had a significant positive effect on height compared to the control, but this effect was greatest for the Vexar tubing treatment. For diameter at four months, both the flexible fencing and Plantskydd treatments had a significant positive effect on western redcedar diameter compared to the control, and Sitka spruce in both the control and co-planting treatments had a significantly larger diameter than the western redcedar control.

In year 10, the flexible net fencing led to significantly higher deformity. In year 10, western redcedar height was significantly taller with Vexar tubing, and all Sitka spruce were significantly taller than the western redcedar control. Vexar and flexible fencing had a significant positive effect on western redcedar diameter, and all Sitka spruce had a significantly larger diameter than the western redcedar control.

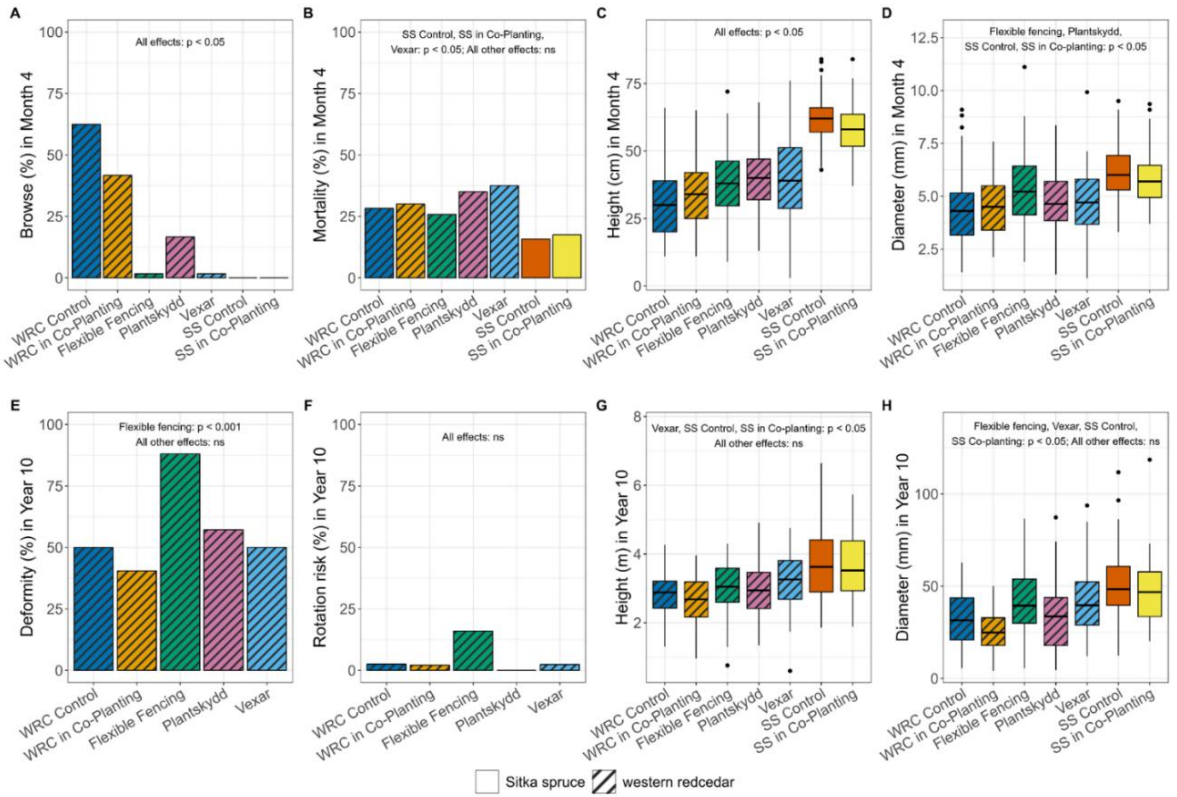

Figure 2.11. Western redcedar (WRC) (hatched bars) and Sitka spruce (SS) (solid bars) growth responses to a randomized block trial of six different treatments as part of the Treatment Strips at Pack Forest trial. Treatments were the following: (1) no action WRC control, (2) SS co-planting (both WRC and SS were measured), (3) flexible fencing, (4) Plantskydd application, (5) Vexar tubing, and (6) a no treatment SS control. In month 4, the presence or absence of browse (A) and mortality (B), height (C), and diameter at root collar (D) were measured. There was no documented browse for SS (A) so it was removed from model testing. In year 10, WRC deformity (E) was measured as a binary Yes or No with presence of any of the following indicating deformity: spike knot, crook, sweep, pistol butt, lean or bole damage (refer to definitions in Figure 2.6.). WRC rotation risk (F) was a field-based determination as to whether the individual tree would likely make it to timber harvest age based on degree of deformities. In year 10, height (G) and diameter (H) at 1 m for both WRC and SS were measured. Discrepancies between original model test results and pairwise test results occurred, so original model results were prioritized and added in text at the top of each figure.

Economic Results

The large fenced exclosure was the most expensive browse deterrent as reported by managers, followed by chemical repellent, Vexar tubing, and Sitka spruce co-planting. Most of the cost associated with the chemical repellent is from reapplication of the repellent at regular intervals. In contrast, the large fenced exclosure treatment requires a large upfront cost with fewer expenses later. If one were to remove the large fence, this would be an additional cost that is not reported in Table 2.3. For Sitka spruce co-planting, the cost of removing the Sitka spruce differed among managers ($210–378 per acre in 2026), and likely depend on the labor structure for each forest operation. For Vexar tubing, one manager reported that no maintenance is needed as the tubes degrade quickly, while another reported the need to regularly adjust the tubes to prevent deformities to the leader and ensure that the tube is protecting the bulk of the tree canopy as the tree grows.

Table 2.3. Reported treatment costs in dollars per acre (assuming 106 TPH [430 TPA]) reported by forest managers in western Washington. When two managers reported different costs for the same treatment, costs were averaged. All costs were converted to 2026 dollars. See Table S2.10 for original cost estimates.

Treatment	Materials	Installation	Maintenance	Total
Chemical repellent	$25.80	$90.30	$864.30[a]	$980.40
Large fenced exclosure		$866.54[b]	$206.48[c]	$1,073.02
Sitka spruce co-planting	$250.90	$194.33	$279.65[d]	$724.88
Vexar tubing	$447.20	$348.20	$73.10[e]	$868.50

[a] Includes labor estimates for regular reapplication of repellent.
[b] Materials and installation labor were contracted together.
[c] Includes labor cost of slashing and removing hardwoods; does not include additional herbicide or fixing holes in fence.
[d] Includes labor cost to remove Sitka spruce 5–10 years after planting.
[e] Includes labor cost of moving tubes up as the tree grows and/or making sure leaders are not caught in the tubing.

2.4 Discussion

How do the various browse prevention techniques (fencing, chemical repellent, tubing, co-planting with Sitka spruce) affect the survival and growth of Douglas-fir and western redcedar regeneration?

The six experimental trials allow for a comparison of browse prevention techniques used to grow and establish trees in the Pacific Northwest, USA. Responses were notably different for the two study species, Douglas-fir and western redcedar, indicating that strategies should be adjusted by species. Strategies that reduce ungulate browse but allow for increased understory vegetation resulted in mixed responses for Douglas-fir, likely due to competition for resources. However, western redcedar benefited from a complete removal of herbivory, such as in the large fenced exclosures, rather than a reduction of herbivory risk (e.g., chemical repellents or Sitka spruce co-planting), where preferential browsing on western redcedar still led to higher rates of mortality and less growth.

First, the two large fencing trials at Pack Forest and near Riffle Lake were successful at establishing and growing fully stocked western redcedar stands, a tree species that otherwise is challenging to establish in this region (Vourc'h et al., 2002; Martin et al., 2002). Fencing at Pack Forest allowed for a recovery in height for western redcedar early in the trial, and at the end of year 3, western redcedar was on average taller than Douglas-fir inside the fence. For western redcedar, rotation risk outside the fence was pronounced in year 8, whereas inside the fence there were few timber quality (i.e., rotation risk) issues. The Small Fence and Weeding Trial at Pack Forest shows similar success for western redcedar in an exclosure, allowing the western redcedar to compete with Douglas-fir in height and diameter, despite Douglas-fir generally being a faster-growing species (Omari et al., 2021).

Douglas-fir response to fencing treatments may be explained by vegetation dynamics. Within the small fence and weeding trial, the fencing and no-weeding treatment significantly reduced Douglas-fir diameter by year 7 compared to the unfenced control. Douglas-fir growth was likely reduced by the presence of invasive species in the unweeded plots, which can influence the success of exclosures (Hart et al., 2020): Himalayan blackberry (*Rubus armeniacus* Focke) overtopped fences and extended over Douglas-fir seedlings, creating robust competition for sunlight (Figure 2.12.). This is consistent with other studies that have noted that herbivory presence can improve unprotected Douglas-fir survival by reducing competing vegetation (Stokely et al., 2018).

Other studies have noted a benefit of vegetation control when paired with tree shelters (Takanobu Yagi, 2022) and the weeding treatment may have slightly reduced the negative impact on Douglas-fir. This is evident in the weeding treatments not having statistically smaller diameters and heights compared to the leading Douglas-fir control. Greater consistency and application of weeding treatments may have been needed for this to be a definitive conclusion. The treatments were also on the edges of a laminated root rot pocket, which could have caused a growth decline in Douglas-fir, although we would expect these effects to be limited in the first years of growth (Buckland et al., 1954) and to equally affect all treatments. In the absence of abnormally high vegetation inside fencing, Douglas-fir can benefit from fencing, as shown in the Fencing and Plantskydd trial on the Olympic Peninsula, where fencing reduced browse, increased survival, and improved height and diameter.

Figure 2.12. Vegetation and invasive species present in the unweeded and fenced treatment as part of the Small Fence and Weeding Trial at Pack Forest. Competition from the invasive species Himalayan blackberry likely reduced Douglas-fir growth in this treatment compared to the control.

Western redcedar was likely less affected by vegetation, competition and root rot due to its greater shade and root rot tolerance (Carter and Klinka, 1992; Goheen and Willhite, 2021). In some instances, Himalayan blackberry presence may aid western redcedar growth by deterring browse while allowing for continued growth in low light conditions, which is not as viable for shade-intolerant Douglas-fir (Harrington, 2006). Together, results indicate that the fencing treatments particularly benefit western redcedar, and that Douglas-fir response is more variable, potentially depending on vegetation competition—especially invasive species vegetation—inside the fenced units.

The chemical browse repellent showed mixed results as a browse deterrent, consistent with previous studies (Andelt et al., 1992). Plantskydd significantly decreased browse and increased

height and diameter in month 4 of the Pack Forest Treatment Strips trial, but these positive effects were lost by year 10. Similarly, in year 4 of the Fencing and Plantskydd trial on the Olympic Peninsula, the Plantskydd treatment did not significantly affect survival, height, or diameter. Variability in treatment effect over time is due at least in part to the need to apply repellents repeatedly to assure seedling protection (Puettmann et al., 2024). Frequent precipitation in western Washington make regular applications challenging, because Plantskydd needs to be applied during a 24-hour, rain-free window (Bobsin, 2023). Migration patterns of deer and elk contribute to outcomes as well, with repellents being a particularly useful tool if browse is seasonal and application timing can be precise (Nolte, 1998). Repellents are also more effective where alternative forage is readily available; deer and elk are less selective if forage is limited (Nolte, 1998). Nevertheless, early positive effects of Plantskydd in the Treatment Strips trial suggest that Plantskydd may have potential as a valuable browse deterrent on a short-term basis, when applications can be applied regularly, or at critical windows of ungulate migration. Results from this study indicate that it is challenging to use repellent to achieve long-term browse prevention.

Third, the three studies that explored Sitka spruce co-planting with seedlings had different outcomes. In the Co-Planting and Tubing Trial near Eatonville, co-planting of Sitka spruce paired with Douglas-fir was superior for Douglas-fir compared to Vexar tubing, with deformity being higher for Vexar tubing, and height and diameter being larger for co-planting. However, the two trials of co-planted Sitka spruce with western redcedar, showed high browse pressure in the first year of the experiment. Treatment Strips at Pack Forest showed high browse for the western redcedar-Sitka spruce co-planting trial at the early 4-month mark; at the co-planting site at Port Blakely, high initial browse led to low survival for western redcedar at year 1. Port Blakely

managers reported that low survival of western redcedar in co-planting was due to elk presence on site within the first week after planting. For the Treatment Strips trial, co-planting mortality was not significantly different from the western redcedar control at month 4, and co-planting treatment led to the lowest western redcedar mean diameter and height of all treatments in year 10. This may partially be due to the competitive effects of Sitka spruce on western redcedar, whereas Sitka spruce was seemingly unaffected by the co-planting treatment in terms of height and diameter. Competition from Sitka spruce must be balanced by the need for Sitka spruce to be comparable in size at planting and growing close to western redcedar for Sitka spruce to effectively protect western redcedar from browse. The Co-Planting and Tubing Trial near Eatonville tied the Sitka spruce and Douglas-fir together to ensure proximity of the species, which may have improved early experimental results—perhaps increased Douglas-fir growth occurred in response to competition with spruce (Woodruff et al., 2002).

Collectively, these results indicate that although the Sitka spruce co-planting may be a useful tool for Douglas-fir regeneration, Sitka spruce may not be a sufficient physical deterrent to reduce western redcedar browse. However, tying western redcedar and Sitka spruce seedlings together and/or repeated pruning of spruce to free western redcedar height growth may improve the utility of a Sitka spruce-western redcedar co-planting approach and should be further tested with western redcedar. For western redcedar, tree-protection tubing may be the best option after fenced exclosures, as tree shelters have been documented to consistently reduce browse and benefit growth in this study and others (Campbell and Evans, 1988; Puettmann et al., 2024; Takanobu Yagi, 2022). Vexar tubing outperformed the other treatments in the Treatment Strips trial with western redcedar being significantly taller in year 10, consistent with other tubing trials (Thyroff et al., 2022). Port Blakely Tree Farm has a newly harvested 14.5-hectare stand planted entirely

with western redcedar and protected with Vexar tubing (average height of seedlings is 1.5 meters at 3.5 years after planting) (Dixon, 2025).

What are the tradeoffs of browse prevention tools when considering ease of installation, maintenance, and cost?

Effectiveness of certain treatments is not the only consideration when planning management action: many of these treatments require significant in-field labor. Installation of robust browse prevention is often motivated by a strong objective of landowners to add western redcedar to the forest—for example, adding diversity to the forest to meet ecological goal, responding to a forest health issue like laminated root rot (Goheen and Willhite, 2021), or to grow high-value western redcedar monocultures. Labor costs for a particular technique should be compared to the costs of no action, (e.g. allowing root rot to spread) (Bormann et al., 2007).

The success of large fencing exclosures for western redcedar was achieved through a robust effort to install and maintain the fences. Installation costs were substantial (Table 2.3.) in addition to typical planting costs that average $705–985 per acre for seedlings and labor (Table S2.10). The costs of large fenced exclosures may be offset by the high market value of western redcedar or reusing fence materials for a future project, although upfront costs may make fencing inaccessible to many landowners. Forest managers for both Large Fence Trials regularly walked the full fence perimeter to ensure trial success, patching holes and ensuring the fence was secured to the ground so that deer and elk could not get under the fence (Vercauteren et al., 2006). At times, deer and elk had to be chased out of the fenced units to preserve the seedlings. Moreover, production records from these trials indicate that additional vegetation inside the fence required extensive pre-commercial thinning efforts to reduce hardwood species. Lastly, our study highlights that invasive species can limit the success of exclosures (Hart et al., 2020). Vegetation control can be more

complicated with the addition of western redcedar in a planting unit as western redcedar is more sensitive to glyphosate than Douglas-fir (Reynolds et al., 1986) and damage from herbicide spray on western redcedar may not be visible until the subsequent year. In addition, not all locations are suitable for a large exclosure: deer and elk can jump over fences on steep slopes that would be inaccessible on flat ground (Iijima and Oka, 2023; Vercauteren et al., 2006). Although large fenced exclosures may be an ideal option for western redcedar regeneration, labor, materials, and site requirements may limit large-scale adoption of this practice.

When large-fence trials are not an option, managers may consider Vexar tubing, co-planting, or repellents, but these options also have high labor requirements (Table 2.3.). Ideally, tree tubes degrade quickly and do not need to be removed, but past studies and this study document that tubing can increase deformities (Puettmann et al., 2024). The process of tube removal may be comparable to the labor required to remove Sitka spruce from co-planting sites 10 years after planting, which deters some managers from applying the Sitka spruce co-planting technique (Dryden, 2025). Managers note that Sitka spruce co-planting is double the costs for seedlings and planting plus the cost of removing the Sitka spruce through slashing (Table 2.3.) (Dryden, 2025). For repellents, this study as well as others highlight that repellents require a concerted application effort for benefits to be achieved (Bobsin, 2023; Puettmann et al., 2024), and this in-field labor may be out of reach for many landowners. Lastly, treatments should be avoided when maintenance requirements are unreasonable. The costs of repeated application of chemical deterrents, and repositing Vexar tubing could also be high, with lower likelihood of complete browse protection. Lessons learned from these trials suggest that if managers are interested in growing a high-value forage species like western redcedar, significant labor inputs are required.

Using the results of this study, what impact does browse have on the regeneration and development of diverse forests in the Pacific Northwest?

This study provides a unique vantage point for understanding the impacts of browse on forest systems in the Pacific Northwest. One example of herbivory influencing species composition across the landscape is the pronounced difference in western redcedar survival inside and outside the fenced exclosure in the Large Fence Trial near Riffle Lake, despite the Sitka spruce co-planting treatment outside the exclosure.

In the absence of prolific hunting and predation by carnivores, ungulates have increased across the landscape, resulting in an increased interaction with forested systems (Kay, 2001; Rooney, 2001). Hunting can change deer behavior and lead to reduced browse, irrespective of the number of deer killed (Martin et al., 2010). Reintroducing western redcedar into plantings to restore its presence in young forests where it is notably absent, without also reducing ungulate abundance or altering their behavior, is a big challenge (LePage and Banner, 2014).

Although not the focus of this study, nor the focus of data collection efforts, vegetation differences within fenced exclosures compared to outside exclosures were striking. Plot notes from the large fence trial at Pack Forest document a higher presence of bitter cherry (*Prunus emarginata* (Douglas ex Hook.) D. Dietr.), red alder (*Alnus rubra* Bong.), black cottonwood (*Populus trichocarpa* Torr. & Gray) and red elderberry (*Sambucus racemosa* L.) inside the fence. Similarly, the Fencing and Plantskydd Trial on the Olympic Peninsula saw an increase in forbs within the fenced unit ($p = 0.03$). The vegetation responses suggest that deer and elk populations are not only impacting western redcedar presence but also affecting vegetation composition, which concurs with other documentation of ungulate-caused reduction in herbs and shrubs (Rooney, 2001). Parker et al. (2020) observed that browsing by deer can reduce horizontal

and vertical structure and impact composition of vegetation strata. Ramirez et al. (2019) found that species richness and Shannon diversity declined steadily over time in unfenced units. Fenced units developed woody tree species with palatable broadleaved species, whereas unfenced units were not associated with any particular tree species (Ramirez et al., 2019). Ungulate impacts can vary substantially by species, as plant species have different tolerance levels and adaptations for browse (Burney et al., 2018; Endress et al., 2016; Vourc'h et al., 2001). These observations depict the impact on ungulates in unfenced areas as well as the potential reduction in foraging habitat from installing fencing. When fenced units are in place, managers interested in promoting wildlife habitat may choose to remedy reduced forage species by removing fencing after successful forest regeneration, or pursuing extended early-seral habitat by implementing variable density planting in other areas of the forest (Ettl et al., 2026).

Deer herbivory gives less palatable species an advantage (Leopold et al., 1947) and the landscape-wide long-term effects of this pressure are not well understood. Indirect effects from herbivory pressure can cascade through a system, where tree density is associated with a multitude of other ecological processes relating to vertebrates (Wisdom et al., 2006). Herbivory as a disturbance agent interacts and overlaps with other episodic forest disturbances, and large spatial and temporal scales of these effects are not well understood (Wisdom et al., 2006). Others have questioned the implications of long-term exclosures, where the natural system can develop herbivore free for years if not decades (Larson and Paine, 2007). Our study confirms that exclusion of ungulate herbivores increases the density of long-lived trees, especially high-value timber species like western redcedar that are also attractive browse species (Larson and Paine, 2007; Woodward et al., 1994). Forming a deeper understanding of our current position in the cyclical nature of wildlife and silvicultural interactions (Leopold, 1936) by studying direct and

indirect impacts of both, may help achieve concurrent forestry and wildlife management objectives.

2.5 Conclusion

Six experimental trials show that although species react differently to various browse prevention methods, effective protection options are available for both Douglas-fir and western redcedar. Certain treatments were consistently beneficial for western redcedar, such as the large fenced exclosures, but the labor and material requirements of this treatment may prohibit adoption and lead managers to select individual-tree protection options. For all techniques, there must be a significant motivation for managers to seek diversity and overcome the challenges of installing and maintaining browse deterrents, but this synthesis shows that some options may be worthy of that effort. Future work should further explore plant composition changes due to ungulate browsing, because our study demonstrates a notable difference in forest response when browse is absent.

Table S2.4. Model results for Co-Planting and Tubing Trial near Eatonville.

Response	Term	Estimate	Std. Error	Statistic	p-value	df
Height, Year 5	Intercept	3.0315	0.0475	63.758	<0.0001	—
Height, Year 5	Vexar Treatment	-0.6286	0.0761	-8.2567	<0.0001	—
Deform, Year 5	—	—	—	37.359	<0.0001	1
Rotation Risk, Year 5	—	—	—	0.2855	0.5931	1
Diameter, Year 5	Intercept	35.492	0.7839	45.279	<0.0001	—
Diameter, Year 5	Vexar Treatment	-9.3369	1.2849	-7.2664	<0.0001	—
Number of Leaders, Year 5	Intercept	0.4282	0.0442	9.6802	<0.0001	—
Number of Leaders, Year 5	Vexar Treatment	-0.0758	0.0725	-1.0452	0.2959	—

Table S2.5. Model results for Large Fence Trial at Pack Forest.

Response	Term	Estimate	Std. Error	Statistic	p-value	df
Height, Year 1	Intercept	46.453	1.0990	42.269	<0.0001	—
Height, Year 1	Fence effect × DF	-3.8595	1.6902	-2.2834	0.0232	—
Height, Year 1	Species Effect	-10.592	1.5099	-7.0151	<0.0001	—
Height, Year 1	Fence effect × WRC	9.8898	2.2702	4.3564	<0.0001	—
Browse, Year 1	—	—	—	27.275	<0.0001	1
Diameter, Year 1	Intercept	8.9411	0.1824	49.023	<0.0001	—
Diameter, Year 1	Fence effect × DF	0.2466	0.2805	0.8790	0.3802	—
Diameter, Year 1	Species Effect	-5.0480	0.2506	-20.146	<0.0001	—
Diameter, Year 1	Fence effect × WRC	0.1110	0.3768	0.2947	0.7685	—
Browse, Year 3	—	—	—	146.08	<0.0001	1
Height, Year 3	Intercept	68.349	3.0460	22.439	<0.0001	—
Height, Year 3	Fence effect × DF	24.880	4.6610	5.3380	<0.0001	—
Height, Year 3	Species Effect	-24.478	4.1103	-5.9552	<0.0001	—

Response	Term	Estimate	Std. Error	Statistic	p-value	df
Height, Year 3	Fence effect × WRC	35.357	6.1406	5.7579	<0.0001	—
Diameter, Year 3	Intercept	14.591	0.5786	25.219	<0.0001	—
Diameter, Year 3	Fence effect × DF	0.4340	0.8853	0.4902	0.6244	—
Diameter, Year 3	Species Effect	-6.6786	0.7807	-8.5542	<0.0001	—
Diameter, Year 3	Fence effect × WRC	6.5551	1.1664	5.6200	<0.0001	—
Deformity, Year 8	Intercept	0.5436	0.1711	3.1774	0.0015	—
Deformity, Year 8	Fence effect × DF	-0.3238	0.2425	-1.3349	0.1819	—
Deformity, Year 8	Species Effect	0.9678	0.3326	2.9097	0.0036	—
Deformity, Year 8	Fence effect × WRC	-1.8928	0.3977	-4.7590	<0.0001	—
Number of Leaders, Year 8	Intercept	0.0847	0.0791	1.0719	0.2838	—
Number of Leaders, Year 8	Fence effect × DF	-0.0349	0.1149	-0.3039	0.7612	—
Number of Leaders, Year 8	Species Effect	0.5716	0.1118	5.1125	<0.0001	—
Number of Leaders, Year 8	Fence effect × WRC	-0.5862	0.1526	-3.8411	0.0001	—
Rotation Risk, Year 8	Intercept	-3.1570	0.4168	-7.5736	<0.0001	—
Rotation Risk, Year 8	Fence effect × DF	0.0736	0.5900	0.1247	0.9008	—
Rotation Risk, Year 8	Species Effect	4.9348	0.5207	9.4763	<0.0001	—
Rotation Risk, Year 8	Fence effect × WRC	-7.3728	1.2039	-6.1239	<0.0001	—
Height, Year 8	Intercept	3.8701	0.1103	35.090	<0.0001	—
Height, Year 8	Fence effect × DF	0.3596	0.1588	2.2644	0.0239	—
Height, Year 8	Species Effect	-2.5418	0.1836	-13.845	<0.0001	—
Height, Year 8	Fence effect × WRC	0.8898	0.2321	3.8332	0.0001	—
Diameter, Year 8	Intercept	45.555	2.2422	20.317	<0.0001	—
Diameter, Year 8	Fence effect × DF	3.7755	3.2433	1.1641	0.2449	—
Diameter, Year 8	Species Effect	-21.618	5.6097	-3.8537	0.0001	—

Response	Term	Estimate	Std. Error	Statistic	p-value	df
Diameter, Year 8	Fence effect × WRC	7.4582	6.3374	1.1769	0.2398	—

Abbreviations: DF, Douglas-fir; WRC, western redcedar

Table S2.6. Model results for Large Fence and Co-Planting Trial near Riffle Lake.

Response	Statistic	p-value	df
Survival, Year 1	398.43	<0.0001	1

Table S2.7. Model results for Fencing and Plantskydd Trial on Olympic Peninsula.

Response	Effect	Group	Term	Estimate	Std. Error	Statistic	p-value	df
Survival, Year 4	fixed	—	Intercept	1.1540	0.5358	2.1537	0.0313	—
Survival, Year 4	fixed	—	Fence	0.8090	0.4120	1.9635	0.0496	—
Survival, Year 4	fixed	—	Plantskydd	-0.0314	0.3757	-0.0835	0.9335	—
Survival, Year 4	ran_pars	block	sd__(Intercept)	0.7969	—	—	—	—
Height, Year 4	fixed	—	Intercept	1.2675	0.1706	7.4309	0.0099	2.4377
Height, Year 4	fixed	—	Fence	0.7558	0.0821	9.2101	<0.0001	190.03
Height, Year 4	fixed	—	Plantskydd	0.0306	0.0851	0.3595	0.7196	190.02
Height, Year 4	ran_pars	block	sd__(Intercept)	0.2752	—	—	—	—
Height, Year 4	ran_pars	Residual	sd__Observation	0.4677	—	—	—	—
Diameter, Year 4	fixed	—	Intercept	34.827	3.4014	10.239	0.0026	2.8070
Diameter, Year 4	fixed	—	Fence	9.3455	2.1313	4.3848	<0.0001	194.03
Diameter, Year 4	fixed	—	Plantskydd	0.3550	2.1821	0.1627	0.8709	194.10
Diameter, Year 4	ran_pars	block	sd__(Intercept)	5.1905	—	—	—	—
Diameter, Year 4	ran_pars	Residual	sd__Observation	12.148	—	—	—	—
Browse, Year 4	—	—	—	—	—	0.5738	0.4487	1

Table S2.8. Model results for Treatment Strips at Pack Forest.

Response	Effect	Group	Term	Estimate	Std. Error	Statistic	p-value	df
Browse, Month 4	fixed	—	Intercept	0.5368	0.2686	1.9988	0.0456	—
Browse, Month 4	fixed	—	SS Co-Planting	-0.8903	0.2696	-3.3020	0.0010	—
Browse, Month 4	fixed	—	Flexible Fencing	-4.7149	0.7489	-6.2954	<0.0001	—
Browse, Month 4	fixed	—	Plantskydd	-2.2153	0.3163	-7.0045	<0.0001	—
Browse, Month 4	fixed	—	SS Control	-27.511	63206.0	-0.0004	0.9997	—
Browse, Month 4	fixed	—	SS in Co-Planting	-26.753	43264.3	-0.0006	0.9995	—
Browse, Month 4	fixed	—	Vexar	-4.7149	0.7489	-6.2954	<0.0001	—
Browse, Month 4	ran_pars	rep	sd__(Intercept)	0.4591	—	—	—	—
Mortality, Month 4	fixed	—	Intercept	-1.3338	0.8615	-1.5482	0.1216	—
Mortality, Month 4	fixed	—	SS Co-Planting	0.1645	0.4023	0.4090	0.6826	—
Mortality, Month 4	fixed	—	Flexible Fencing	-0.2628	0.4156	-0.6324	0.5271	—
Mortality, Month 4	fixed	—	Plantskydd	0.6142	0.3912	1.5700	0.1164	—
Mortality, Month 4	fixed	—	SS Control	-1.5475	0.4699	-3.2930	0.0010	—
Mortality, Month 4	fixed	—	SS in Co-Planting	-1.3058	0.4584	-2.8484	0.0044	—
Mortality, Month 4	fixed	—	Vexar	0.8181	0.3873	2.1124	0.0347	—
Mortality, Month 4	ran_pars	rep	sd__(Intercept)	1.9820	—	—	—	—
Height, Month 4	fixed	—	Intercept	30.893	1.4117	21.884	<0.0001	19.193
Height, Month 4	fixed	—	SS Co-Planting	3.9959	1.5196	2.6296	0.0087	778.27
Height, Month 4	fixed	—	Flexible Fencing	7.5594	1.5158	4.9871	<0.0001	778.12
Height, Month 4	fixed	—	Plantskydd	8.3541	1.5263	5.4734	<0.0001	778.13
Height, Month 4	fixed	—	SS Control	30.762	1.5024	20.475	<0.0001	778.07

Response	Effect	Group	Term	Estimate	Std. Error	Statistic	p-value	df
Height, Month 4	fixed	—	SS in Co-Planting	26.703	1.5024	17.773	<0.0001	778.07
Height, Month 4	fixed	—	Vexar	8.5924	1.5161	5.6674	<0.0001	778.27
Height, Month 4	ran_pars	rep	sd__(Intercept)	2.2631	—	—	—	—
Height, Month 4	ran_pars	Residual	sd__Observation	11.392	—	—	—	—
Diameter, Month 4	fixed	—	Intercept	4.3642	0.2881	15.148	<0.0001	6.9984
Diameter, Month 4	fixed	—	SS Co-Planting	0.1100	0.1749	0.6289	0.5296	777.05
Diameter, Month 4	fixed	—	Flexible Fencing	0.7755	0.1740	4.4566	<0.0001	777.02
Diameter, Month 4	fixed	—	Plantskydd	0.4209	0.1752	2.4022	0.0165	777.02
Diameter, Month 4	fixed	—	SS Control	1.7983	0.1725	10.427	<0.0001	777.01
Diameter, Month 4	fixed	—	SS in Co-Planting	1.4330	0.1725	8.3086	<0.0001	777.01
Diameter, Month 4	fixed	—	Vexar	0.3253	0.1740	1.8692	0.0620	777.05
Diameter, Month 4	ran_pars	rep	sd__(Intercept)	0.6387	—	—	—	—
Diameter, Month 4	ran_pars	Residual	sd__Observation	1.3077	—	—	—	—
Deform Risk, Year 10	fixed	—	Intercept	0.1260	0.5161	0.2441	0.8071	—
Deform Risk, Year 10	fixed	—	WRC in Co-Planting	-0.4900	0.4611	-1.0625	0.2880	—
Deform Risk, Year 10	fixed	—	Flexible Fencing	2.0733	0.5628	3.6841	0.0002	—
Deform Risk, Year 10	fixed	—	Plantskydd	0.2681	0.4712	0.5689	0.5694	—
Deform Risk, Year 10	fixed	—	Vexar	-0.1652	0.4698	-0.3516	0.7252	—
Deform Risk, Year 10	ran_pars	plot	sd__(Intercept)	0.6699	—	—	—	—
Rotation Risk, Year 10	fixed	—	Intercept	-3.7203	1.0438	-3.5642	0.0004	—
Rotation Risk, Year 10	fixed	—	WRC in Co-Planting	-0.1643	1.4277	-0.1151	0.9084	—
Rotation Risk, Year 10	fixed	—	Flexible Fencing	2.0227	1.0845	1.8651	0.0622	—

Response	Effect	Group	Term	Estimate	Std. Error	Statistic	p-value	df
Rotation Risk, Year 10	fixed	—	Plantskydd	-16.027	186.96	-0.0857	0.9317	—
Rotation Risk, Year 10	fixed	—	Vexar	-0.0809	1.4308	-0.0565	0.9549	—
Rotation Risk, Year 10	ran_pars	plot	sd__(Intercept)	0.3170	—	—	—	—
Height, Year 10	fixed	—	Intercept	2.7998	0.1664	16.825	<0.0001	10.833
Height, Year 10	fixed	—	WRC in Co-Planting	-0.1549	0.1843	-0.8404	0.4013	312.16
Height, Year 10	fixed	—	Flexible Fencing	0.1674	0.1821	0.9191	0.3587	312.87
Height, Year 10	fixed	—	Plantskydd	0.0379	0.1893	0.2003	0.8413	312.15
Height, Year 10	fixed	—	SS Control	0.9221	0.1818	5.0727	<0.0001	312.22
Height, Year 10	fixed	—	SS in Co-Planting	0.8574	0.1819	4.7141	<0.0001	312.42
Height, Year 10	fixed	—	Vexar	0.3863	0.1895	2.0392	0.0423	312.35
Height, Year 10	ran_pars	plot	sd__(Intercept)	0.1644	—	—	—	—
Height, Year 10	ran_pars	Residual	sd__Observation	0.8563	—	—	—	—
Diameter, Year 10	fixed	—	Intercept	33.193	2.8321	11.720	<0.0001	38.225
Diameter, Year 10	fixed	—	WRC in Co-Planting	-6.5762	3.6581	-1.7977	0.0732	301.83
Diameter, Year 10	fixed	—	Flexible Fencing	8.5587	3.6443	2.3485	0.0195	302.79
Diameter, Year 10	fixed	—	Plantskydd	0.9598	3.7187	0.2581	0.7965	301.73
Diameter, Year 10	fixed	—	SS Control	17.339	3.5875	4.8332	<0.0001	301.92
Diameter, Year 10	fixed	—	SS in Co-Planting	14.288	3.6231	3.9437	0.0001	302.30
Diameter, Year 10	fixed	—	Vexar	8.8614	3.7425	2.3678	0.0185	302.08
Diameter, Year 10	ran_pars	plot	sd__(Intercept)	1.6115	—	—	—	—
Diameter, Year 10	ran_pars	Residual	sd__Observation	16.826	—	—	—	—

Abbreviations: DF, Douglas-fir; WRC, western redcedar; SS, Sitka spruce

Table S2.9. Model results for small fence and weeding trial at Pack Forest.

Response	Effect	Group	Term	Estimate	Std. Error	Statistic	p-value	df
Survival, Year 2	fixed		Intercept	-1.2805	0.8632	-1.4834	0.1380	—
Survival, Year 2	fixed		F/NW x DF	-18.4288	79.4806	-0.2319	0.8166	—
Survival, Year 2	fixed		F/W x DF	-0.4275	0.9755	-0.4382	0.6612	—
Survival, Year 2	fixed		W x DF	-1.8863	1.3155	-1.4339	0.1516	—
Survival, Year 2	fixed		Species Effect	0.3083	0.8846	0.3485	0.7275	—
Survival, Year 2	fixed		F/NW x WRC	-0.3410	106.7636	-0.0032	0.9975	—
Survival, Year 2	fixed		F/W x WRC	-0.0891	1.0454	-0.0852	0.9321	—
Survival, Year 2	fixed		W x WRC	2.3513	1.3732	1.7122	0.0869	—
Survival, Year 2	ran_pars	plot	sd__(Intercept)	0.4199	—	—	—	—
Height, Year 2	fixed		Intercept	100.6729	11.8043	8.5285	<0.0001	40.7923
Height, Year 2	fixed		F/NW x DF	-47.7556	12.0065	-3.9775	0.0001	412.4352
Height, Year 2	fixed		F/W x DF	-41.0051	11.3867	-3.6011	0.0004	412.7524
Height, Year 2	fixed		W x DF	-53.0489	11.9914	-4.4239	<0.0001	411.0681
Height, Year 2	fixed		Species Effect	-44.2159	10.9891	-4.0236	0.0001	412.3688
Height, Year 2	fixed		F/NW x WRC	88.7670	12.9648	6.8468	<0.0001	412.1432
Height, Year 2	fixed		F/W x WRC	81.2048	12.3163	6.5933	<0.0001	412.6510
Height, Year 2	fixed		W x WRC	48.3529	13.0638	3.7013	0.0002	411.3771

Response	Effect	Group	Term	Estimate	Std. Error	Statistic	p-value	df
Height, Year 2	ran_pars	plot	sd__(Intercept)	11.7177	—	—	—	—
Height, Year 2	ran_pars	Residual	sd__Observation	28.6462	—	—	—	—
Diameter, Year 2	fixed		Intercept	13.0864	1.8731	6.9865	<0.0001	34.1140
Diameter, Year 2	fixed		F/NW x DF	-6.4690	1.8705	-3.4583	0.0006	412.2810
Diameter, Year 2	fixed		F/W x DF	-4.5197	1.7740	-2.5477	0.0112	412.5775
Diameter, Year 2	fixed		W x DF	-4.2565	1.8680	-2.2787	0.0232	411.0581
Diameter, Year 2	fixed		Species Effect	-3.9624	1.7120	-2.3144	0.0211	412.2188
Diameter, Year 2	fixed		F/NW x WRC	8.8349	2.0198	4.3742	<0.0001	412.0149
Diameter, Year 2	fixed		F/W x WRC	7.7782	1.9189	4.0536	0.0001	412.4815
Diameter, Year 2	fixed		W x WRC	2.8147	2.0351	1.3831	0.1674	411.3297
Diameter, Year 2	ran_pars	plot	sd__(Intercept)	1.9592	—	—	—	—
Diameter, Year 2	ran_pars	Residual	sd__Observation	4.4624	—	—	—	—
Deformity, Year 7	fixed		Intercept	0.9400	0.7885	1.1921	0.2332	—
Deformity, Year 7	fixed		F/NW x DF	-0.3853	0.8132	-0.4738	0.6357	—
Deformity, Year 7	fixed		F/W x DF	-0.9150	0.8130	-1.1254	0.2604	—
Deformity, Year 7	fixed		W x DF	-0.3698	0.9109	-0.4059	0.6848	—
Deformity, Year 7	fixed		Species Effect	0.3281	0.8163	0.4019	0.6878	—
Deformity, Year 7	fixed		F/NW x WRC	-1.5709	1.0061	-1.5614	0.1184	—
Deformity, Year 7	fixed		F/W x WRC	-0.3338	0.9928	-0.3362	0.7367	—

Response	Effect	Group	Term	Estimate	Std. Error	Statistic	p-value	df
Deformity, Year 7	fixed		W x WRC	-0.3995	1.1659	-0.3426	0.7319	—
Deformity, Year 7	ran_pars	plot	sd__(Intercept)	0.8086	—	—	—	—
Rotation Risk, Year 7	fixed		Intercept	-0.8072	1.2151	-0.6643	0.5065	—
Rotation Risk, Year 7	fixed		F/NW x DF	-1.1986	1.0806	-1.1092	0.2674	—
Rotation Risk, Year 7	fixed		F/W x DF	-3.1003	1.3941	-2.2239	0.0262	—
Rotation Risk, Year 7	fixed		W x DF	-18.9479	128.6464	-0.1473	0.8829	—
Rotation Risk, Year 7	fixed		Species Effect	1.0070	0.9068	1.1105	0.2668	—
Rotation Risk, Year 7	fixed		F/NW x WRC	-18.0971	139.5030	-0.1297	0.8968	—
Rotation Risk, Year 7	fixed		F/W x WRC	0.1623	1.4653	0.1107	0.9118	—
Rotation Risk, Year 7	fixed		W x WRC	19.5078	128.6463	0.1516	0.8795	—
Rotation Risk, Year 7	ran_pars	plot	sd__(Intercept)	1.6528	—	—	—	—
Height, Year 7	fixed		Intercept	2.8065	0.3550	7.9067	0.0010	4.2766
Height, Year 7	fixed		F/NW x DF	-0.4791	0.2729	-1.7559	0.0803	255.0988
Height, Year 7	fixed		F/W x DF	0.2330	0.2742	0.8498	0.3962	255.2926
Height, Year 7	fixed		W x DF	-0.1303	0.3007	-0.4333	0.6652	255.0181
Height, Year 7	fixed		Species Effect	-1.6128	0.2472	-6.5242	<0.0001	255.2298
Height, Year 7	fixed		F/NW x WRC	2.0906	0.3213	6.5073	<0.0001	255.2582
Height, Year 7	fixed		F/W x WRC	1.4724	0.3179	4.6314	<0.0001	255.2228
Height, Year 7	fixed		W x WRC	0.1540	0.3679	0.4186	0.6759	255.0270

Response	Effect	Group	Term	Estimate	Std. Error	Statistic	p-value	df
Height, Year 7	ran_pars	plot	sd__(Intercept)	0.4997	—	—	—	—
Height, Year 7	ran_pars	Residual	sd__Observation	0.7639	—	—	—	—
Diameter, Year 7	fixed		Intercept	32.1307	5.7313	5.6061	0.0001	11.4920
Diameter, Year 7	fixed		F/NW x DF	-12.1489	5.9108	-2.0554	0.0410	226.7370
Diameter, Year 7	fixed		F/W x DF	-2.2570	6.0938	-0.3704	0.7114	227.2229
Diameter, Year 7	fixed		W x DF	-7.6658	6.6158	-1.1587	0.2478	225.9940
Diameter, Year 7	fixed		Species Effect	-21.7394	6.0848	-3.5727	0.0004	227.3725
Diameter, Year 7	fixed		F/NW x WRC	36.8355	7.4866	4.9202	<0.0001	227.2393
Diameter, Year 7	fixed		F/W x WRC	30.0794	7.5465	3.9859	0.0001	227.1837
Diameter, Year 7	fixed		W x WRC	6.3772	8.8305	0.7222	0.4709	226.1157
Diameter, Year 7	ran_pars	plot	sd__(Intercept)	5.9804	—	—	—	—
Diameter, Year 7	ran_pars	Residual	sd__Observation	16.1489	—	—	—	—

Table S2.10. Treatment costs gathered from forest managers in western Washington. Acre estimates assume 430 trees per acre (106 trees per hectare) planted. All costs are converted to 2026 USD using the U.S. Bureau of Labor Statistics CPI series.

Treatment	Item / Activity	Source	Year	Original cost	2026 cost	× 430 seedlings	2026 per-acre total
Chemical repellent	Cost of repellent product	ONRC	2021	$0.05	$0.06	$25.80	$25.80
Chemical repellent	Cost of repellent product	Pack Forest	2015	$0.04	$0.06	$25.80	$25.80
Chemical repellent	Labor for initial spray	Pack Forest	2015	$0.15	$0.21	$90.30	$90.30
Chemical repellent	Labor for repeat spray	Pack Forest	2016	$0.37	$0.51	$219.30	$219.30
Chemical repellent	Labor for repeat spray	Pack Forest	2017	$0.37	$0.50	$215.00	$215.00
Chemical repellent	Labor for repeat spray	Pack Forest	2018	$0.38	$0.50	$215.00	$215.00
Chemical repellent	Labor for repeat spray	Pack Forest	2019	$0.39	$0.50	$215.00	$215.00
Large fence exclosure	Hardwood slashing and removal	Port Blakely	2015	$71.00	$96.77	—	$96.77
Large fence exclosure	Hardwood slashing and removal	Port Blakely	2018	$85.00	$109.71	—	$109.71
Large fence exclosure	Labor and materials for fence installation	Port Blakely	2011	$586.72	$866.54	—	$866.54
Sitka spruce co-planting	Labor for additional planting time	Pack Forest	2015	$0.33	$0.45	$193.50	$193.50
Sitka spruce co-planting	Labor for additional planting time	Pilchuck Tree Farm	2026	$0.50	$0.50	$217.50	$217.50
Sitka spruce co-planting	Labor for additional planting time	Port Blakely	2011	$0.27	$0.40	$172.00	$172.00
Sitka spruce co-planting	Labor for removing Sitka spruce	Pack Forest	2025	$0.48	$0.49	$210.70	$210.70
Sitka spruce co-planting	Labor for removing Sitka spruce	Pilchuck Tree Farm	2026	$250.00	$250.00	—	$250.00
Sitka spruce co-planting	Labor for removing Sitka spruce	Port Blakely	2020	$300.00	$378.24	—	$378.24
Sitka spruce co-planting	Sitka spruce seedling costs	Pack Forest	2015	$0.40	$0.56	$240.80	$240.80
Sitka spruce co-planting	Sitka spruce seedling costs	Pilchuck Tree Farm	2026	$0.60	$0.60	$261.00	$261.00
Vexar tubing	Bamboo	Port Blakely	2021	$0.16	$0.20	$86.00	$86.00

Treatment	Item / Activity	Source	Year	Original cost	2026 cost	× 430 seedlings	2026 per-acre total
Vexar tubing	Labor for adjusting tubes	Pack Forest	2019	$0.13	$0.17	$73.10	$73.10
Vexar tubing	Labor for adjusting tubes	Pack Forest	2017	$0.13	$0.17	$73.10	$73.10
Vexar tubing	Labor for installation of tubes	Pack Forest	2015	$0.50	$0.70	$301.00	$301.00
Vexar tubing	Labor for installation of tubes	Port Blakely	2021	$318.23	$395.40	—	$395.40
Vexar tubing	Labor for tubing maintenance	Port Blakely	2026	$0.00	—	—	$0.00
Vexar tubing	Tubes	Port Blakely	2021	$0.71	$0.88	$378.40	$378.40
Vexar tubing	Tubing materials (tubes, bamboo)	Pack Forest	2015	$0.72	$1.00	$430.00	$430.00
No treatment	Average Seedling Costs - High	Pack Forest	2026	$1	$1	$430.00	$430.00
No treatment	Average Seedling Costs – Low	Pack Forest	2026	$0.65	$0.65	$279.50	$279.50
No treatment	Average Labor Costs for Planting – High	Pack Forest	2026	$1	$1	$430.00	$430.00
No treatment	Average Labor Costs for Planting – Low	Pack Forest	2026	$0.70	$0.70	$301.00	$301.00

CHAPTER 3. EVALUATING REMOTE SENSING AND MACHINE LEARNING METHODS FOR PREDICTING UNDERSTORY BIOMASS IN POST-HARVEST FORESTS

3.0 ABSTRACT

Forest understory vegetation contributes to aboveground carbon budgets and affects terrestrial ecosystem function, yet quantification of understory biomass at large spatial scales is difficult to achieve. Increasingly, forest management operations are aided by unmanned aerial vehicles (UAVs) that collect imagery and airborne light detection and ranging (LiDAR) data, potentially providing a dataset for understory monitoring. In this study, we evaluated the suitability of two different remote sensing datasets for predicting low understory biomass amounts (field average of 2 Mg ha^{-1}) using five different machine learning models. We compared (A) LiDAR and multispectral imagery with (B) structure-from-motion (SfM) photogrammetry and multispectral imagery. We also tested and compared models using only multispectral imagery from the two acquisitions. Remotely sensed data was temporally linked to ground plots in open post-harvest conditions, where we employed a method for quick in-field biomass estimation via calibrated photos. Our best model was a stochastic gradient boosting model built with Acquisition A, using both LiDAR and multispectral data (testing R^2=0.43, training R^2=0.67). The multispectral-only model from Acquisition A performed similarly (testing R^2=0.44, training R^2=0.53), despite larger bias in shaded areas, suggesting an alternative streamlined method for creating wall-to-wall estimates. Acquisition B was unfit for this type of modeling under all tested conditions, indicating that data acquisition and post-processing may determine feasibility for certain utilities. Our study provides a framework for evaluating low

amounts of understory biomass efficiently using limited ground measurements and remotely sensed data.

3.1 Introduction

The early-seral stage, characterized by a flush of rapid understory growth, can exceed biomass accumulation in mature forests (Bormann et al., 2015) and play an important role in forest carbon budgets. Understory vegetation in the early-seral period can influence forest development pathways and contribute to carbon storage over a longer timeframe (Prescott and Sajedi, 2008). Dense understory environments can inhibit tree growth and natural seedling regeneration that results in prolonged open canopy conditions (Freund et al., 2014). Some forest managers intentionally aim to create this extended open-canopy condition to increase forest structural diversity, provide forage for critical wildlife species, and promote culturally important species (Swanson et al., 2011). Tracking and monitoring early-seral vegetation in post-harvest conditions is essential to understanding forest dynamics and management options.

Traditional understory biomass estimates involve destructive sampling or equations built with vegetation biometric data like percentage cover and plant height (Paul et al., 2016), requiring numerous in-field hours that can result in limited geographic inference. Remote sensing techniques offer an opportunity to quantify understory biomass at a scale that is meaningful to forest managers and researchers (Li et al., 2015). However, remotely sensed monitoring of early-seral vegetation in forested systems—especially small shrubs—has been limited. Technologies that accurately measure total aboveground biomass (AGB), principally dominated by overstory trees, have limited capability to quantify understory conditions (Fernández-Guisuraga et al., 2022b). Aerial LiDAR effectively captures the structure and height

of dominant overstory trees, yet occlusion of the understory from LiDAR pulses limits inference in the understory (Hull and Shipley, 2019) and LiDAR sensors can greatly underestimate vegetation height (Streutker and Glenn, 2006). Satellite imagery has been successfully linked to total AGB (Khan et al., 2024)—and in open canopy conditions, shrub biomass (Berner et al., 2018)—but spatial resolution limits fine-scale estimates.

For short and low density vegetation in open early-seral forests, conditions may be most similar to an agricultural field where remote sensing is used to monitor crop height, cover, and biomass (Jimenez-Berni et al., 2018; Pittman et al., 2015), as well as detect weeds (Andújar et al., 2013; Shahbazi et al., 2021). For these studies, crop biomass can be of interest as a proxy for drought-tolerant genotypes (Li et al., 2022). Estimation performance varies with different crop species (Prabhakara et al., 2015) and among studies of the same species: for predicting sorghum biomass, model performance ranges from 0.11 R^2 (Li et al., 2022) to 0.89 R^2 (Masjedi et al., 2020). At the low end of biomass values, there can be additional error (Prabhakara et al., 2015). Numerous factors may influence model performance including equipment selection, sample size, and acquisition timing.

Researchers have investigated a variety of methods to map understory biomass in forested systems. Some approaches use aerial data acquisitions: researchers paired photo-based understory cover board estimates, a tool to visually measure understory, with aerial LiDAR to predict vegetation structure ($R^2 = 0.44$) (Campbell et al., 2018). Shrestha et al. (2021) used traditional understory measurements and a LiDAR sensor affixed to an unmanned aerial vehicle (UAV) to effectively quantify understory biomass in open conditions in the southeast United States ($R^2 = 0.51$). Due to the common issue of understory occlusion with aerial data acquisitions, researchers have found success when remotely sensed data are collected from the

ground level (Li et al., 2021). Terrestrial Laser Scanning (TLS) offers close-proximity, high-resolution data from a horizontal rather than vertical vantage point and has been used in conjunction with aerial LiDAR to predict horizontal vegetation cover with a testing accuracy of 85% (Batchelor et al., 2023). Similarly, close-range photogrammetry with a GoPro resulted in poor total plot biomass estimates (R^2 = 0.08 to 0.21) but predictions were improved when the lowest stratum of vegetation was removed (R^2 = 0.74 to 0.85) (Cova et al., 2023). These ground-based methods require special remote sensing data collection campaigns that are not typical of normal forest management operations.

Building on this body of work, this study aims to further explore remote sensing datasets that may already be routinely collected for forest managers to quantify understory biomass. Increasingly, forest management operations are aided by UAVs, which offer information at stand and large spatial scales that can guide management decisions. Unlike other remote sensing methods, UAVs offer flexible acquisition timing, high-density point clouds, and high spatial resolution (Fernández-Guisuraga et al., 2022a). These acquisitions allow for relatively low-cost and replicable measurement and analysis of experimental treatments compared to expansive field plots. UAVs may be affixed with a LiDAR sensor, or more typically for forest management, just a multispectral or red, green, blue (RGB) camera. Camera imagery can be stitched together to create structure-from-motion (SfM) photogrammetric point clouds that can be analyzed using the same techniques used for LiDAR point clouds (Fernández-Guisuraga et al., 2022a). Zhang et al. (2022) used an ultralow-flying drone and SfM to predict understory vegetation biomass based on a canopy height model. These techniques can have utility for certain forestry questions but lack of clarity about tradeoffs can make a single approach challenging to select.

Our study is part of a larger experiment called the T3 Watershed Experiment, a 20,000-acre operational-scale experiment in the Olympic Experimental State Forest (OESF), Washington, U.S.A., aimed at expanding forest management options through the implementation of novel forest treatments. Several prescriptions within this experiment include a variable retention harvest followed by planting in ways that encourage and extend the early-seral forest stage, where understory biomass and species diversity can flourish (Swanson et al., 2011). Understory responses to these treatments have implications for co-benefits such as carbon sequestration, ungulate habitat and forage, and presence of culturally important species. A major goal of our study is to create baseline understory biomass estimates immediately post-harvest, upon which future work within the T3 Watershed Experiment can be built. A challenge for this goal is that baseline conditions at the study sites require modeling only very small amounts of understory (field measurements averaged 2 Mg ha^{-1}), placing additional pressure on the remote sensing technology to capture sufficient information for accurate quantification.

Machine learning models can leverage remote sensing datasets to produce predictions that capture complex and non-linear relationships with less sensitivity to noise (Thapa et al., 2023). For predicting total AGB—not just the understory—non-parametric machine learning models are often employed, such as k-nearest neighbor, artificial neural networks, support vector machine, random forest, gradient boosting, and maximum entropy (Tian et al., 2023). These machine learning methods offer tradeoffs in performance versus explainability of the model, as well as handling small datasets and noise (D. Lu et al., 2016). Nevertheless, when comparing model performance, data type and quality can matter more than model selection in overall model performance (Almeida et al., 2019).

For our study, we have two remotely sensed datasets: Acquisition A—UAV acquired LiDAR and multispectral imagery collected in 2024, and Acquisition B—UAV SfM photogrammetry and multispectral imagery collected in 2025. By pairing these remotely sensed datasets with photo-based understory ground plot measurements, our study aims to answer the following questions:

1. How do remote sensing approaches—UAV LiDAR with multispectral imagery versus UAV SfM photogrammetry with multispectral imagery—compare in their ability to predict understory biomass?

2. How and under what conditions can remote sensing aid in measuring understory biomass and novel treatment effectiveness?

3. Which machine learning model provides the most accurate predictions of understory biomass in open post-harvest conditions?

We seek to answer these questions while prioritizing feasibility and repeatability for researchers and managers in terms of available data and resources.

3.2 Materials and Methods

Study Area

The Olympic Peninsula is located in the northwest portion of Washington state (WA), U.S.A. The western portion of the Peninsula is characterized by temperate rainforests, which are predominantly wet, evergreen, and coniferous. Our study was conducted across two experimental sites on land managed by the Washington Department of Natural Resources (DNR) and within the Olympic Experimental State Forest (OESF) on the Olympic Peninsula: (1) the T3 Watershed

Experiment near the Hoh and Clearwater watershed, and (2) the Ethnoforestry field trials study site near La Push, WA (Figure 3.1.). Mean annual temperature in this region is 10.4°C (14.9°C for May–September), and average annual precipitation is 2959 mm (average of 90 mm for May–September) (PRISM Climate Group, Oregon State University, 2026).

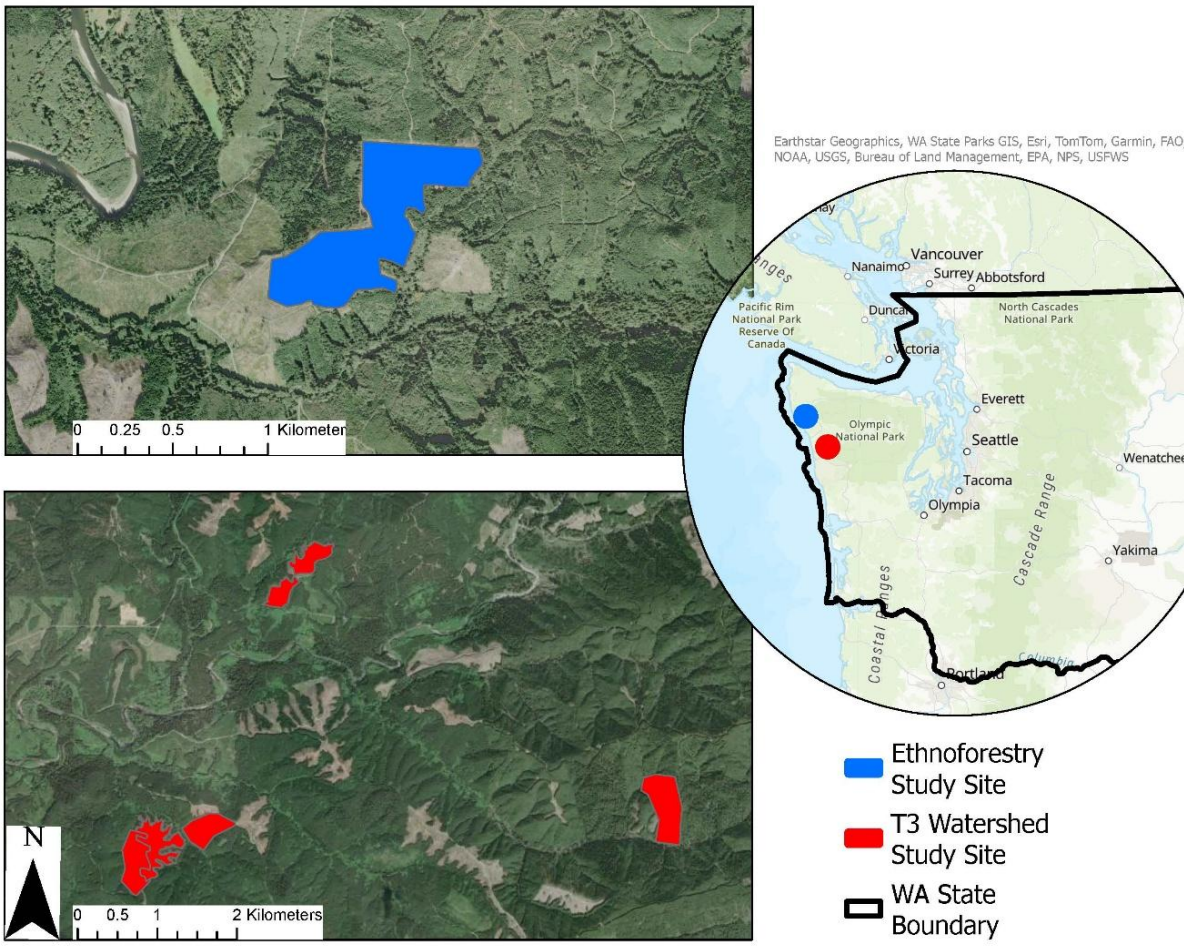

Figure 3.1. Two experimental sites within the Olympic Experimental State Forest in WA were analyzed in this study: the Ethnoforestry field trials study site near La Push, WA (blue, top frame) and various harvested units part of a much larger 20,000-acre experiment called the T3 Watershed Experiment (red, bottom frame).

T3 Watershed Experiment study site

This study evaluates post-harvest conditions on three separate treatments that are part of the larger T3 Watershed Experiment: Variable Density Planting (VDP), Complex Early Seral (CES), and Polyculture (Poly). All T3 Watershed Experimental treatment units were harvested in 2024–2025 with various silvicultural designs. Woody debris from the harvests were left on site. Pre-harvest conditions for the study sites were dominated by a dense western hemlock (*Tsuga heterophylla* (Raf.) Sarg.)/Douglas-fir (*Pseudotsuga menziesii* (Mirb.) Franco) overstory. For the purposes of this study, data collection was concentrated in open-canopy, post-harvest conditions and performed before herbicide applications and planting. In year 2025, understory species composition included a mixture of (1) graminoids including velvet grass (*Holcus lanatus* L.), spike bentgrass (*Agrostis exarata* Trin.), and small flowered woodrush (*Luzula parviflora* (Ehrh.) Desv.); (2) diverse forbs including fragrant bedstraw (*Galium triflorum* Michx.), woodland ragwort (*Senecio sylvaticus* L.), Siberian springbeauty (*Claytonia sibirica* L.), redwood-sorrel (*Oxalis oregana* Nutt.), and many others; and (3) a mixture of shrubs and ferns that were likely growing prior to timber harvest and survived, including salal (*Gaultheria shallon*), red huckleberry (*Vaccinium parvifolium* Sm.), western sword fern (*Polystichum munitum* (Kaulf.) C. Presl), and deer fern (*Blechnum spicant* (L.) Sm).

Ethnoforestry field trials study site

The Ethnoforestry field-trials study site is part of an existing randomized-block experiment to explore people-focused understory management (see Bobsin, 2023). Pre-harvest conditions for the study sites were dominated by a dense western hemlock/Douglas-fir overstory. The unit received a variable retention harvest in 2018, an herbicide application in August 2020,

and planting from January to April 2021. Woody debris from the harvests were left on site. The units were planted with Douglas-fir and red alder (*Alnus rubra* Bong.) as well as five understory species: whitebark raspberry (*Rubus leucodermis* Douglas ex Torr. & A. Gray), Roemer's fescue (*Festuca idahoensis* Elmer spp. *roemeri* (Pavlick) S. Aiken), salmonberry (*Rubus spectabilis* Pursh), tall Oregon grape (*Mahonia aquifolium* (Pursh) Nutt.), and Nootka rose (*Rosa nutkana* C. Presl). In addition, understory regenerated naturally at this site over time with a similar mixture of graminoids, forbs, shrubs, and ferns as the units in the T3 Watershed Experiment. Dominant species at this site included hairy cat's ear (*Hypochaeris radicata* L.*),* purple foxglove (*Digitalis purpurea* L.), spike bentgrass, velvetgrass, red elderberry (*Sambucus racemosa* L.), salal, several blackberry species (*Rubus* spp.), and many others.

Ground Data: Understory Biomass

Field measurements for understory biomass and species cover were collected on all study sites throughout the summers of 2024 and 2025. Understory-biomass ground plots were measured by comparing the live understory biomass within the boundaries of the plot to a set of images in a Biomass Booklet created for this purpose. This booklet contains 31 images of 3 m x 3 m plots with associated dry weight values (Mg ha^{-1}). Each image represents a different set of understory species with varying levels of biomass, identified through traditional methods of drying and weighing vegetation. Field crews matched plot images with conditions in ground plots to obtain biomass measurements (Figure 3.2.). For example, if their ground plots were predominantly sword fern, crews looked for images within the Biomass Booklet that contained sword fern and determined which image most closely aligned with ground conditions. In certain situations, no single photo would perfectly capture ground conditions. To mitigate this, the field crews took measurements from two sides of the plot and averaged those biomass totals. In

addition, the crews were allowed to add or subtract a percentage from any given photo if no single image captured field conditions. For example, if their ground plot contained twice as much sword fern as the best sword fern image within the booklet, the crew could double the amount of biomass in the associated image and record this on their data sheet.

This method allows for fast ocular biomass estimates for plots of similar conditions and species distribution. To expand the condition options within the Biomass Booklet to better reflect early-seral conditions on all of the harvested study sites, plots outside the boundaries of the study area were photographed and received traditional biomass measurements: all vegetation within a 3 m x 3 m quadrat was removed, dried in ovens to a constant mass, and weighed. Total biomass (Mg ha^{-1}) was calculated based on the dry weight values. New images and their associated biomass values were added to the booklet to represent these early-seral conditions for future use.

Figure 3.2. An example of a calibrated photo from the Biomass Booklet, which contains a series of photos with corresponding biomass values. Text at the bottom of each image specifies dried weight for the vegetation in the photo and the corresponding dominant species in the plot, and photos are labeled for easy data entry (F2 label in the top right). Field crews matched 3 m x 3 m plot conditions with the best-fit photo to create quick ocular estimates that were then used to create our predictive model.

Plot locations were distributed throughout the harvested units and stratified to capture the range of site conditions, while remaining limited to open-canopy areas. Biomass plots were georeferenced using a Javad Triumph 2, a survey grade GNSS receiver, so they could be spatially connected to remote sensing data (San Jose, CA, USA). Previous studies using post-processed Javad Triumph 2 data in Pacific Northwest forested conditions found a horizontal accuracy of 1.76 m, but this study found on average, slightly better results due to the open-canopy conditions (McGaughey et al., 2017). Due to this slight offset, plot locations as recorded with the Javad Triumph 2 (Javad) were not perfectly aligned with remotely sensed data. A matching procedure outlined in Kruper, 2024 was used to spatially adjust plot locations, using the LiDAR data as the locational standard. A series of LiDAR visible objects, such as stumps and downed logs, were used as reference points to adjust Javad plot locations to better match corresponding reference

points in the LiDAR data. All adjustments were performed manually in ESRI ArcGIS Pro (ESRI, 2022).

In most instances, plot locations were identified by two points at opposite corners to represent the full 3 m by 3 m square. When the two points were brought into ArcGIS, plot boundaries were not perfectly square. To resolve this and create a best match of in-field conditions, a center point between the two georeferenced points was generated and then a perfect 3 m x 3 m square was calculated around that center point. A small fraction of the ground plot data was taken with one central georeferenced point, for which the 3 m x 3 m square was calculated around that center point. For the Ethnoforestry field trials study site, this process was completed with 1.5 m x 1.5 m square plot boundaries, but these plots were related back to the biomass booklet at the 3 m x 3 m scale and therefore estimates were still at the 3 m x 3 m scale.

Due to various georeferencing issues, such as a missing plot corner location, some plots had to be removed from each dataset. The final data included 191 ground plots measured in 2024 for Acquisition A (53 from T3 Watershed Experiment and 138 from Ethnoforestry field trials) and 183 in 2025 for Acquisition B (25 from T3 Watershed Experiment and 158 from Ethnoforestry field trials).

UAV Remotely Sensed Data

There were two separate remotely sensed data acquisitions across the study sites: Acquisition A in 2024 using UAV lidar and multispectral imagery, and Acquisition B in 2025 using UAV SfM photogrammetry and multispectral imagery (Table 3.1). Remotely sensed data were matched with the ground data from the respective summers, creating two temporally linked datasets. For both acquisitions, ground data and remotely sensed data were separated in time by

no more than two months. The two acquisitions had overlapping areas flown, including all the Ethnoforestry field trials study site, as well as non-overlapping additional study areas within the T3 Watershed Experiment for both flights (roughly half of the flight area in Acquisition A was reflown for Acquisition B). For Acquisition A, remote sensing data were acquired for 91.1 hectares; for Acquisition B, remote sensing data was acquired for 215 hectares.

Table 3.1. Study site information for the two areas where field and remote sensing data were acquired. For Acquisition A (A), field and remote sensing data were both acquired during the summer of 2024. For Acquisition B (B), field and remote sensing data were both acquired during the summer of 2025.

Study Site	Year Harvested	Year Herbicide	Year Planted	Hectares Flown for A	# of Ground Plots for A	Hectares Flown for B	# of Ground Plots for B
T3 Watershed Experiment	2024-2025	NA	NA	72.5	53	116.3	25
Ethnoforestry field trials	2018	2020	2021	18.6	138	98.7	158

Acquisition A

In the summer of 2024, both UAV LiDAR and multispectral imagery data were collected by the natural resource consulting firm West Fork Environmental. LiDAR data were collected using a DJI Matrice 600 Pro UAV, with a Surveyor 32 LiDAR instrument, manufactured by LiDAR USA, with a Pandar XT32 scanner, made by Hesai. LiDAR flight height was 60 meters above ground level. Point density ranged from 402 to 702 points m^{-2}. Multispectral imagery was acquired with a DJI Matrice 210 UAV, with an attached Altum-PT sensor made by Ag Eagle, formerly known as MicaSense. Imagery was collected at 120 meters above ground level. The Altum-PT sensor resolutions include 2064 × 1544 (3.2 MP per multispectral band), 4112 × 3008 (12 MP panchromatic), and 320 × 256 thermal infrared. For multispectral bands, the spectral ranges were the following: Blue (475 ± 16 nm), Green (560 ± 16 nm), Red (668 ± 14 nm), Red Edge (717 ± 12 nm), and Near-infrared (842 ± 57 nm). Processing was done with Agisoft

Metashape. A calibration panel was used prior to takeoff and immediately following acquisition to calibrate the imagery in metashape. Photo alignment was performed with high accuracy, a no tie point limit, and 40,000 key points per photo limit. An orthomosaic surface was created using a DEM built within the Metashape software using the imagery dense point cloud. Spatial resolution for the imagery was 0.05 m.

A ground model was provided by the vendor using the following procedure and created with R programming software (R Core Team, 2022): extract the lowest points in the LiDAR point cloud (from 0–0.15 m aboveground level); run the lidR classify_ground function using the Progressive Morphological Filter (PMF) option with a window sizes set to 3, 12 and 3 meters and linearly spaced elevation thresholds between 0.1 m and 1.5 m; and generate a DTM using a Triangulated Irregular Network interpolation method at a resolution of 0.5 m.

Acquisition B

In the summer of 2025, DNR used a DJI Mavic 3 Multispectral UAV to collect multispectral imagery, which was used to create a point cloud using SfM photogrammetry. The UAV was flown 122 m (400 ft) above ground level. For this acquisition, the RGB camera had a 20 MP resolution and a maximum image size of 5280 × 3956. The multispectral camera had a 5 MP effective resolution and captured four bands—Green (560 ± 16 nm), Red (650 ± 16 nm), Red Edge (730 ± 16 nm), and Near-infrared (860 ± 26 nm)—at a maximum image size of 2592 × 1944. Spatial resolution for the imagery was 0.04 m. Processing was done with Agisoft Metashape. Photo alignment was performed with high accuracy, a no tie point limit, and 40,000 key points per photo limit. The point cloud was created using densest possible point cloud without filtering noise. Point density ranged from 33 to 155 points m^{-2}. For camera optimization, there was no adaptive camera model fitting, and fitting all other parameters (f, k1, k2, k3, k4,

cx+cy, p1, p2, b1, b2). An orthomosaic surface was built from tie points, with a low poly surface count. Ground sampling distance varied but was on average ~2.5 cm per pixel.

Two different ground models were assessed for use: (1) an aerial LiDAR derived DTM from the Washington State LiDAR portal, and (2) a ground model generated from the SfM photogrammetric point cloud data, following the process outlined for the Acquisition A dataset. Option two, the generated ground model, was used for all further data processing and analysis.

Remotely Sensed Data Processing

All data processing was completed using R (R Core Team, 2022), and for the data processing stage, generative artificial intelligence (OpenAI, 2025) was used to explore functions, refine code, and debug code. The authors have reviewed and edited all outputs and take full responsibility for the content of this publication. Data processing was divided into two phases for both Acquisition A and B: (1) processing stand-scale data at the full geographic extent of the acquisitions to be used for model prediction, and (2) processing plot-scale data at the 3 m x 3 m (or 1.5 m x 1.5 m for Ethnoforestry field trials) scale for the creation of the models.

All data processing described in this section was the same for Acquisition A and B. Although the two acquisitions captured different multispectral bands, only the bands common to both were retained for the final models making the datasets equivalent in usable statistics. To make the two datasets match, statistics on multiband reflectance, panchromatic band and long-wave infrared were removed from Acquisition A, and statistics generated from the green multi-reflectance band and the red multi-reflectance band were removed from Acquisition B.

Stand-Scale Data Processing

The FUSION software (version 4.61) was used to process the Acquisition A LiDAR and Acquisition B SfM photogrammetric point cloud data (McGaughey, 2024). Data for entire acquisition areas was run through the GridMetrics function to generate statistics on the point cloud. Points were normalized using the ground DTM. All points above zero were considered, ground points were ignored, a cellsize of 3 m was used to match the ground plot size, and statistics were generated using the following height strata (meters above ground): 0.5, 1.0, 1.5, 2.0, 2.5, 3.0, 3.5.

For image processing, composite images were created following Xie et al. (2018). The following images were used in the analysis: RGB, False Color Near-Infrared (NIR), False Color Red Edge, Normalized Difference Vegetation Index (NDVI) using NIR and Red, NDVI using NIR and Red Edge, Modified Simple Ratio (MSR) using NIR and Red, MSR using NIR and Red Edge, Chlorophyll Index (CI) using NIR and Green, CI using NIR and Red Edge, NDVI using NIR, and weighted Red + Red Edge, MSR using NIR and weighted Red and Red Edge, Chlorophyll Index using NIR and weighted Red and Red Edge.

The aggregate function within Spatial Data Analysis (terra) package within R studio (Hijmans et al., 2026) was used to extract statistics at a 3 m resolution for all image layers. The following statistics were generated for each 3 m section of each composite image: max, min, mean, standard deviation (sd), 25th quantile, 75th quantile and coefficient of variation.

The results of this stand level processing were a series of files containing statistics for all flown units at a 3 m x 3 m scale to match the scale of ground plots.

Plot-Scale Data Processing

Plot level data processing matched as much as possible the stand level data processing. The georeferenced and adjusted 3 m × 3 m ground (1.5 m x 1.5 m for Ethnoforestry field trials) plot locations were used to extract statistical information from all remotely sensed datasets, with point-based statistics generated using the FUSION software. First, LiDAR and SfM point cloud data were clipped to plot locations using the PolyClipData function. Plot elevations were normalized using the ClipData function and the ground DTM. This output was fed to the CloudMetrics function using parameters that matched the GridMetrics call applied to stand-level data; statistics were generated for height strata at 0.5 m increments from 0.5 to 3.5 m above ground.

For image processing at the plot level, data for each georeferenced plot location was extracted from all of the generated composite images using the extract function within the terra package, producing the same statistics as the aggregate function noted above: max, min, mean, standard deviation (sd), 25th quantile, 75th quantile and coefficient of variation.

Data cleaning

Plot-scale statistics for the point clouds and multispectral imagery were joined for model building. Datasets created with Acquisition A and B were compared so that only shared columns across the two datasets were kept (330 columns for each dataset), making differences in multispectral bands available across the acquisitions irrelevant. Certain columns contained many NA values due to statistics being generated for height thresholds that the low-lying vegetation did not reach. For example, if the generated statistic was “standard deviation for all returns between 2.5 and 3 m”, but vegetation within the plot did not reach that height, then an NA value

would be generated. “N/A” values were then replaced with zeros for columns where no data values should logically be zero, such as point cloud statistics on counts or proportion. Subsequently, all columns with greater than 30% “N/A” values were removed; this threshold was chosen because it was a natural breakpoint in the column-wise distribution of “N/A” values. Next, using the softImpute function within the softImpute package in R, a Principal Component Analysis (PCA) based imputation with 10 principal component was used to fill in remaining “N/A" values (Hastie et al., 2015; Mazumder et al., 2010). Next, columns with a variance lower than 0.01 were dropped and highly correlated columns were filtered using the findCorrelation function in the caret R package (Kuhn, 2008). Of the predictors that had a correlation higher than 0.95, the predictor that was more highly correlated with the entire dataset was dropped.

This resulted in 188 available predictors: 59 variables from the point cloud data and 129 variables from the multispectral imagery data. A full list of variables used in model building is available in the Supplementary Materials (Table S3.4). Broadly, major categories of variables that were culled based on criteria listed in the methods section include: all point cloud intensity metrics, metrics related to points in certain elevation strata where there were insufficient points, multispectral metrics that were only available with one acquisition but not the other, and multispectral metrics that were highly correlated.

The data were split into training and testing data, 80% train and 20% test, randomized across all samples (n=152 for A and n=146 for B). Predictor variables were mean-centered and scaled to unit variance using statistics derived from the training data, and the same transformations were applied to the corresponding test datasets. We then subset the 129 multispectral columns from each dataset and saved them separately, leaving us with four datasets for model building: (1) Acquisition A LiDAR and multispectral data, (2) Acquisition A

multispectral data only, and (3) Acquisition B SfM photogrammetry point cloud and multispectral data, and (4) Acquisition B multispectral data only.

Machine Learning Models

Five machine learning models were fit to each of the four datasets: random forest (rf), stochastic gradient boosting (gbm), extreme gradient boosting (xgbTree), k-nearest neighbors algorithm (knn), and generalized linear model (glmnet). Hyperparameter tuning was performed on all models using the caret package, using 5-fold cross-validation repeated 3 times in the training data. All hyperparameter combinations, with final hyperparameter choices, were applied to all 4 datasets and are available in Table S3.5. A small feed-forward neural network with two hidden layers was also implemented and tuned. However, it is omitted because it showed signs of significant overfitting, which can be expected in this use case due to limited and highly variable data. All models were fit to maximize the coefficient of determination, and this value as well as RMSE were computed.

Prediction

Stand-scale data were filtered and cleaned, following the same process as the plot level data. Data were scaled using statistics derived from the training dataset. The two best models were used to predict understory biomass (Mg ha^{-1}) across all available stands. Ground data were collected in open-canopy conditions, so areas with existing canopy cover were removed from understory biomass totals for each experimental unit. Removal of these values was done using the mask function in the terra package, in which tree polygons generated in FUSION were buffered, unioned and then masked from the final predictive raster. In addition, ArcGIS was used

to draw freehand polygons around heavily shaded regions and were also removed from the final prediction rasters. Prediction totals were generated using the global function in the terra package.

3.3 Results

Model Performance

The predictive performance of Acquisition A was superior to all models produced with Acquisition B dataset (Figure 3.3.). The best models were the stochastic gradient boosting models from the Acquisition A dataset, with the highest coefficients of determination and lowest RMSE values (LiDAR and multispectral: R^2 = 0.43, RMSE = 0.76 Mg ha^{-1}, relative error = 0.46; multispectral only: R^2= 0.44, RMSE = 0.75 Mg ha^{-1}, relative error = 0.47). Acquisition A random forest models also performed comparably but tended to be overfit evident by the high training coefficients of determination, and much lower testing coefficients of determination (LiDAR and multispectral: R^2=0.39, RMSE = 0.78 Mg ha^{-1}, relative error = 0.48).

For Acquisition B, all tested machine learning models were overfit, determined similarly by high training R^2 values and low testing R^2 values, indicating that the mean of the data would create a better prediction than these models. Visual inspection of Acquisition B SfM point cloud suggests poor spatial registration in the imagery contributed to poor model performance.

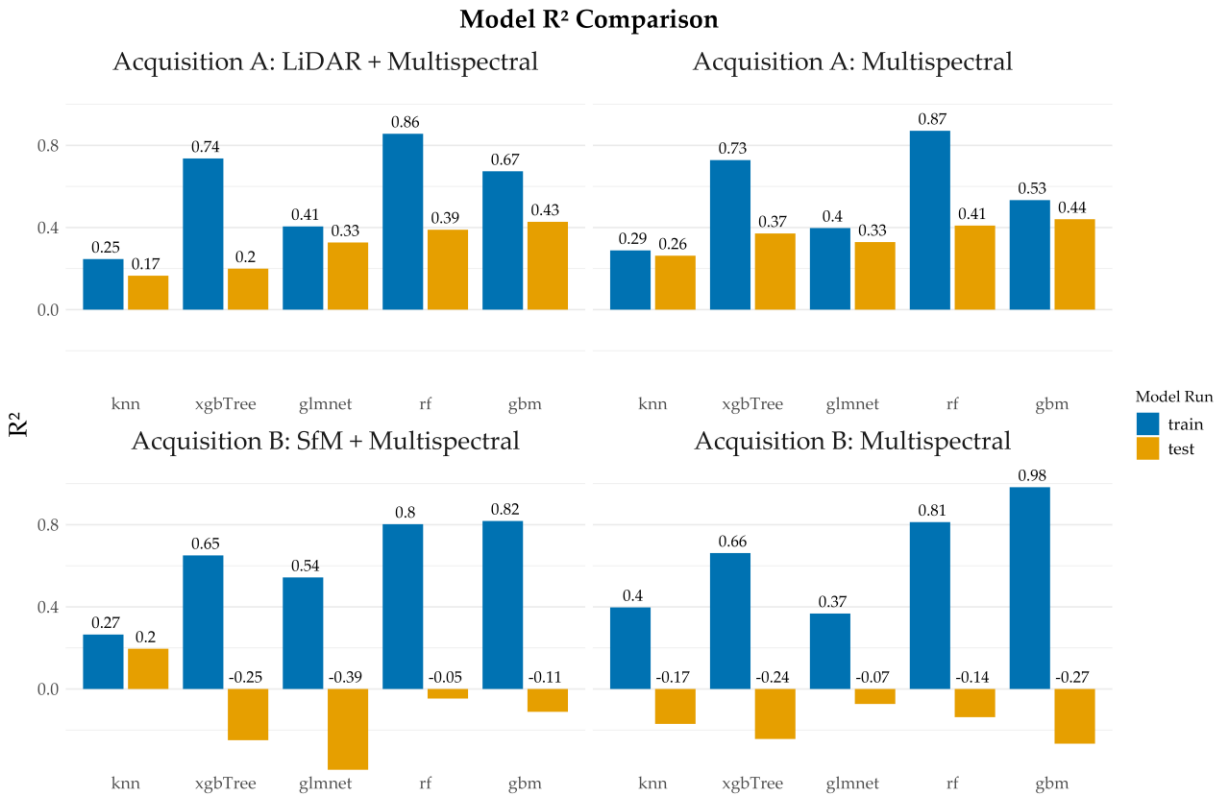

Figure 3.3. Coefficient of determination (R^2) training and testing data model results for Acquisition A and B. The following datasets were tested: (1) Acquisition A LiDAR and multispectral data, (2) Acquisition A multispectral data only, and (3) Acquisition B SfM photogrammetry point cloud and multispectral data, and (4) Acquisition B multispectral data only. The following models were trained and tested: k-nearest neighbors algorithm (knn), extreme gradient boosting (xgbTree), generalized linear model (glmnet), random forest (rf), and stochastic gradient boosting (gbm).

All tested models predicted higher values where trees created shade in the imagery, but this tendency was more extreme with the multispectral only models. Although Acquisition A multispectral-only model resulted in better model statistics than Acquisition A LiDAR and multispectral model, the multispectral-only model predicted higher biomass values overall, and upon visual inspection, seemed to overpredict in these shaded regions. All models also predicted high biomass values in leave-tree zones, where trees were left after harvest. Ground plots were not taken under existing canopy, nor were they stratified to include areas that would be shaded in the imagery, so predictions in these areas were outside the scope of the model capabilities and

not considered in final stand biomass estimates (Figure 3.4.). Biomass estimates produced from our best model, Acquisition A LiDAR and multispectral model, for each stand can be found in Table 3.2.

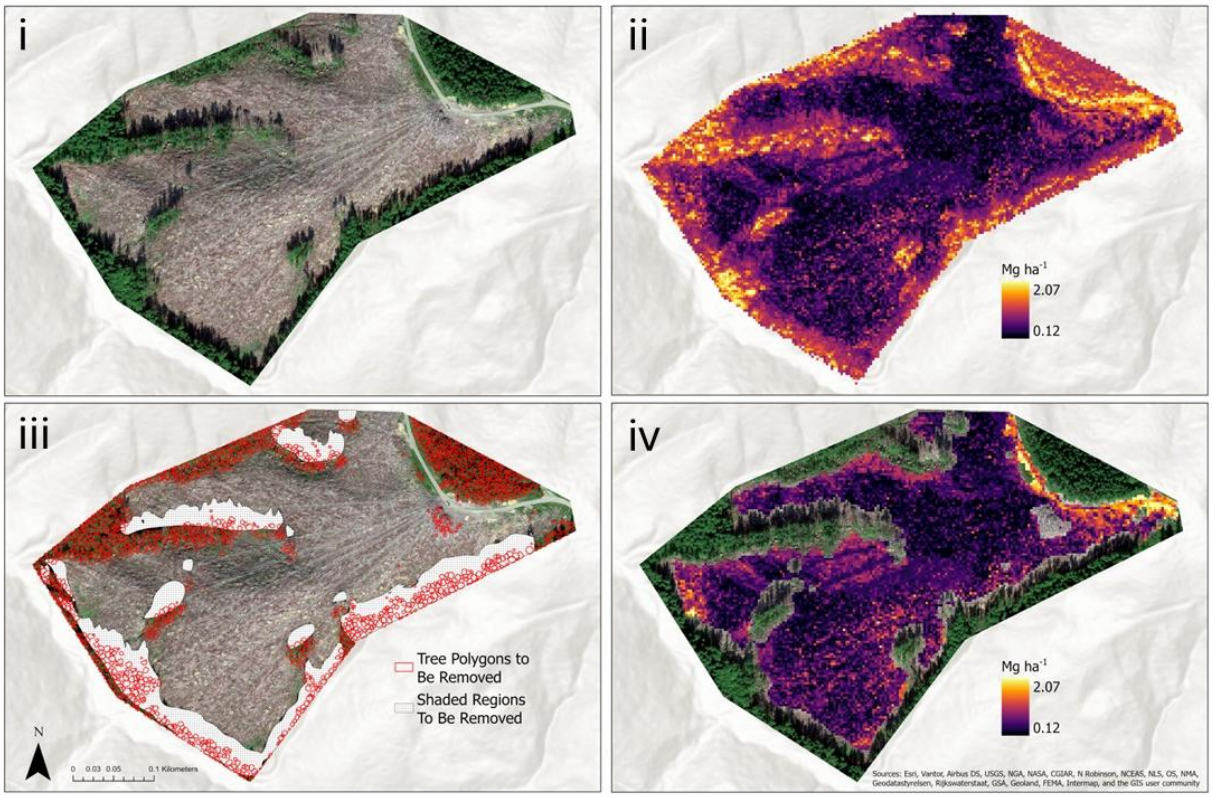

Figure 3.4. Images are of the Variable Density Polyculture unit within the T3 Watershed Experiment. These four panels show the filtering process for generating wall-to-wall understory biomass predictions using our best performing model, the LiDAR and multispectral stochastic gradient boosting model built with Acquisition A. Panels are the following: i) Aerial image of harvested unit at time of data collection, ii) biomass predictions in Mg $ha^{-1}$of the entire unit, including areas outside of the scope of the model, such as shaded and closed canopy regions, iii) shaded and closed canopy regions to be removed from the final model predictions, iv) final model predictions to be used as baseline estimates for future experimental work and forest management decisions.

Table 3.2. Biomass estimates for stands measured with Acquisition A. These predictions do not include leave-tree areas or areas that were shaded in the imagery, as those were areas where the model had less predictive power. Acquisition B models were not used for prediction because of their poor performance.

Stand Name	Number ha predicted	Total Area Estimate (Mg)	Average (Mg ha^{-1})	Standard Deviation Predicted (Mg ha^{-1})
Variable Density Polyculture	9.1	4.4 Mg	0.49	0.27
Polyculture	10	6.8 Mg	0.67	0.30
Complex Early Seral	9.1	4.3 Mg	0.48	0.20
Ethnoforestry Field Trials North	6.4	8.9 Mg	1.4	0.34
Ethnoforestry Field Trials South	8.0	11 Mg	1.4	0.38

Variable Importance Scores

The top five predictors for all created models were multispectral variables (Table 3.3.). Bands that were particularly important include red edge, MSR, CI using NIR and Red Edge, and NIR. These results indicate that for our tested models, LiDAR metrics were not as important as multispectral metrics.

Table 3.3. The top five most important predictors using relative ranking for the two best models created with Acquisition A (A). Multispectral data were the most important for all tested models. Statistics were calculated for each band within each composite image, so certain bands of composite images scored higher than others. "q" stands for quantile.

Tested Dataset	Best Model	Most Important Variables	Importance Scores
A: LiDAR and Multispectral	stochastic gradient boosting	Red-edge, band 1, 75^{th} q	100
		Modified Simple Ratio, band 1, 75^{th} q	68
		Chlorophyll Index red-edge, band 1, 25^{th} q	37
		Near-infrared, band 1, min value	34
		Red-edge, band 1, min value	33
A: Multispectral only	stochastic gradient boosting	Red-edge, band 1, 75th q	100
		Modified Simple Ratio, band 1, 75th q	68
		Chlorophyll Index red-edge, band 1, 25th q	42
		Near-infrared, band 1, min value	37
		Red-edge, band 1, min value	30

3.4 Discussion

We connected ground-based understory biomass estimates to two distinct UAV data acquisitions to identify feasibility of using these common datasets to predict wall-to-wall understory biomass for forest management and research. Three research questions guided the analysis:

1. How do remote sensing approaches—UAV LiDAR with multispectral imagery versus UAV SfM photogrammetry with multispectral imagery—compare in their ability to predict understory biomass?;
2. How and under what conditions can remote sensing aid in measuring understory biomass and novel treatment effectiveness?; and
3. Which machine learning model provides the most accurate predictions of understory biomass in open post-harvest conditions?

In addition, this work sought to document baseline conditions for experimental units as part of a larger long-term experiment.

Through the combination of UAV LiDAR, multispectral imagery and ground biomass plots, we calculated coarse estimates of biomass across the entire stand, functional for estimating low, medium, and high biomass amounts. We created a pathway for limited in-field data collection using a set of calibrated photos called the Biomass Booklet, that can be linked to commonly acquired forestry remote sensing data with very little additional field work. Furthermore, we identified the weaknesses in the approach—even in open-canopy conditions with high spatial resolution UAV-based data, SfM photogrammetry alone was ill-suited for this type of research. The combination of low biomass values and poor spatial registration likely resulted in relatively low estimation performance for all models tested.

How do remote sensing approaches—UAV LiDAR with multispectral imagery versus UAV SfM photogrammetry with multispectral imagery—compare in their ability to predict understory biomass?

Acquisition A was able to generate predictions for understory biomass across management units, but model estimation performance was relatively low (R^2 = 0.43). Although other researchers have had better modeling success with biomass estimates when average biomass levels are significantly higher (Alonzo et al., 2020; Zhang et al., 2022), our study reflects variability in the field and the challenges of measuring and predicting extremely low biomass values (Li et al., 2022). Our model results from Acquisition A suggest that comparable predictions can be generated using multispectral data alone, significantly reducing data processing time compared to processing both imagery and LiDAR data. Upon visual inspection of the wall-to-wall estimates, the multispectral-only model may be less useful in areas with leave trees, where shade may reduce model performance. Based on our variable importance scores, the multispectral statistics were of highest utility for all our models, which we suspect were effectively capturing presence and absence of low-lying vegetation. Our study site also had a high degree of woody slash, which at times, was taller than the vegetation, and could be affecting our model performance as an additional layer of occlusion and source of error in point filtering (Wing et al., 2012). When vegetation height is a greater determinant for total volume and therefore total biomass, and overtopping the coarse woody debris, we suspect that the LiDAR-based statistics will have higher relevance and our model performance may improve.

In contrast, Acquisition B, using SfM and multispectral imagery, was unfit for this type of analysis under all tested conditions, which is not particularly surprising considering SfM is a technique with mixed results for low-lying vegetation (Zahawi et al., 2015). We analyzed this

dataset with two different ground models: one using the public access DTM from the WA State LiDAR portal and one with a ground model generated from the SfM point cloud. SfM photogrammetry extracts keypoints from individual photos, finds keypoint matches between photos, and uses algorithms to reconstruct feature and camera locations (Dandois and Ellis, 2013). Through visual inspection of the point cloud with both ground models, we suspect this dataset had poor spatial registration between photos, leading to floating points and a high degree of noise. This noise may be tolerable for some types of analysis, but due to our small plot size (3 m x 3 m) and minimal low-lying modeled vegetation, vegetation size (branch and foliage) likely made image matching challenging. Moreover, photos must capture all vegetation angles to generate sufficient signatures. Through comparing the multispectral-only models from Acquisition A and B, we can see that the quality of the Acquisition B multispectral-only data was also poor, meaning that this issue likely extended to the post-processing and stitching together of the orthomosaic imagery. Cunliffe et al. (2016) used SfM motion photogrammetry to model biomass at a fine scale, but they employed systematically acquired convergent image data, nadir image data, and high-precision ground-control points, which required multiple flights over the same area. In our case, post-processing of the Acquisition B dataset was done following standard protocol for forest management where a high level of optimization is not needed. A lack of precision in feature matching within Acquisition B likely caused poor performance in the corresponding models.

Differences in model performance between the two Acquisitions may also be attributed to equipment. For example, Acquisition A multispectral imagery was acquired with an Altum-PT sensor, whereas Acquisition B used the Mavic 3 Multispectral camera. Product performance

differences for the cameras, as well as differences in position and altitude sensing instrumentation, may account for at least part of the performance discrepancies.

How and under what conditions can remote sensing aid in measuring understory biomass and novel treatment effectiveness?

Our study benefited from numerous advantages that made low biomass understory estimates possible, despite understory predictions being more challenging to generate than upper canopy predictions (Fernández-Guisuraga et al., 2022b). First, we had temporally linked remote sensing and ground datasets that were no more than two months apart in time. Understory biomass can grow quickly, so timing of data acquisition influences matching of on-the-ground conditions with remote sensing signatures, and discrepancies in data collection timing can complicate study outcomes (Prabhakara et al., 2015). Second, knowing that understory biomass is difficult to measure when tall trees are present, we focused our analysis on open-canopy conditions. Because our study was conducted on the Olympic Peninsula, where forests are extremely dense, plots under existing canopy cover were unlikely to generate reasonable model predictions. Based on other studies in more open forests (Olsoy et al., 2024), we suspect this process could be replicated in other locations with some existing tree cover, such as low-density dry forests. Third, our remotely sensed data set was extremely high density (33–702 points m^{-2}), which would be achievable only with a UAV and professional-grade equipment.

A key component of this work that made this remote sensing study feasible was the Biomass Booklet, a set of calibrated photos for quick visual understory biomass estimates. This tool allowed for minimal ground crew work: crews were tasked to take plots in designated areas, they established georeferenced plot information, measured a 3 m x 3 m square, and then chose an

estimated biomass value. Georeferencing can be completed once for multiple plots; crews measured Javad locations once and subsequently measured the distance and azimuth to this Javad location for multiple plot locations, which can then be reconstructed using R programming to create a map of all plot locations. Therefore, the in-field process can be fast and efficient—expanding this operation to include more ground points may improve model performance with little additional time. However, these biomass values are inherently subjective estimates, and they have the potential for large error or bias. Models generated from these estimates can be expected to have lower performance than using actual dried and weighed biomass estimates. For our purposes, we are hoping to track broad trends in understory change between novel harvest regimes, so absolute accuracy is less important than tiered (relative) values that indicate whether management activity is warranted.

Despite these advantages, our model performance in terms of R^2 is lower compared to other field-based studies of understory biomass, most of which measure orders of magnitude more understory biomass than our study. Our study had an average biomass of 1.3 Mg ha^{-1} for 2024 field measurements compared to 8.2 Mg ha^{-1} (Zhang et al., 2022) and 26 Mg ha^{-1} (Alonzo et al., 2020). Because of the plants that we were measuring and predicting, our study may be comparable to those in the agricultural field, where model performance is highly variable (Li et al., 2022). Moreover, in accordance with agricultural research, a typical practice in this field is to eliminate points close to the ground that capture rocks or raised soil that may create additional noise in the data (Walter et al., 2019). This can be done through reassigning points between 0 and 5 cm to a height of 0 cm (Walter et al., 2019). We tested whether removing these low-lying points improved our model performance for models built with Acquisition A, but we found no improvement, concluding that ground noise was not affecting model performance.

Additional estimation error may be due to the complexity of growth forms and habits of early-seral plants. For example, sprouting species (e.g., bigleaf maple) may generate numerous small-diameter stems that cumulatively account for a substantial amount of biomass but may be challenging to measure or estimate individually (Matula et al., 2015), potentially contributing to field-data bias. Ruderal plants can produce high densities of biomass rapidly, and intermediate deciduous shrubs have branches that rapidly spread foliage laterally. In contrast, most conifers take years to develop a full array of needle age classes, are determinant (growth is fixed before bud breaks), and have crown shapes that limit outward growth. Differences in growth forms and respective differences in biomass accumulation, may make accurate predictions of the early-seral environment more challenging than a conifer-dominated system.

Which machine learning model provides the most accurate predictions of understory biomass in open post-harvest conditions?

For Acquisition A, the stochastic gradient boosting model had the best predictive capacity and lowest error rate. Although the random forest model was a close second in model fit, R^2 values were higher in the training versus testing dataset, indicating that these models were overfit to the training dataset. This issue was exacerbated for Acquisition B, indicating the models were mostly fit to noise in the data rather than distinguishing a true pattern. Ultimately, data quality (determined by acquisition and post processing) was much more important than model selection, with Acquisition A models being superior to Acquisition B models under all conditions.

Future work will explore replicating these methods with larger vegetation and greater biomass quantities, which may improve model performance because vegetation will more often overtop slash, be more easily captured by multispectral cameras, and have larger three-

dimensional form that can be measured with LiDAR height and structure metrics. A minimum vegetation biomass may exist for this analysis in which vegetation is robust and visible but not yet producing closed-canopy occlusion. For future use of the Biomass Booklet, observer bias could be reduced by (1) setting up calibration plots for crews, and (2) including more than two observers for each plot and keeping estimates independent.

3.5 Conclusion

Our study tested model capability to predict understory biomass for two datasets across open-canopy experimental units. We concluded that remotely sensed data quality is more important than model selection and that acquisition methods, including post-processing procedures, can dictate feasibility of this type of study. Poor spatial registration can result in poor-performing models. However, the combination of high-quality UAV-acquired multispectral imagery and LiDAR produced a model that can predict tiered understory biomass values at a scale that is useful to forest managers. Future work should explore whether combining the Biomass Booklet, a set of calibrated photos for measuring understory biomass, with other remote sensing methods improves model accuracy. This framework should also be employed in areas with denser understory to assess whether model performance improves when more vegetation is present.

Table S3.4. This table shows the final variables used in model building. For both Acquisition A and B, one model was built with both point cloud and multispectral data and one model was built with multispectral data only.

Variable Type for Predictive Modeling	List of Predictors
Point Cloud Variables Used	Return.1.count.above.0.00, Elev.minimum, Elev.maximum, Elev.mode, Elev.variance, Elev.CV, Elev.IQ, Elev.skewness, Elev.kurtosis, Elev.MAD.median, Elev.MAD.mode, Elev.L1, Elev.L2, Elev.L3, Elev.L4, Elev.L.CV, Elev.L.skewness, Elev.L.kurtosis, Elev.P01, Elev.P05, Elev.P10, Elev.P20, Elev.P25, Elev.P30, Elev.P40, Elev.P80, Elev.P99, Canopy.relief.ratio, Percentage.all.returns.above.0.00, X.All.returns.above.0.00.....Total.first.returns., Percentage.all.returns.above.mean, Percentage.all.returns.above.mode, X.All.returns.above.mode.....Total.first.returns., First.returns.above.mean, First.returns.above.mode, All.returns.above.mean, All.returns.above.mode, Total.first.returns, Total.all.returns, Elev.strata..below.0.50..total.return.count, Elev.strata..below.0.50..return.proportion, Elev.strata..below.0.50..min, Elev.strata..below.0.50..max, Elev.strata..below.0.50..mean, Elev.strata..below.0.50..mode, Elev.strata..below.0.50..median, Elev.strata..below.0.50..stddev, Elev.strata..below.0.50..CV, Elev.strata..below.0.50..skewness, Elev.strata..below.0.50..kurtosis, Elev.strata..0.50.to.1.00..total.return.count, Elev.strata..0.50.to.1.00..return.proportion, Elev.strata..1.00.to.1.50..total.return.count, Elev.strata..1.00.to.1.50..return.proportion, Elev.strata..1.50.to.2.00..total.return.count, Elev.strata..1.50.to.2.00..return.proportion, Elev.strata..2.00.to.2.50..total.return.count, Elev.strata..2.00.to.2.50..return.proportion, Profile.area

Multispectral Variables Used	blue_reflectance_band_1_max, blue_reflectance_band_1_min, blue_reflectance_band_1_mean, blue_reflectance_band_1_sd, blue_reflectance_band_1_q25, blue_reflectance_band_1_q75, blue_reflectance_band_1_coef_var, cigreen_band_1_max, cigreen_band_1_min, cigreen_band_1_mean, cigreen_band_1_sd, cigreen_band_1_q25, cigreen_band_1_q75, cigreen_band_1_coef_var, ciredедge_band_1_max, ciredедge_band_1_min, ciredедge_band_1_sd, ciredедge_band_1_q25, ciredедge_band_1_q75, ciredедge_band_1_coef_var, ciredrededge_band_1_max, ciredrededge_band_1_min, ciredrededge_band_1_mean, ciredrededge_band_1_sd, ciredrededge_band_1_q25, ciredrededge_band_1_q75, ciredrededge_band_1_coef_var, green_reflectance_band_1_max, green_reflectance_band_1_min, green_reflectance_band_1_mean, green_reflectance_band_1_sd, green_reflectance_band_1_q25, green_reflectance_band_1_q75, green_reflectance_band_1_coef_var, msr_band_1_max, msr_band_1_min, msr_band_1_mean, msr_band_1_sd, msr_band_1_q25, msr_band_1_q75, msr_band_1_coef_var, msrrededge_band_1_min, msrrededge_band_1_mean, msrrededge_band_1_sd, msrrededge_band_1_q25, msrrededge_band_1_q75, msrrededge_band_1_coef_var, msrredrededge_band_1_min, msrredrededge_band_1_mean, msrredrededge_band_1_sd, msrredrededge_band_1_q25, msrredrededge_band_1_coef_var, NIR_band_1_coef_var, NIR_band_2_coef_var, NIR_band_3_coef_var, nir_re_g_band_1_max, nir_re_g_band_1_min, nir_re_g_band_1_mean, nir_re_g_band_1_sd, nir_re_g_band_1_q25, nir_re_g_band_1_q75, nir_re_g_band_1_coef_var, nir_re_g_band_2_coef_var, nir_re_g_band_3_coef_var, nir_reflectance_band_1_max, nir_reflectance_band_1_min, nir_reflectance_band_1_mean, nir_reflectance_band_1_sd, nir_reflectance_band_1_q25, nir_reflectance_band_1_q75, nir_reflectance_band_1_coef_var, nvdinir_band_1_max, nvdinir_band_1_min, nvdinir_band_1_mean, nvdinir_band_1_sd, nvdinir_band_1_q25,

	nvdinir_band_1_q75, nvdinir_band_1_coef_var, nvdirededge_band_1_max, nvdirededge_band_1_min, nvdirededge_band_1_mean, nvdirededge_band_1_sd, nvdirededge_band_1_q25, nvdirededge_band_1_q75, nvdirededge_band_1_coef_var, nvdiredrededge_band_1_min, nvdiredrededge_band_1_mean, nvdiredrededge_band_1_sd, nvdiredrededge_band_1_q25, nvdiredrededge_band_1_q75, nvdiredrededge_band_1_coef_var, red_reflectance_band_1_max, red_reflectance_band_1_min, red_reflectance_band_1_mean, red_reflectance_band_1_sd, red_reflectance_band_1_q25, red_reflectance_band_1_q75, red_reflectance_band_1_coef_var, rededge_band_1_max, rededge_band_1_min, rededge_band_1_sd, rededge_band_1_q75, rededge_band_1_coef_var, rededge_band_2_coef_var, rededge_band_3_coef_var, rededge_reflectance_band_1_max, rededge_reflectance_band_1_min, rededge_reflectance_band_1_mean, rededge_reflectance_band_1_sd, rededge_reflectance_band_1_q25, rededge_reflectance_band_1_q75, rededge_reflectance_band_1_coef_var, RGB_band_1_max, RGB_band_1_sd, RGB_band_1_q25, RGB_band_1_q75, RGB_band_1_coef_var, RGB_band_2_max, RGB_band_2_min, RGB_band_2_sd, RGB_band_2_q25, RGB_band_2_q75, RGB_band_2_coef_var, RGB_band_3_max, RGB_band_3_min, RGB_band_3_sd, RGB_band_3_q25, RGB_band_3_q75, RGB_band_3_coef_var.

Table S3.5. All hyperparameter combinations and final hyperparameter choices for all machine learning models tested with the four datasets: Acquisition A (A) LiDAR and multispectral (MS), A MS only, Acquisition B (B) SfM and MS, B MS.

Model	Parameter	Values Tested	A Full	B Full	A MS	B MS
GLMNet	Alpha (mixing percentage)	seq(0, 1, 0.1)	1	1	1	1
	Lambda (regularization strength)	$10^{seq(-5, -1, 0.1)}$	0.1	0.0126	0.1	0.0126

Model	Parameter	Values Tested	A Full	B Full	A MS	B MS
KNN	k (number of neighbors)	1:15	15	3	14	3
RF	mtry (number randomly selected predictors)	2, 3, 4, 5, 13, 62, 94	3	62	—	—
	mtry (number randomly selected predictors)	2, 3, 4, 5, 11, 43, 64, 129	—	—	5	129
GBM	n.trees (boosting iterations)	250, 500, 750, 1000, 1250, 1500	250	500	500	1000
	interaction.depth (maximum tree depth)	1, 2, 3	3	1	1	1
	shrinkage (learning rate)	0.01, 0.05, 0.1	0.01	0.05	0.01	0.1
	n.minobsinnode (minimum terminal node size)	5, 10	10	5	10	10
xgbTree	eta (learning rate)	0.3, 0.4	0.3	0.4	0.3	0.3
	max_depth (maximum tree depth)	1, 2	1	1	1	1
	subsample (subsample percentage)	0.5, 0.75	0.75	0.5	0.75	0.75
	nrounds (boosting iterations)	50, 100	50	50	50	50
	colsample_bytree (column subsample ratio)	1	1	1	1	1

CHAPTER 4. SUMMARY

Forest landowners and managers interested in multiple objectives need tools beyond those available for monoculture forestry, and this dissertation addresses three areas of consideration: species selection and stocking, seedling regeneration, and monitoring. The discoveries within this dissertation may be applied differently depending on whether the reader is a small forest landowner or a manager of United States Forest Service land. This chapter aims to put results into the context of the user to provide a greater contribution to the theories and practices of sustainable forest management, while identifying areas for further research.

First, we observed that mixed-species forestry offers an opportunity to meet ecological objectives while sustaining individual tree growth. Small forest landowners who are not focused on maximizing volume yield can use the pairs with observed bilateral positive growth as a template and guide for experimentation. Small changes in management can encourage the occurrence of these species pairings: bigleaf maple could be favored as a leave-tree in monoculture Douglas-fir thinning operations and western hemlock can be a go-to species for underplanting red alder forests. For private timber producers open to diversifying species composition — perhaps to reduce risks associated with climatic change and accelerated tree dieback — the high-value pairing of Douglas-fir and western redcedar offers a strong option, as a 50:50 mix may meet growth maximization for both species. Or, depending on site conditions, producers may prefer a Douglas-fir and western hemlock mix, where a 50:50 ratio may meet Douglas-fir growth maximization. Higher timber value pairs (Douglas-fir and western redcedar; Douglas-fir and western hemlock) may also be appropriate for managers of federal or state lands who may have objectives that fall along the continuum of ecologically focused with a no-harvest

regime to timber production focused. These pairs have the potential to achieve goals of timber production while gaining the possible benefits (drought tolerance, aesthetics, wildlife value) of mixed species forests.

The growth outcomes of these pairings will likely be more driven by the cumulative impact of other growing factors such as site condition, stand density, stand age and tree size than species mixing. Understanding the limits and applicability of these pairings is a worthy endeavor for anyone seeking to incorporate additional species into long-term forest planning. Questions remain regarding whether these pairs can produce more timber than a monoculture forest, and under what circumstances overyielding may occur. This question can at least be partially addressed through models constructed to predict plot-scale basal area for different species ratios rather than the individual tree growth models used in this study. Outcomes of this work would have implications for timber management throughout the Pacific Northwest and research should be conducted to determine widespread adoption of these pairings.

Planning for mixed-species plantations, including species selection, means little if seedlings are not successfully regenerated. Chapter 2 draws on quantitative data from multiple sources to move beyond conventional wisdom and anecdotal accounts of browse deterrents. Small forest landowners who are working across fewer hectares, may choose to focus on individual tree protection options: co-planting for Douglas-fir and Vexar tubing for western redcedar. Individual tree protection may be best suited for interplanting mixed species operations, where a second species such as western redcedar is being infilled at low densities into an existing plantation. For high stocking, where a high density of western redcedar is trying to be achieved, landowners should consider fenced exclosures, as our results indicate significant growth benefits for western redcedar with this technique.

The high timber market value of western redcedar makes it an obvious choice for integration into mixed-species forest plantings, yet planting this species is limited in part due to extreme challenges with browse (LePage and Banner, 2014). Considering western redcedar's regional dieback (Andrus et al., 2024), the larger forest research and management community must identify solutions for western redcedar regeneration in high-priority growth zones in a way that does not meaningfully restrict forage for wildlife and reduce habitat connectivity. Collaborative projects involving both wildlife specialists and foresters can help elucidate the current wildlife and forestry relationship, identify needs and barriers for both communities, and advance goals of species diversity across the landscape.

Chapter 3 lays the groundwork for monitoring of one important forest response within this larger experiment; however, the methods can be easily applied to other areas of interest in the post-harvest landscape, such as live seedling counts and coarse woody debris measurements. We can learn something from the contrast of our results generated with structure-from-motion (SfM) photogrammetry versus the higher performing technique from Cunliffe et al. (2016), who employed systematically acquired convergent image data, nadir image data, and high-precision ground-control points, which required multiple flights over the same area. This contrast highlights that there are superior ways to collect, process and analyze data depending on the objectives, and that remote sensing methods must be matched to the correct use-case. State and federal agencies are cautioned against using the same acquisition framework for all cases, and technical staff should be well-versed in the tradeoffs of different strategies.

Remote sensing technologies, particularly those involving unmanned aerial vehicles (UAVs), are advancing quickly and our study represents technological capacity at just one point in time. Advancements in everything from aircrafts, sensors, positioning hardware, and

processing techniques may facilitate increased use of this technology for small forest landowners and large private timberlands alike. Artificial Intelligence (AI) can aid with the technical coding required to process remote sensing data, democratizing this technology for a larger pool of users. AI may also advance point cloud analysis to identify new trends, creating an area for significant improvement. Future work should continue to explore technological capabilities of remote sensing methods to answer emerging questions because outcomes may change as methods advance.

The forest research community has an opportunity for collective engagement on management needs, from small forest landowners to large public entities, which can result in further clarification of the ideas outlined in this dissertation. The European triplet network provides us with an example of coordinated research to explore mixed-species plantings. Paired installations of mixed-species forests throughout the Pacific Northwest, could help us trial untested pairs, and these could be installed on private and public lands, creating a cooperative approach to learning. The infrastructure of this network could then be leveraged as unforeseen issues arise in our forests, with new experimental installations to address evolving issues. The forestry community is normalized to working on long time spans, with delayed returns. As an example, this dissertation relies heavily on decades of data collection as part of permanent plot networks. We must again consider what the next generation of managers will need to know and start the process of shared learning now.

CHAPTER 5. REFERENCES

Adler, P.B., Smull, D., Beard, K.H., Choi, R.T., Furniss, T., Kulmatiski, A., Meiners, J.M., Tredennick, A.T., Veblen, K.E., Comita, L., 2018. Competition and coexistence in plant communities: intraspecific competition is stronger than interspecific competition. Ecology Letters 21, 1319–1329. https://doi.org/10.1111/ele.13098

Almeida, D.R.A., Broadbent, E.N., Zambrano, A.M.A., Wilkinson, B.E., Ferreira, M.E., Chazdon, R., Meli, P., Gorgens, E.B., Silva, C.A., Stark, S.C., Valbuena, R., Papa, D.A., Brancalion, P.H.S., 2019. Monitoring the structure of forest restoration plantations with a drone-lidar system. International Journal of Applied Earth Observation and Geoinformation 79, 192–198. https://doi.org/10.1016/j.jag.2019.03.014

Alonzo, M., Dial, R.J., Schulz, B.K., Andersen, H.-E., Lewis-Clark, E., Cook, B.D., Morton, D.C., 2020. Mapping tall shrub biomass in Alaska at landscape scale using structure-from-motion photogrammetry and lidar. Remote Sensing of Environment 245, 111841. https://doi.org/10.1016/j.rse.2020.111841

Amoroso, M.M., Turnblom, E.C., 2006. Comparing productivity of pure and mixed Douglas-fir and western hemlock plantations in the Pacific Northwest. Canadian Journal of Forest Research 36, 1484–1496. https://doi.org/10.1139/x06-042

Andelt, W.F., Baker, D.L., Burnham, K.P., 1992. Relative preference of captive cow elk for repellent-treated diets. The Journal of Wildlife Management 56, 164–173. https://doi.org/10.2307/3808805

Andrus, R.A., Peach, L.R., Cinquini, A.R., Mills, B., Yusi, J.T., Buhl, C., Fischer, M., Goodrich, B.A., Hulbert, J.M., Holz, A., Meddens, A.J.H., Moffett, K.B., Ramirez, A., Adams, H.D., 2024. Canary in the forest?—Tree mortality and canopy dieback of western redcedar linked to drier and warmer summers. Journal of Biogeography 51, 103–119. https://doi.org/10.1111/jbi.14732

Andújar, D., Rueda-Ayala, V., Moreno, H., Rosell-Polo, J.R., Escolá, A., Valero, C., Gerhards, R., Fernández-Quintanilla, C., Dorado, J., Griepentrog, H.-W., 2013. Discriminating Crop, Weeds and Soil Surface with a Terrestrial LIDAR Sensor. Sensors 13, 14662–14675. https://doi.org/10.3390/s131114662

Anthropic, 2025. Claude (Claude Sonnet 4.6).

Antos, J.A., Filipescu, C.N., Negrave, R.W., 2016. Ecology of western redcedar (Thuja plicata): Implications for management of a high-value multiple-use resource. Forest Ecology and Management 375, 211–222. https://doi.org/10.1016/j.foreco.2016.05.043

Batchelor, J.L., Hudak, A.T., Gould, P., Moskal, L.M., 2023. Terrestrial and Airborne Lidar to Quantify Shrub Cover for Canada Lynx (Lynx canadensis) Habitat Using Machine Learning. Remote Sensing 15, 4434-. https://doi.org/10.3390/rs15184434

Beguin, J., Tremblay, J.-P., Thiffault, N., Pothier, D., Côté, S.D., 2016. Management of forest regeneration in boreal and temperate deer–forest systems: challenges, guidelines, and research gaps. Ecosphere 7, e01488. https://doi.org/10.1002/ecs2.1488

Berner, L.T., Jantz, P., Tape, K.D., Goetz, S.J., 2018. Tundra plant above-ground biomass and shrub dominance mapped across the North Slope of Alaska. Environmental Research Letters 13, 35002-. https://doi.org/10.1088/1748-9326/aaaa9a

Bigger, C.M., 1988. Effects of harvest intensity on nutrient removal, nutrient leaching and growth of seedlings in individual stands of high and low productivity red alder and Douglas-fir. ProQuest Dissertations & Theses.

Binkley, D., 2003. Seven decades of stand development in mixed and pure stands of conifers and nitrogen-fixing red alder. Can. J. For. Res. 33, 2274–2279. https://doi.org/10.1139/x03-158

Black, H.C., Scheringer, E.J., Hooven, E.F., 1979. Animal Damage to Coniferous Plantations In Oregon and Washington. Pt.1, a Survey, 1963-1975 (No. 25), Special Publication. Oregon State University, School of Forestry, Corvallis, OR.

Blackstone, K.M.S., McNickle, G.G., Ritzi, M.V., Nelson, T.M., Hardiman, B.S., Montague, M.S., Jacobs, D.F., Couture, J.J., 2025. Niche Overlap in Forest Tree Species Precludes a Positive Diversity–Productivity Relationship. Plants 14. https://doi.org/10.3390/plants14152271

Bobsin, C.R., 2023. Ethnoforestry and adaptive management: generating new pathways to manage forests on the Olympic Peninsula, WA. University of Washington Libraries, Seattle.

Bormann, B.T., Bobsin, C.R., McGaughey, R.J., Gordon, J.C., Morrissette, B.A., Kruper, A., 2023. The Wind River alder strip revisited: Lessons for post-fire management on recent and future western Washington and Oregon fires. Forest Ecology and Management 537, 120959. https://doi.org/10.1016/j.foreco.2023.120959

Bormann, B.T., Darbyshire, R.L., Homann, P.S., Morrissette, B.A., Little, S.N., 2015. Managing early succession for biodiversity and long-term productivity of conifer forests in southwestern Oregon. Forest Ecology and Management 340, 114–125. https://doi.org/10.1016/j.foreco.2014.12.016

Bormann, B.T., Haynes, R.W., Martin, J.R., 2007. Adaptive Management of Forest Ecosystems: Did Some Rubber Hit the Road? Bioscience 57, 186–191. https://doi.org/10.1641/B570213

Brassard, B.W., Chen, H.Y.H., Bergeron, Y., Paré, D., 2011. Differences in fine root productivity between mixed- and single-species stands. Functional Ecology 25, 238–246. https://doi.org/10.1111/j.1365-2435.2010.01769.x

Bravo, F., Hann, D.W., Maguire, D.A., 2001. Impact of competitor species composition on predicting diameter growth and survival rates of Douglas-fir trees in southwestern Oregon. Canadian Journal of Forest Research 31, 2237–2247. https://doi.org/10.1139/x01-164

Brodie, J.D., 1979. Animal Damage to Coniferous Plantations in Oregon and Washington: Part II, An Economic Evaluation. Oregon State University, School of Forestry, Corvallis, OR.

Brooks, J.R., Meinzer, F.C., Coulombe, R., Gregg, J., 2002. Hydraulic redistribution of soil water during summer drought in two contrasting Pacific Northwest coniferous forests. Tree Physiology 22, 1107–1117. https://doi.org/10.1093/treephys/22.15-16.1107

Buckland, D.C., Molnar, A.C., Wallis, G.W., 1954. Yellow laminated root rot of douglas fir. Can. J. Bot. 32, 69–81. https://doi.org/10.1139/b54-009

Burney, O.T., Tognetti, R., Jacobs, D.F., 2018. Species selection – A fundamental silvicultural tool to promote forest regeneration under high animal browsing pressure. Forest Ecology and Management 408, 67–74. https://doi.org/10.1016/j.foreco.2017.10.037

Campbell, D.L., Evans, J., 1988. Evaluation of Seedling Protection Materials in Western Oregon (No. TN OR-5). United States Department of the Interior, Bureau of Land Management, Oregon State Office, Portland, OR.

Campbell, M.J., Dennison, P.E., Hudak, A.T., Parham, L.M., Butler, B.W., 2018. Quantifying understory vegetation density using small-footprint airborne lidar. Remote Sensing of Environment 215, 330–342. https://doi.org/10.1016/j.rse.2018.06.023

Carsky, G., 2019. Effects of thinning on stand-structure dynamics and growth in pure and mixed Douglas-fir and western hemlock stands in coastal British Columbia. University of British Columbia. https://doi.org/10.14288/1.0376213

Carter, R.E., Klinka, K., 1992. Variation in shade tolerance of Douglas fir, western hemlock, and western red cedar in coastal British Columbia. Forest Ecology and Management 55, 87–105. https://doi.org/10.1016/0378-1127(92)90094-P

Chen, H.Y.H., Klinka, K., Mathey, A.H., Wang, X., Varga, P., Chourmouzis, C., 2003. Are mixed-species stands more productive than single-species stands: an empirical test of three forest types in British Columbia and Alberta. Canadian Journal of Forest Research 33, 1227–1237. https://doi.org/10.1139/x03-048

Clifton, B.C., Smith, D., 2018. Comparison of Deterrents to Reduce Elk Rubbing and Herbivory in a Skagit River Restoration Planting, Washington. Skagit River System Cooperative, La Conner, WA.

Coates, K., Pollack, J., Barker, J., 1985. The Effect of Deer Browsing on the Early Growth of Three Conifer Species in the Queen Charlotte Islands. BC Ministry of Forest, research report RR85002-PR.

Cockle, A., Ettl, G., 2010. Survival and Growth of Western Redcedar and Douglas-Fir Planted in a Variable Retention Harvest Unit in the Western Cascades, Washington, in: A Tale of Two Cedars: International Symposium on Western Redcedar and Yellow-Cedar.

Cole, E., Newton, M., 2023. Density effects on growth and dominance in pure and mixed stands of red alder and western hemlock in western Oregon. Forest Ecology and Management 537, 120950-. https://doi.org/10.1016/j.foreco.2023.120950

Coll, L., Ameztegui, A., Collet, C., Löf, M., Mason, B., Pach, M., Verheyen, K., Abrudan, I., Barbati, A., Barreiro, S., Bielak, K., Bravo-Oviedo, A., Ferrari, B., Govedar, Z., Kulhavy, J., Lazdina, D., Metslaid, M., Mohren, F., Pereira, M., Peric, S., Rasztovits, E., Short, I., Spathelf, P., Sterba, H., Stojanovic, D., Valsta, L., Zlatanov, T., Ponette, Q., 2018. Knowledge gaps about mixed forests: What do European forest managers want to know and what answers can science provide? Forest Ecology and Management 407, 106–115. https://doi.org/10.1016/j.foreco.2017.10.055

Collet, C., Ningre, F., Barbeito, I., Arnaud, A., Piboule, A., 2014. Response of tree growth and species coexistence to density and species evenness in a young forest plantation with two competing species. Annals of Botany 113, 711–719. https://doi.org/10.1093/aob/mct285

Collins, D.B., 2001. Investigation into the productivity of single- and mixed-species, second-growth stands of western hemlock and western redcedar. University of British Columbia. https://doi.org/10.14288/1.0099569

Cortini, F., Comeau, P.G., 2008. Effects of red alder and paper birch competition on juvenile growth of three conifer species in southwestern British Columbia. Forest Ecology and Management 256, 1795–1803. https://doi.org/10.1016/j.foreco.2008.03.022

Courbaud, B., Toigo, M., Perot, T., Ecosystèmes montagnards, Institut national de recherche en sciences et technologies pour l'environnement et l'agriculture, Bontemps, J.-D., French National Forest Office, Laboratoire d'Etudes des Ressources Forêt-Bois, Institut National de la Recherche Agronomique (INRA)-AgroParisTech, Ecosystèmes forestiers, Institut national de recherche en sciences et technologies pour l'environnement et l'agriculture,

Piedallu, C., Vallet, P., 2015. Overyielding in mixed forests decreases with site productivity. The Journal of Ecology 103, 502–512. https://doi.org/10.1111/1365-2745.12353
Courtin, P., Harper, G., 2018. Assessment of a 14-year-old Mixed Western Redcedar:Red Alder Plantation in Southwestern British Columbia. B.C. Exten. Note 121.
Cova, G.R., Prichard, S.J., Rowell, E., Drye, B., Eagle, P., Kennedy, M.C., Nemens, D.G., 2023. Evaluating Close-Range Photogrammetry for 3D Understory Fuel Characterization and Biomass Prediction in Pine Forests. Remote Sensing 15, 4837-. https://doi.org/10.3390/rs15194837
CPI Inflation Calculator [WWW Document], 2026. Bureau of Labor Statistics. URL https://www.bls.gov/data/inflation_calculator.htm (accessed 4.28.26).
Crouch, G.L., 1968. Forage Availability in Relation to Browsing of Douglas-Fir Seedlings by Black-Tailed Deer. The Journal of Wildlife Management 32, 542–553. https://doi.org/10.2307/3798934
Cunliffe, A.M., Brazier, R.E., Anderson, K., 2016. Ultra-fine grain landscape-scale quantification of dryland vegetation structure with drone-acquired structure-from-motion photogrammetry. Remote Sensing of Environment 183, 129–143. https://doi.org/10.1016/j.rse.2016.05.019
Curtis, R.O., 1982. A simple index of stand density for Douglas-fir [Pseudotsuga menziesii, Forest mensuration]. Forest science 28, 92–94. https://doi.org/10.1093/forestscience/28.1.92
Dandois, J.P., Ellis, E.C., 2013. High spatial resolution three-dimensional mapping of vegetation spectral dynamics using computer vision. Remote Sensing of Environment 136, 259–276. https://doi.org/10.1016/j.rse.2013.04.005
De Montigny, L., 2007. Growth and survival of Douglas-fir and western redcedar planted at different densities and species mixtures. Technical report.
Devine, W.D., Harrington, C.A., 2009. Western redcedar response to precommercial thinning and fertilization through 25 years posttreatment. Canadian Journal of Forest Research 39, 619–628. https://doi.org/10.1139/X08-199
Diaz, D.D., 2023. Leveraging Open Data to Support Forest Mapping, Modeling, and Policy Analysis in the Pacific Northwest, USA. ProQuest Dissertations & Theses.
Dixon, S., 2025. Port Blakely Tree Farm western redcedar planting data.
Dryden, J., 2025. Personal Correspondence.
Eis, S., 1974. Root System Morphology of Western Hemlock, Western Red Cedar, and Douglas-fir. Canadian Journal of Forest Research 4, 28–38. https://doi.org/10.1139/x74-005
Endress, B.A., Naylor, B.J., Pekin, B.K., Wisdom, M.J., 2016. Aboveground and belowground mammalian herbivores regulate the demography of deciduous woody species in conifer forests. Ecosphere 7, n/a. https://doi.org/10.1002/ecs2.1530
Erickson, H.E., Harrington, C.A., Marshall, D.D., 2009. Tree growth at stand and individual scales in two dual-species mixture experiments in southern Washington State, USA. Canadian Journal of Forest Research 39, 1119–1132. https://doi.org/10.1139/X09-040
Eskelson, B.N., Huberman, Y.L., 2023. Conifer performance, stand productivity, and understory cover in varying densities of mixed conifer-broadleaf stands in southwestern British Columbia. Canadian Journal of Forest Research 53, 430–443. https://doi.org/10.1139/cjfr-2022-0211
ESRI, 2022. ArcGIS Pro (Version 3.0.0).

Ettl, G.J., Bobsin, C.R., Bormann, B.T., Holt, D.E., 2026. Variable Density Planting: Using Marigolds as a Model System to Describe a Silvicultural Approach to Increase Structural Diversity. Forests 17, 401-. https://doi.org/10.3390/f17040401

Fang, C., Comeau, P.G., Harper, G.J., 2019. Effects of red alder on growth of Douglas-fir and western redcedar in southwestern British Columbia. Forest Ecology and Management 434, 244–254. https://doi.org/10.1016/j.foreco.2018.12.023

Felton, A., Lindbladh, M., Brunet, J., Fritz, Ö., 2010. Replacing coniferous monocultures with mixed-species production stands: An assessment of the potential benefits for forest biodiversity in northern Europe. Forest Ecology and Management 260, 939–947. https://doi.org/10.1016/j.foreco.2010.06.011

Feng, Y., Schmid, B., Loreau, M., Forrester, D.I., Fei, S., Zhu, Jianxiao, Tang, Z., Zhu, Jiangling, Hong, P., Ji, C., Shi, Y., Su, H., Xiong, X., Xiao, J., Wang, S., Fang, J., 2022. Multispecies forest plantations outyield monocultures across a broad range of conditions. Science (American Association for the Advancement of Science) 376, 865–868. https://doi.org/10.1126/science.abm6363

Fernández-Guisuraga, J.M., Calvo, L., Suárez-Seoane, S., 2022a. Monitoring post-fire neighborhood competition effects on pine saplings under different environmental conditions by means of UAV multispectral data and structure-from-motion photogrammetry. Journal of Environmental Management 305, 114373-. https://doi.org/10.1016/j.jenvman.2021.114373

Fernández-Guisuraga, J.M., Suárez-Seoane, S., Fernandes, P.M., Fernández-García, V., Fernández-Manso, A., Quintano, C., Calvo, L., 2022b. Pre-fire aboveground biomass, estimated from LiDAR, spectral and field inventory data, as a major driver of burn severity in maritime pine (Pinus pinaster) ecosystems. Forest Ecosystems 9, 100022-. https://doi.org/10.1016/j.fecs.2022.100022

Forrester, D.I., Bonal, D., Dawud, S., Gessler, A., Granier, A., Pollastrini, M., Grossiord, C., 2016. Drought responses by individual tree species are not often correlated with tree species diversity in European forests. The Journal of Applied Ecology 53, 1725–1734. https://doi.org/10.1111/1365-2664.12745

Forrester, D.I., Plaga, B.N.E., Bauhus, J., 2025. The Effects of Tree Size, Stand Density, and Tree-Species Mixing on Stand Level and Tree Level Light Absorption and Light-Use Efficiency: A Review. Current Forestry Reports 11, 15–15. https://doi.org/10.1007/s40725-025-00247-7

Fox, J., 2003. Effect Displays in R for Generalised Linear Models. Journal of Statistical Software 8, 1–27. https://doi.org/10.18637/jss.v008.i15

Fox, J., Weisberg, S., 2019. An R Companion to Applied Regression, 3rd Edition. Thousand Oaks, CA.

Freund, J.A., Franklin, J.F., Larson, A.J., Lutz, J.A., 2014. Multi-decadal establishment for single-cohort Douglas-fir forests. Can. J. For. Res. 44, 1068–1078. https://doi.org/10.1139/cjfr-2013-0533

Fried, J.S., Boyle, J.R., Tappeiner II, J.C., Cromack Jr., K., 1990. Effects of bigleaf maple on soils in Douglas-fir forests. Can. J. For. Res. 20, 259–266. https://doi.org/10.1139/x90-038

Goheen, E.M., Willhite, E.A., 2021. Field Guide to Common Diseases and Insect Pests of Oregon and Washington Conifers, Revised. ed, R6-FHPRO-2021-01. USDA Forest Service, Pacific Northwest Region, Portland, OR.

Gourley, M., Vomocil, M., Newton, M., 1990. Forest weeding reduces the effect of deer-browsing on Douglas fir. Forest Ecology and Management 36, 177–185. https://doi.org/10.1016/0378-1127(90)90024-6
Gunther, E., 1973. Ethnobotany of western Washington: the knowledge and use of indigenous plants by Native Americans, Rev. ed. ed. University of Washington Press, Seattle.
Hamdan, K., Schmidt, M., 2012. influence of bigleaf maple on chemical properties of throughfall, stemflow, and forest floor in coniferous forest in the Pacific Northwest. Canadian Journal of Forest Research 42, 868–878. https://doi.org/10.1139/x2012-042
Harper, G., Omari, K., Kranabetter, M., Courtin, P., 2023. Assessment of a 20-year-old mixed western redcedar/red alder plantation in southwestern British Columbia. Forest Ecology and Management 529, 120737-. https://doi.org/10.1016/j.foreco.2022.120737
Harrington, T.B., 2006. Five-year growth responses of Douglas-fir, western hemlock, and western redcedar seedlings to manipulated levels of overstory and understory competition. Canadian Journal of Forest Research 36, 2439–2453. https://doi.org/10.1139/x06-139
Hart, P.J., Ibanez, T., Uehana, S., Pang-Ching, J., 2020. Forest regeneration following ungulate removal in a montane Hawaiian wet forest. Restoration Ecology 28, 757–765. https://doi.org/10.1111/rec.13116
Hartig, F., 2022. DHARMa: Residual Diagnostics for Hierarchical (Multi-Level / Mixed) Regression Models.
Hastie, T., Mazumder, R., Lee, J., Zadeh, R., 2015. Matrix Completion and Low-rank SVD via Fast Alternating Least Squares. Journal of Machine Learning Research 16, 3367–3402.
Heiderman, R.R., Kimsey, M.J., 2023. Pacific Northwest conifer forest stand carrying capacity under future climate scenarios. Natural Resource Modeling 36. https://doi.org/10.1111/nrm.12381
Hijmans, R.J., Brown, A., Barbosa, M., 2026. terra: Spatial Data Analysis.
Himes, A., Puettmann, K., 2020. Tree species diversity and composition relationship to biomass, understory community, and crown architecture in intensively managed plantations of the coastal Pacific Northwest, USA. Canadian Journal of Forest Research 50, 1–12. https://doi.org/10.1139/cjfr-2019-0236
Höwler, K., Vor, T., Seidel, D., Annighöfer, P., Ammer, C., 2019. Analyzing effects of intra- and interspecific competition on timber quality attributes of Fagus sylvatica L.—from quality assessments on standing trees to sawn boards. European Journal of Forest Research 138, 327–343. https://doi.org/10.1007/s10342-019-01173-7
HSC, 2017. Effects of species mixtures on growth and yield of red alder and western red cedar. In: Hardwood Silviculture Cooperative Annual Report 2017. Oregon State University.
Hull, I.T., Shipley, L.A., 2019. Testing the Ability of Airborne LiDAR to Measure Forage Resources for Wild Ungulates in Conifer Forests. Journal of Forestry 117, 492–503. https://doi.org/10.1093/jofore/fvz040
Iijima, H., Oka, T., 2023. Fences are more effective than repellents in reducing deer browsing on planted two conifer species but their effectiveness is reduced by higher deer density, deeper snow, and steeper slope. Forest Ecology and Management 546, 121328-. https://doi.org/10.1016/j.foreco.2023.121328
Jactel, H., Bauhus, J., Boberg, J., Bonal, D., Castagneyrol, B., Gardiner, B., Gonzalez-Olabarria, J.R., Koricheva, J., Meurisse, N., Brockerhoff, E.G., 2017. Tree Diversity Drives Forest

Stand Resistance to Natural Disturbances. Current Forestry Reports 3, 223–243. https://doi.org/10.1007/s40725-017-0064-1
Jamrozik, M.J., 2016. Effects of bigleaf maple on the growth and morphology of mature conifers in the southern coastal forests of British Columbia. (Master of Science). Simon Fraser University.
Jansen, K., von Oheimb, G., Bruelheide, H., Härdtle, W., Fichtner, A., 2021. Tree species richness modulates water supply in the local tree neighbourhood: evidence from wood δ13C signatures in a large-scale forest experiment. Proceedings of the Royal Society B: Biological Sciences 288, 20203100. https://doi.org/10.1098/rspb.2020.3100
Martin, J.-L., Archaux, F., Baltzinger, C., 2002. Interaction among deer browsing, hunting, and tree regeneration. Canadian Journal of Forest Research 32, 1254–1264. https://doi.org/10.1139/x02-043
Martin, J.-L., Stockton, S.A., Allombert, S., Gaston, A.J., 2010. Top-down and bottom-up consequences of unchecked ungulate browsing on plant and animal diversity in temperate forests: lessons from a deer introduction. Biological Invasions 12, 353–371. https://doi.org/10.1007/s10530-009-9628-8
Jimenez-Berni, J.A., Deery, D.M., Rozas-Larraondo, P., Condon, A. (Tony) G., Rebetzke, G.J., James, R.A., Bovill, W.D., Furbank, R.T., Sirault, X.R.R., 2018. High Throughput Determination of Plant Height, Ground Cover, and Above-Ground Biomass in Wheat with LiDAR. Frontiers in Plant Science 9, 237-. https://doi.org/10.3389/fpls.2018.00237
Käber, Y., Bigler, C., HilleRisLambers, J., Hobi, M., Nagel, T.A., Aakala, T., Blaschke, M., Brang, P., Brzeziecki, B., Carrer, M., Cateau, E., Frank, G., Fraver, S., Idoate-Lacasia, J., Holik, J., Kucbel, S., Leyman, A., Meyer, P., Motta, R., Samonil, P., Seebach, L., Stillhard, J., Svoboda, M., Szwagrzyk, J., Vandekerkhove, K., Vostarek, O., Zlatanov, T., Bugmann, H., 2023. Sheltered or suppressed? Tree regeneration in unmanaged European forests. The Journal of Ecology 111, 2281–2295. https://doi.org/10.1111/1365-2745.14181
Kay, C.E., 2001. Long-term aspen exclosures in the Yellowstone ecosystem, in: Shepperd, W.D., Binkley, D., Bartos, D.L., Stohlgren, T.J., Eskew, L.G. (Eds.), Sustaining Aspen in Western Landscapes: Symposium Proceedings, Proceedings RMRS-P-18. U.S. Department of Agriculture, Forest Service, Rocky Mountain Research Station, Fort Collins, CO, pp. 225–242.
Keeton, W.S., Franklin, J.F., 2005. Do remnant old-growth trees accelerate rates of succession in mature Douglas-fir forests? Ecological monographs 75, 103–118. https://doi.org/10.1890/03-0626
Kelty, M.J., 1992. Comparative productivity of monocultures and mixed-species stands, in: Kelty, M.J., Larson, B.C., Oliver, C.D. (Eds.), The Ecology and Silviculture of Mixed-Species Forests: A Festschrift for David M. Smith. Springer Netherlands, Dordrecht, pp. 125–141. https://doi.org/10.1007/978-94-015-8052-6_8
Khan, M.N., Tan, Y., Gul, A.A., Abbas, S., Wang, J., 2024. Forest Aboveground Biomass Estimation and Inventory: Evaluating Remote Sensing-Based Approaches. Forests 15, 1055-. https://doi.org/10.3390/f15061055
Kimball, B.A., Russell, J.H., DeGraan, J.P., Perry, K.R., 2008. Screening Hydrolyzed Casein as a Deer Repellent for Reforestation Applications. Western Journal of Applied Forestry 23, 172–176. https://doi.org/10.1093/wjaf/23.3.172

Knowe, S.A., Carrier, B.D., Dobkowski, A., 1995. Effects of Bigleaf Maple Sprout Clumps on Diameter and Height Growth of Douglas-Fir. Western Journal of Applied Forestry 10, 5–11. https://doi.org/10.1093/wjaf/10.1.5

Kobe, R.K., Coates, K.D., 1997. Models of sapling mortality as a function of growth to characterize interspecific variation in shade tolerance of eight tree species of northwestern British Columbia. Canadian Journal of Forest Research 27, 227–236. https://doi.org/10.1139/x96-182

Krishna, M., Chandra Garkoti, S., 2022. Evergreen and deciduous tree species show distinct strategies to synchronize with seasonality in mid-elevational forests of central Himalaya. Forest Ecology and Management 526, 120567. https://doi.org/10.1016/j.foreco.2022.120567

Kruper, A., 2024. Western Redcedar on the Olympic Peninsula: Locating This Culturally, Economically, and Ecologically Important Species Using Remote Sensing Methodologies. ProQuest Dissertations & Theses.

Kuhn, M., 2008. Building Predictive Models in R Using the caret Package. Journal of Statistical Software 28, 1–26. https://doi.org/10.18637/jss.v028.i05

Larson, A.J., Paine, R.T., 2007. Ungulate Herbivory: Indirect Effects Cascade into the Treetops. Proceedings of the National Academy of Sciences - PNAS 104, 5–6. https://doi.org/10.1073/pnas.0610198103

Lenth, R.V., Piaskowski, J., 2026. emmeans: Estimated Marginal Means, aka Least-Squares Means.

Leopold, A., 1936. Deer and Dauerwald in Germany: history. Journal of Forestry 34, 366–375.

Leopold, A., Sowls, L.K., Spencer, D.L., 1947. A Survey of Over-Populated Deer Ranges in the United States. The Journal of Wildlife Management 11, 162–177. https://doi.org/10.2307/3795561

LePage, P., Banner, A., 2014. Long-term recovery of forest structure and composition after harvesting in the coastal temperate rainforests of northern British Columbia. Forest Ecology and Management 318, 250–260. https://doi.org/10.1016/j.foreco.2014.01.031

Leuschner, C., Meinzer, F.C., 2024. Drought resistance and drought adaptation of Douglas-fir (*Pseudotsuga menziesii*) – A review. Perspectives in Plant Ecology, Evolution and Systematics 65, 125829. https://doi.org/10.1016/j.ppees.2024.125829

Li, A., Glenn, N.F., Olsoy, P.J., Mitchell, J.J., Shrestha, R., 2015. Aboveground biomass estimates of sagebrush using terrestrial and airborne LiDAR data in a dryland ecosystem. Agricultural and Forest Meteorology 213, 138–147. https://doi.org/10.1016/j.agrformet.2015.06.005

Li, J., Schachtman, D.P., Creech, C.F., Wang, L., Ge, Y., Shi, Y., 2022. Evaluation of UAV-derived multimodal remote sensing data for biomass prediction and drought tolerance assessment in bioenergy sorghum. The Crop Journal 10, 1363–1375. https://doi.org/10.1016/j.cj.2022.04.005

Li, S., Wang, T., Hou, Z., Gong, Y., Feng, L., Ge, J., 2021. Harnessing terrestrial laser scanning to predict understory biomass in temperate mixed forests. Ecological Indicators 121, 107011. https://doi.org/10.1016/j.ecolind.2020.107011

Liu, C.L.C., Kuchma, O., Krutovsky, K.V., 2018. Mixed-species versus monocultures in plantation forestry: Development, benefits, ecosystem services and perspectives for the future. Global Ecology and Conservation 15, e00419. https://doi.org/10.1016/j.gecco.2018.e00419

Löf, M., Sandell Festin, E., Szydło, M., Brunet, J., 2023. Restoring mixed forests through conversion of Norway spruce stands: effects of fencing and mechanical site preparation on performance of planted beech and natural tree regeneration. European Journal of Forest Research 142, 763–772. https://doi.org/10.1007/s10342-023-01554-z

Lu, D., Chen, Q., Wang, G., Liu, L., Li, G., Moran, E., 2016. A survey of remote sensing-based aboveground biomass estimation methods in forest ecosystems. International Journal of Digital Earth 9, 63–105. https://doi.org/10.1080/17538947.2014.990526

Lu, H., Mohren, G.M., den Ouden, J., Goudiaby, V., Sterck, F.J., 2016. Overyielding of temperate mixed forests occurs in evergreen–deciduous but not in deciduous–deciduous species mixtures over time in the Netherlands. Forest Ecology and Management 376, 321–332. https://doi.org/10.1016/j.foreco.2016.06.032

Masjedi, A., Crawford, M.M., Carpenter, N.R., Tuinstra, M.R., 2020. Multi-Temporal Predictive Modelling of Sorghum Biomass Using UAV-Based Hyperspectral and LiDAR Data. Remote Sensing 12. https://doi.org/10.3390/rs12213587

Matula, R., Damborská, L., Nečasová, M., Geršl, M., Šrámek, M., 2015. Measuring Biomass and Carbon Stock in Resprouting Woody Plants. PloS one 10, e0118388-. https://doi.org/10.1371/journal.pone.0118388

Mazumder, R., Hastie, T., Tibshirani, R., 2010. Spectral Regularization Algorithms for Learning Large Incomplete Matrices. Journal of Machine Learning Research 11, 2287–2322.

McGaughey, R.J., 2024. FUSION/LDV: Software for LIDAR Data Analysis and Visualization. U.S. Department of Agriculture, Forest Service, Pacific Northwest Research Station.

McGaughey, R.J., Ahmed, K., Andersen, H.-E., Reutebuch, S.E., 2017. Effect of Occupation Time on the Horizontal Accuracy of a Mapping-Grade GNSS Receiver under Dense Forest Canopy. Photogrammetric engineering and remote sensing 83, 861–868. https://doi.org/10.14358/PERS.83.12.861

McNellis, B.E., Smith, A.M.S., Hudak, A.T., Strand, E.K., 2021. Tree mortality in western U.S. forests forecasted using forest inventory and Random Forest classification. Ecosphere 12, e03419. https://doi.org/10.1002/ecs2.3419

Miller, R.E., Murray, M.D., 1978. The effects of red alder on growth of Douglas-fir. Utilization and management of alder For. Serv. Gen. Tech. Rep., 386–306.

Mitchell, K.J., 1964. Height growth losses due to animal feeding in Douglas fir plantations, Vancouver Island, B.C. Forestry Chronicle 40, 298–307. https://doi.org/10.5558/tfc40298-3

Murray, J.F., 2021. Planting Sitka Spruce and Western Redcedar in the Same Hole to Mitigate Browsing Damage. Tree Planters' Notes 64, 55–62.

Nishimura, N., Hara, T., Miura, M., Manabe, T., Yamamoto, S., 2003. Tree competition and species coexistence in a warm-temperate old-growth evergreen broad-leaved forest in Japan. Plant Ecology 164, 235–248. https://doi.org/10.1023/a:1021224429091

Nolte, D.L., 1998. Efficacy of selected repellents to deter deer browsing on conifer seedlings: Vertebrate deteriogens. International biodeterioration & biodegradation 42, 101–107.

Oliver, C.D., Larson, B.A., 1996. Forest Stand Dynamics, Update Edition. John Wiley & Sons, New York.

Olsoy, P.J., Zaiats, A., Delparte, D.M., Germino, M.J., Richardson, B.A., Roser, A.V., Forbey, J.S., Cattau, M.E., Caughlin, T.T., 2024. Demography with drones: detecting growth and survival of shrubs with unoccupied aerial systems. Restoration Ecology 32, n/a. https://doi.org/10.1111/rec.14106

Omari, K., Kranabetter, J.M., de Montigny, L., 2021. Productivity of coastal Douglas-fir and western redcedar in response to species mixture, planting density, and soil carbon:nitrogen ratio. Canadian Journal of Forest Research 51, 668–674. https://doi.org/10.1139/cjfr-2020-0223

OpenAI, 2025. ChatGPT (GPT-4o) [Large language model].

Pardos, M., del Río, M., Pretzsch, H., Jactel, H., Bielak, K., Bravo, F., Brazaitis, G., Defossez, E., Engel, M., Godvod, K., Jacobs, K., Jansone, L., Jansons, A., Morin, X., Nothdurft, A., Oreti, L., Ponette, Q., Pach, M., Riofrío, J., Ruíz-Peinado, R., Tomao, A., Uhl, E., Calama, R., 2021. The greater resilience of mixed forests to drought mainly depends on their composition: Analysis along a climate gradient across Europe. Forest Ecology and Management 481, 118687. https://doi.org/10.1016/j.foreco.2020.118687

Parker, H.A., Larkin, J.T., Heggenstaller, D., Duchamp, J., Tyree, M.C., Rushing, C.S., Just Domoto, E., Larkin, J.L., 2020. Evaluating the impacts of white-tailed deer (Odocoileus virginianus) browsing on vegetation in fenced and unfenced timber harvests. Forest Ecology and Management 473, 118326-. https://doi.org/10.1016/j.foreco.2020.118326

Paul, K.I., Roxburgh, S.H., Chave, J., England, J.R., Zerihun, A., Specht, A., Lewis, T., Bennett, L.T., Baker, T.G., Adams, M.A., Huxtable, D., Montagu, K.D., Falster, D.S., Feller, M., Sochacki, S., Ritson, P., Bastin, G., Bartle, J., Wildy, D., Hobbs, T., Larmour, J., Waterworth, R., Stewart, H.T., Jonson, J., Forrester, D.I., Applegate, G., Mendham, D., Bradford, M., O'Grady, A., Green, D., Sudmeyer, R., Rance, S.J., Turner, J., Barton, C., Wenk, E.H., Grove, T., Attiwill, P.M., Pinkard, E., Butler, D., Brooksbank, K., Spencer, B., Snowdon, P., O'Brien, N., Battaglia, M., Cameron, D.M., Hamilton, S., McAuthur, G., Sinclair, J., 2016. Testing the generality of above-ground biomass allometry across plant functional types at the continent scale. Global Change Biology 22, 2106–2124. https://doi.org/10.1111/gcb.13201

Pedersen, T.L., 2024. patchwork: The Composer of Plots.

Pittman, J., Arnall, D., Interrante, S., Moffet, C., Butler, T., 2015. Estimation of Biomass and Canopy Height in Bermudagrass, Alfalfa, and Wheat Using Ultrasonic, Laser, and Spectral Sensors. Sensors 15, 2920–2943. https://doi.org/10.3390/s150202920

Postma, J.A., Hecht, V.L., Hikosaka, K., Nord, E.A., Pons, T.L., Poorter, H., 2021. Dividing the pie: A quantitative review on plant density responses. Plant, Cell and Environment 44, 1072–1094. https://doi.org/10.1111/pce.13968

Prabhakara, K., Hively, W.D., McCarty, G.W., 2015. Evaluating the relationship between biomass, percent groundcover and remote sensing indices across six winter cover crop fields in Maryland, United States. International Journal of Applied Earth Observation and Geoinformation 39, 88–102. https://doi.org/10.1016/j.jag.2015.03.002

Prescott, C.E., Sajedi, T., 2008. The role of salal in forest regeneration problems in coastal British Columbia: problem or symptom? Forestry Chronicle 84, 29–36. https://doi.org/10.5558/tfc84029-1

Pretzsch, H., 2022. Facilitation and competition reduction in tree species mixtures in Central Europe: Consequences for growth modeling and forest management. Ecological Modelling 464, 109812. https://doi.org/10.1016/j.ecolmodel.2021.109812

Pretzsch, H., 2014. Canopy space filling and tree crown morphology in mixed-species stands compared with monocultures. Forest Ecology and Management 327, 251–264. https://doi.org/10.1016/j.foreco.2014.04.027

Pretzsch, H., del Río, M., Biber, P., Arcangeli, C., Bielak, K., Brang, P., Dudzinska, M., Forrester, D.I., Klädtke, J., Kohnle, U., Ledermann, T., Matthews, R., Nagel, J., Nagel, R., Nilsson, U., Ningre, F., Nord-Larsen, T., Wernsdörfer, H., Sycheva, E., 2019. Maintenance of long-term experiments for unique insights into forest growth dynamics and trends: review and perspectives. European Journal of Forest Research 138, 165–185. https://doi.org/10.1007/s10342-018-1151-y

Pretzsch, H., Schütze, G., 2021. Tree species mixing can increase stand productivity, density and growth efficiency and attenuate the trade-off between density and growth throughout the whole rotation. Annals of Botany 128, 767–786. https://doi.org/10.1093/aob/mcab077

PRISM Climate Group, Oregon State University, 2026. PRISM Data Explorer.

Puettmann, K.J., 2011. Silvicultural challenges and options in the context of global change: "simple" fixes and opportunities for new management approaches. Journal of Forestry 109, 321–331. https://doi.org/10.1093/jof/109.6.321.

Puettmann, K.J., Cole, L., Newton, M., 2024. Deer browse deterrents and microsite selection influence Callitropsis nootkatensis and Thuja plicata planting success in Southeast Alaska. New Forests 55, 877–895. https://doi.org/10.1007/s11056-023-10008-8

Puettmann, K.J., Hann, D.W., Hibbs, D.E., 1993. Evaluation of the size-density relationships for pure red alder and Douglas-fir stands. Forest science 39, 7–27. https://doi.org/10.1093/forestscience/39.1.7

Python Software Foundation, 2016. Python Language Reference.

R Core Team, 2022. R: A Language and Environment for Statistical Computing.

Radosevich, S.R., Hibbs, D.E., Ghersa, C.M., 2006. Effects of species mixtures on growth and stand development of Douglas-fir and red alder. Canadian Journal of Forest Research 36, 768–782. https://doi.org/10.1139/x05-280

Ramirez, J.I., Jansen, P.A., den Ouden, J., Goudzwaard, L., Poorter, L., 2019. Long-term effects of wild ungulates on the structure, composition and succession of temperate forests. Forest Ecology and Management 432, 478–488. https://doi.org/10.1016/j.foreco.2018.09.049

Reineke, L.H., 1933. Perfecting a Stand-Density Index for Even-Aged Forests. Illus. Journal of agricultural research (Washington, D.C.) 46, 627-.

Rewald, B., Leuschner, C., 2009. Belowground competition in a broad-leaved temperate mixed forest: pattern analysis and experiments in a four-species stand. European Journal of Forest Research 128, 387–398. https://doi.org/10.1007/s10342-009-0276-4

Reynolds, P.E., King, K., Whitehead, R., McKay, T.S., 1986. One-year results for a coastal British Columbia glyphosate conifer release trial. Proceedings of the Western Society of Weed Science 39, 107–117.

Richards, A.E., Forrester, D.I., Bauhus, J., Scherer-Lorenzen, M., 2010. The influence of mixed tree plantations on the nutrition of individual species: a review. Tree physiology 30, 1192–1208. https://doi.org/10.1093/treephys/tpq035

Rooney, T.P., 2001. Deer impacts on forest ecosystems: a North American perspective. Forestry 74, 201–208. https://doi.org/10.1093/forestry/74.3.201

Shahbazi, N., Ashworth, M.B., Callow, J.N., Mian, A., Beckie, H.J., Speidel, S., Nicholls, E., Flower, K.C., 2021. Assessing the Capability and Potential of LiDAR for Weed Detection. Sensors 21. https://doi.org/10.3390/s21072328

Shainsky, L.J., Radosevich, S.R., 1992. Mechanisms of competition between Douglas-fir and red alder seedlings. Ecology (Durham) 73, 30–45. https://doi.org/10.2307/1938718

Shrestha, M., Broadbent, E.N., Vogel, J.G., 2021. Using GatorEye UAV-Borne LiDAR to Quantify the Spatial and Temporal Effects of a Prescribed Fire on Understory Height and Biomass in a Pine Savanna. Forests 12, 38-. https://doi.org/10.3390/f12010038

Slesak, R.A., Agne, M.C., Harrington, C.A., Powers, M.D., 2025. Douglas-fir dominates when grown in dual species mixtures with three western conifers. Forest Ecology and Management 597, 123141-. https://doi.org/10.1016/j.foreco.2025.123141.

Stan, A.B., Daniels, L.D., 2014. Growth releases across a natural canopy gap-forest gradient in old-growth forests. Forest Ecology and Management 313, 98–103. https://doi.org/10.1016/j.foreco.2013.11.004

Stokely, T.D., Verschuyl, J., Hagar, J.C., Betts, M.G., 2018. Herbicides and herbivory interact to drive plant community and crop-tree establishment. Ecological applications 28, 2011–2023. https://doi.org/10.1002/eap.1777

Streutker, D.R., Glenn, N.F., 2006. LiDAR measurement of sagebrush steppe vegetation heights. Remote Sensing of Environment 102, 135–145. https://doi.org/10.1016/j.rse.2006.02.011

Stroh, N., Baltzinger, C., Martin, J.-L., 2008. Deer prevent western redcedar (Thuya plicata) regeneration in old-growth forests of Haida Gwaii: Is there a potential for recovery? Forest Ecology and Management 255, 3973–3979. https://doi.org/10.1016/j.foreco.2008.03.039

Swanson, M.E., Franklin, J.F., Beschta, R.L., Crisafulli, C.M., DellaSala, D.A., Hutto, R.L., Lindenmayer, D.B., Swanson, F.J., 2011. The forgotten stage of forest succession: early-successional ecosystems on forest sites. Frontiers in ecology and the environment 9, 117–125. https://doi.org/10.1890/090157

Yagi, T., 2022. The combined effects of tree shelters, large stock and vegetation control on the early growth of conifer seedlings. Journal of Forest Research 1–9. https://doi.org/10.1080/13416979.2022.2048442

Tappeiner, J.C., Maguire, D.A., Harrington, T.B., Bailey, J.D., 2015. Silviculture and Ecology of Western U.S. Forests, Second edition. Oregon State University Press.

Thapa, B., Lovell, S., Wilson, J., 2023. Remote sensing and machine learning applications for aboveground biomass estimation in agroforestry systems: a review. Agroforestry Systems 97, 1097–1111. https://doi.org/10.1007/s10457-023-00850-2

Thyroff, E.C., Burney, O.T., Oliet, J.A., Redick, C.H., Tognetti, R., Jacobs, D.F., 2022. Toward Identifying Alternatives to Fencing for Forest Restoration: Tube Shelters Outperform Mesh Shelters for Deer Browse Protection of Live Oak, Quercus virginiana. Land 11, 966–966. https://doi.org/10.3390/land11070966

Tian, L., Wu, X., Tao, Y., Li, M., Qian, C., Liao, L., Fu, W., 2023. Review of Remote Sensing-Based Methods for Forest Aboveground Biomass Estimation: Progress, Challenges, and Prospects. Forests 14, 1086. https://doi.org/10.3390/f14061086

Tilman, D., Reich, P.B., Knops, J., Wedin, D., Mielke, T., Lehman, C., 2001. Diversity and Productivity in a Long-Term Grassland Experiment. Science 294, 843–845. https://doi.org/10.1126/science.1060391

Townsend, S., 2019. Sitka Spruce Can Shepherd Your Cedars Toward Maturity. Small Forest Landowner News, Department of Natural Resources. URL https://sflonews.wordpress.com/2019/08/01/sitka-spruce-can-shepherd-your-cedars-toward-maturity/ (accessed 4.14.26).

Turk, T.D., Schmidt, M.G., Roberts, N.J., 2008. The influence of bigleaf maple on forest floor and mineral soil properties in a coniferous forest in coastal British Columbia. Forest Ecology and Management 255, 1874–1882. https://doi.org/10.1016/j.foreco.2007.12.016
Urgenson, L.S., Halpern, C.B., ANDERSON, P.D., 2013. Twelve-year responses of planted and naturally regenerating conifers to variable-retention harvest in the Pacific Northwest, USA. Canadian Journal of Forest Research 43, 46–55. https://doi.org/10.1139/cjfr-2012-0323
Van de Peer, T., Verheyen, K., Kint, V., Van Cleemput, E., Muys, B., 2017. Plasticity of tree architecture through interspecific and intraspecific competition in a young experimental plantation. Forest Ecology and Management 385, 1–9. https://doi.org/10.1016/j.foreco.2016.11.015
Vercauteren, K.C., Lavelle, M.J., Hygnstrom, S., 2006. Fences and Deer-Damage Management: A Review of Designs and Efficacy. Wildlife Society Bulletin 34, 191–200. https://doi.org/10.2193/0091-7648(2006)34%5B191:FADMAR%5D2.0.CO;2
Villemaire-Côté, O., Ruel, J.-C., Sirois, L., 2017. Development of Northern White-Cedar (Thuja occidentalis L.) Plantations within and outside Deer Yards. Forests 8, 326-. https://doi.org/10.3390/f8090326
Vourc'h, G., Vila, B., Gillon, D., Escarré, J., Guibal, F., Fritz, H., Clausen, T.P., Martin, J.-L., 2002. Disentangling the causes of damage variation by deer browsing on young Thuja plicata. Oikos 98, 271–283. https://doi.org/10.1034/j.1600-0706.2002.980209.x
Vourc'h, G., Martin, J.-L., Duncan, P., Escarré, J., Clausen, T.P., 2001. Defensive adaptations of Thuja plicata to ungulate browsing: a comparative study between mainland and island populations. Oecologia 126, 84–93. https://doi.org/10.1007/s004420000491
Walter, J.D.C., Edwards, J., McDonald, G., Kuchel, H., 2019. Estimating Biomass and Canopy Height With LiDAR for Field Crop Breeding. Frontiers in Plant Science 10, 1145-. https://doi.org/10.3389/fpls.2019.01145
Wambsganss, J., Beyer, F., Freschet, G.T., Scherer-Lorenzen, M., Bauhus, J., 2021. Tree species mixing reduces biomass but increases length of absorptive fine roots in European forests. The Journal of Ecology 109, 2678–2691. https://doi.org/10.1111/1365-2745.13675
Wang, X.L., Klinka, K., Chen, H.Y.H., De Montigny, L., 2002. Root structure of western hemlock and western redcedar in single- and mixed-species stands. Canadian Journal of Forest Research 32, 997–1004. https://doi.org/10.1139/x02-026
Washington State Department of Natural Resources, 2025. Olympic Experimental State Forest Tier 3 Upland Management Plan (Management Plan). Washington State Department of Natural Resources, Land Management Division, Olympia, Washington.
Watson, J.V., Liang, J., Tobin, P.C., Lei, X., Rentch, J.S., Artis, C.E., 2015. Large-scale forest inventories of the United States and China reveal positive effects of biodiversity on productivity. Forest Ecosystems 2, 22. https://doi.org/10.1186/s40663-015-0045-4
Wickham, H., 2016. ggplot2: Elegant Graphics for Data Analysis. Springer-Verlag New York.
Wickham, H., Hester, J., Chang, W., Bryan, J., 2026. devtools: Tools to Make Developing R Packages Easier.
Wierman, C.A., Oliver, C.D., 1979. Crown stratification by species in even-aged mixed stands of Douglas-fir – western hemlock. Can. J. For. Res. 9, 1–9. https://doi.org/10.1139/x79-001
Williams, L.J., Paquette, A., Cavender-Bares, J., Messier, C., Reich, P.B., 2017. Spatial complementarity in tree crowns explains overyielding in species mixtures. Nature ecology & evolution 1, 63-. https://doi.org/10.1038/s41559-016-0063

Wing, B.M., Ritchie, M.W., Boston, K., Cohen, W.B., Gitelman, A., Olsen, M.J., 2012. Prediction of understory vegetation cover with airborne lidar in an interior ponderosa pine forest. Remote Sensing of Environment 124, 730–741. https://doi.org/10.1016/j.rse.2012.06.024

Wisdom, M.J., Vavra, M., Boyd, J.M., Hemstrom, M.A., Ager, A.A., Johnson, B.K., 2006. Understanding Ungulate Herbivory-Episodic Disturbance Effects on Vegetation Dynamics: Knowledge Gaps and Management Needs. Wildlife Society Bulletin 34, 283–292. https://doi.org/10.2193/0091-7648(2006)34%255B283:UUHDEO%255D2.0.CO;2

Woodruff, D.R., Bond, B.J., Ritchie, G.A., Scott, W., 2002. Effects of stand density on the growth of young Douglas-fir trees. Canadian Journal of Forest Research 32, 420–427. https://doi.org/10.1139/x01-213

Woodward, A., Jenkins, K.J., Harmon, M.E., 2021. Plant community succession following ungulate exclusion in a temperate rainforest. Ecosphere 12, e03889. https://doi.org/10.1002/ecs2.3889

Woodward, A., Schreiner, E.G., Houston, D.B., Moorhead, B.B., 1994. Ungulate-forest relationships in Olympic National Park: retrospective exclosure studies. Northwest Science 68, 97–111.

Xie, Q., Dash, J., Huang, W., Peng, D., Qin, Q., Mortimer, H., Casa, R., Pignatti, S., Laneve, G., Pascucci, S., Dong, Y., Ye, H., 2018. Vegetation Indices Combining the Red and Red-Edge Spectral Information for Leaf Area Index Retrieval. IEEE journal of selected topics in applied earth observations and remote sensing 11, 1482–1493. https://doi.org/10.1109/JSTARS.2018.2813281

Yoda, K., Kira, T., Hozimu, K., Ogawa, H., 1963. Self-thinning in overcrowded pure stands under cultivated and natural conditoins (Intraspecifc compettiion among higher plants XI). Osaka City University: Journal of the Institute of Polytechnics, D 14, 107–129.

Zahawi, R.A., Dandois, J.P., Holl, K.D., Nadwodny, D., Reid, J.L., Ellis, E.C., 2015. Using lightweight unmanned aerial vehicles to monitor tropical forest recovery. Biological Conservation 186, 287–295. https://doi.org/10.1016/j.biocon.2015.03.031

Zhang, Y., Chen, H.Y.H., Reich, P.B., 2012. Forest productivity increases with evenness, species richness and trait variation: a global meta-analysis. The Journal of Ecology 100, 742–749. https://doi.org/10.1111/j.1365-2745.2011.01944.x

Zhang, Y., Onda, Y., Kato, H., Feng, B., Gomi, T., 2022. Understory biomass measurement in a dense plantation forest based on drone-SfM data by a manual low-flying drone under the canopy. Journal of Environmental Management 312, 114862. https://doi.org/10.1016/j.jenvman.2022.114862